Fakultät für Medizin

Institut für Zellbiologie des Nervensystems

Plasticity of mononuclear phagocytes in an animal model of multiple sclerosis

Delphine Theodorou

Vollständiger Abdruck der von der Fakultät für Medizin der Technischen Universität München zur Erlangung des akademischen Grades eines

Doctor of Philosophy (Ph.D.)

genehmigten Dissertation.

Vorsitzender: Prof. Dr. Roland M. Schmid

Betreuer: Prof. Dr. Martin Kerschensteiner

Prüfer der Dissertation:

1. Prof. Dr. Thomas Misgeld

2. Prof. Dr. Thomas Korn

Die Dissertation wurde am 11.09.2017 bei der Fakultät für Medizin der Technischen Universität München eingereicht und durch die Fakultät für Medizin am 05.11.2017 angenommen.

Table of Contents

1. **Abstract** 4

2. **Introduction** 6

The immune system 6

The immune system in the CNS: immune privilege 8

Mononuclear phagocytes: origins and functions 11

Mononuclear phagocytes: classification 15

Involvement of mononuclear phagocytes in neurological diseases 24

Multiple sclerosis 26

Experimental models of Multiple Sclerosis 34

Questions and specific aims 39

Where do polarized phagocytes originate? 39

Can CNS microenvironments influence phagocyte phenotype? 39

Are phagocyte phenotypes stable or can they display plasticity? 40

3. **Material and Methods** 41

Mouse strains and genotyping 41

Active EAE induction 41

Bone marrow-derived macrophage culture 42

Immunocytochemistry 43

Flow cytometry 44

RNA sequencing analysis 45

Immunohistochemistry and *in situ* confocal microscopy 46

Quantitative analysis of *in situ* images 48

In vivo imaging method, processing and quantifications 50

Statistical analysis 53

4. **Results** 54

Characterization of *iNOS-tdTomato-cre* and *Arginase YFP* mouse lines 54

Absence of iNOS/arginase-1 expression in the healthy spinal cord 59

In situ colocalization of iNOS and arginase-1 with a phagocyte marker in the CNS 61

In situ colocalization of iNOS/arginase-1 with reporter proteins in the CNS 63

Determination of the proportion of resident cells expressing iNOS and arginase-1 signature enzymes 65

The progression of reporter protein expression correlates with the pro- and anti-inflammatory phagocyte phenotypes 69
Transcriptional analysis of macrophages populations isolated from the CNS 73
Importance of CNS compartmentalization for the establishment of mononuclear phagocyte phenotypes *in vivo* 76
Isotropic distribution of mononuclear phagocyte phenotypes in parenchymal lesions at EAE onset *in situ* 79
Mononuclear phagocyte polarization is initiated after CNS entry 81
Highest conversion rate of tdTomato expression in the parenchyma and at the pia/parenchymal border 87
Progression of mononuclear phagocyte phenotypes during EAE evolution 88
Mononuclear phagocytes plasticity occurs mainly in the parenchyma and at the pia/parenchyma border 90
Reporter promoters are still active over the course of EAE 92
Presence of a "*de novo"* macrophages population expressing $M^{Arginase}$ 94

5. **Discussion** 98

6. **References** 107

7. **List of abbreviations** 127

8. **Acknowledgements** 130

9. **Publication** 131

1. Abstract

Mononuclear phagocytes, key regulators of the immune system, have distinct functions depending on the cues and signals received by their local microenvironment. In this study, we used two transgenic mouse lines, which translate the expression of inducible Nitric Oxide Synthase (iNOS) and arginase-1, two well established signatures enzymes of pro- and anti-inflammatory macrophages, into distinct fluorescent signals. These enzymes are competing for the same substrate, the essential amino-acid L-arginine and are in consequence suitable to examine macrophage polarization states. Using a combination of these transgenic phenotype reporter mouse lines and a spinal *in vivo* imaging approach, we investigated the modulation of mononuclear phagocytes phenotype over time and in different compartments of the central nervous system (CNS). To study the role of activated phagocytes in the context of neuroinflammation, we induced experimental autoimmune encephalomyelitis (EAE), a widely used animal model of multiple sclerosis (MS). We showed that, over the course of EAE, iNOS and arginase-1 expression correlate with pro- and anti- inflammatory phagocyte phenotypes. While the expression of iNOS was predominant at early stages of the disease, arginase-1 expression prevailed at later time point including during remission. We could also observe a large proportion of macrophages expressing both markers over the course of the disease. The transcriptional profile of these macrophage populations in the inflamed CNS revealed M^{iNOS}, $M^{iNOS/Arginase}$ and $M^{Arginase}$ cells as distinct populations, however with a strongly overlapping transcriptome that is distinct from the classic M1-M2 phenotypes observed in *in vitro* experiments. We could also appreciate the importance of the spinal cord compartmentalization for the establishment of the phagocyte phenotype. The parenchyma was significantly enriched in M^{iNOS} cells in comparison to the upper meninges where M^{Arg} cells were predominant. Overall, our data show that macrophages enter the CNS unpolarized via

the blood circulation and afterwards start to express iNOS either in the perivascular space, in the meninges or directly in the parenchyma. We observed that polarized macrophages can also adapt their phenotype over the disease course by switching in an unidirectional manner from a pro- to an anti-inflammatory state (M^{iNOS} to $M^{Arginase}$). However, intermediary stage exists where both reporter proteins are expressed, thus suggesting the existence of a rather continuous phenotype spectrum. Lastly, a fate tracking approach showed that roughly 1/3 of arginase-1 expressing-macrophages appear *de novo*, thus revealing two different origins of anti-inflammatory macrophages. Our work provides novel insights into the dynamics of mononuclear phagocytes phenotypes during the formation to the resolution of neuroinflammatory lesions in an animal model of MS.

2. Introduction

The immune system

The immune system offers a complex defense mechanism composed of an intricate network of cells and tissues protecting the host against any invading pathogens, parasites and viruses. In vertebrates, it can be subdivided into two categories: an innate arm of the immune system, which provides fast responses induced by common danger signals and the adaptive immune system with a slower response to danger, based on a highly specific antigen driven immune response also referred to as acquired immunity. The principal actors of the innate immune system are the epithelial barriers acting as a physical obstacle, dendritic cells, mast cells, lymphocyte natural killer (NK) cells, phagocytic leukocytes such as monocytes, macrophages, granulocytes (neutrophils, basophils and eosinophils); whereas the main effectors of the adaptive immune system are T lymphocytes (mainly divided into cluster of differentiation (CD) $CD4^+$ and $CD8^+$ T cell) and B cells (**Figure 1**). Cells belonging to the innate immune system also participate in the transmission of the information and the activation of the adaptive immune system and vice versa.

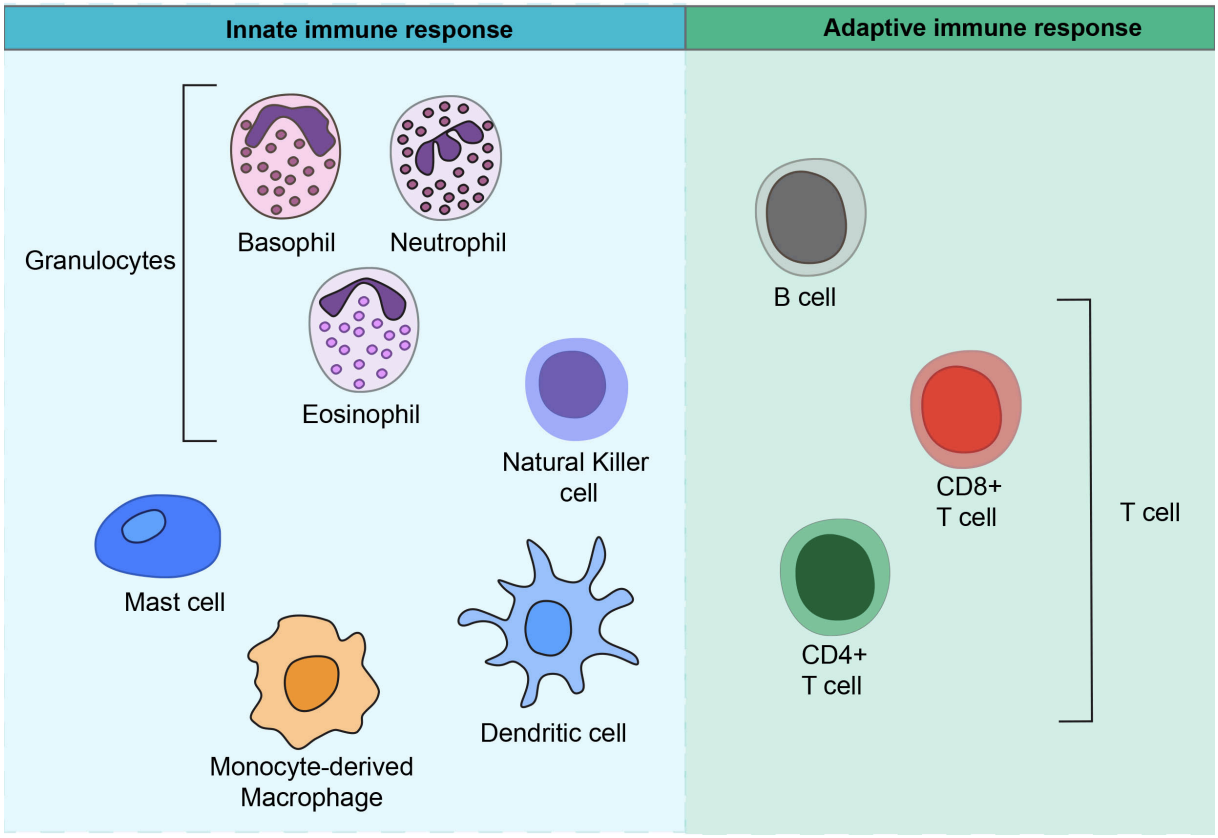

Figure 1: The innate versus adaptive immune response

The actors of the innate immune response are depicted on the left with granulocytes (basophil, neutrophil, eosinophil), mast cell, natural killer, dendritic cell and monocyte-derived macrophage while on the right are represented the actors of the adaptive immune response with B cell, $CD4^+$ T cell, $CD8^+$ T cell. Scheme inspired from Dranoff, 2004.

Several lymphoid organs act as sentinels that control the production and actions of these immune cells. These include the primary lymphoid organs (bone marrow and thymus) and the secondary lymphatic tissues with the spleen, liver, lymph nodes, lymphatic vessels, skin and tonsils. The primary lymphoid organs are responsible for the elimination of cells expressing receptors with high affinity for auto-antigens, while the secondary lymphoid organs provide an environment for possible interactions between immune cells and the induction of an immune reaction. For example, T cell progenitors are generated in the bone marrow and

migrate toward the thymus to undergo a maturation process corresponding to the verification of expression (positive selection) and the specificity of their T cell receptor (TCR) (negative selection). This TCR specificity will be responsible for the recognition of Major Histocompatibility Complexes (MHC class I for $CD8^+$ T cells and class II for $CD4^+$ T cells) presented by professional antigen presenting cells such as monocytes/macrophages, dendritic cells and B-lymphocytes. MHC are cell surfaces proteins that bind antigens derived from pathogens and present them on the cell surface in order to be recognized by T cells.

Cells from the innate and the adaptive immune system have complementary roles during homeostasis and pathology. A deregulation of any of these protective mechanisms may indeed lead to autoimmune-, inflammatory-, metabolic-, allergic- diseases or cancer. Deregulations leading to an autoimmune disorder such as multiple sclerosis will be discussed subsequently.

The immune system in the CNS: immune privilege

Sir Peter Medawar proposed the concept of immune privileged-organs in 1948 after performing heterotopic skin tissues grafts to the brain and to the anterior chamber of the eye in rabbits that did not induce a rejection for an extended period (Medawar, 1948). More precisely, immune privileged-organs can tolerate the presence of immune-stimulatory antigens without the initiation of an inflammatory immune response. Among these are the CNS, testis, eyes, placenta and the fetus during pregnancy. The concept of immune privilege has been considered to be an evolutionary adaptation mechanism to ensure the preservation and defense of vital organs, fundamental for survival during development and reproduction. If we take individually each of these organs, we can understand better why they could be the subjects to such peculiar protection. The eye is protected against inflammatory milieus that could be deleterious for the vision. The placenta and fetus acquired antigens inherited from

the father that could be recognized by the mother´s immune system. Thus, their protection is indispensable to avoid a miscarriage. For a long time, it was believed that these organs were isolated from the others and also from the immune system by actual physical barriers. Nonetheless, it was demonstrated later that antigens and immune cells can also access immune-privileged organs.

If we look more closely at the case of the CNS, and its crucial role as information-processing centre strongly interconnected with other organs, we can understand how fundamental it is to protect it from the consequences of inflammation-associated damage. The CNS must maintain its specific homeostasis even in response to potential changes in its microenvironment involving for example a change of pH or the presence of pathogens in the blood circulation (Prinz & Priller, 2017). For a long period, it was assumed that the CNS was separated from the other organs and the immune system thanks to substantial barriers such as the Blood Brain Barrier (BBB), the blood-cerebrospinal fluid (CSF) barrier composed of epithelial cells and tight junctions and leptomeninges, in order to prevent the entrance of peripheral immune cells coming from the circulation (Shechter et al, 2013; Engelhardt et al, 2017). However, several recent findings led to a re-evaluation of the concept of the CNS immune privilege and show that different immune cells (e.g. memory T cells coming from the periphery) can cross an intact BBB and continually recognize and eliminate malignant or virally infected cells, this process being called immune surveillance.

Meninges

The CNS is surrounded by a layered structure called meninges, which protect the brain and the spinal cord and contain immune cells that fulfill a surveillance role. The meninges are made up by the dura mater (outer part), the arachnoid (middle part) and the pia mater (inner part) with the latter two collectively called leptomeninges (**Figure 2**). In between the pia

matter and the arachnoid mater is located the subarachnoidal space that contains the CSF, originally secreted by the choroid plexus. The CSF directly drains antigens, cytokines, hormones and neurotransmitters via the dural lymphatic vasculature to reach the deep cervical lymph nodes, eventually allowing for peripheral presentation of CNS antigens. However, only few $CD4^{+}T$ cells and monocytes are actually found in the CSF under physiological conditions. In several traumatic and inflammatory pathologies of the CNS, hematopoietic cells can enter the CNS and exert pathological functions.

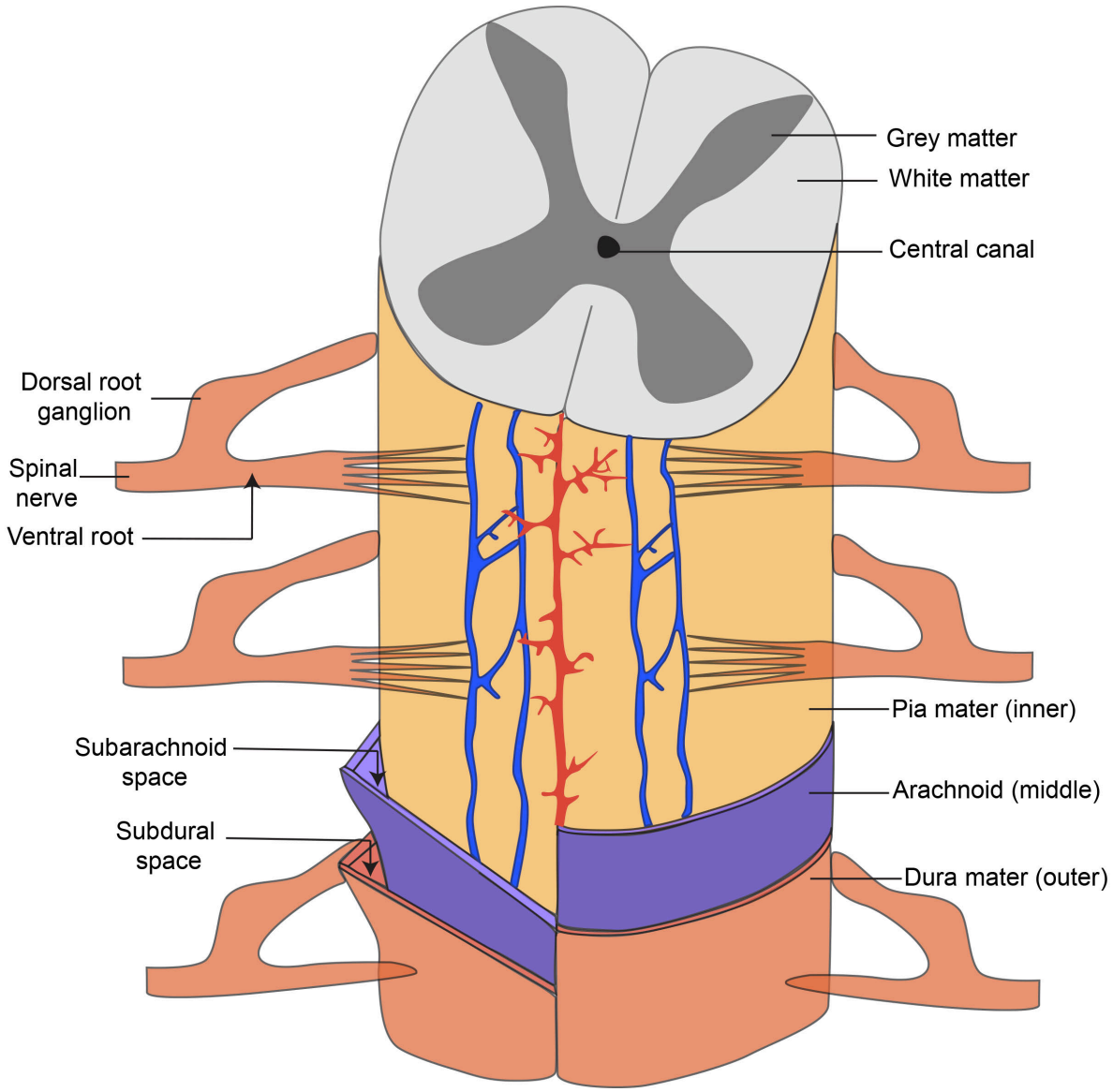

Figure 2: Scheme representing the spinal cord and its meninges

Figure 2: Scheme representing the spinal cord and its meninges

The different meninges layers are depicted on this scheme (pia mater (yellow), arachnoid (purple) and dura mater (orange)). The subarachnoid space is located between the arachnoid and pia mater while the subdural space is located between the dura mater and arachnoid. Vasculature is represented in red and blue. Scheme inspired from spinal cord anatomy and Pearson education.

Several hypotheses exist regarding the leukocytes invasion paths (e.g. of T cells) into the CNS. One suggests the entrance via the BBB, or an invasion of the CSF via the choroid plexus and the leptomeningeal vessels (Schwartz et al, 2014; Shechter et al, 2013). Another possibility of leukocytes invasion would be their entrance via the vasculature in order to reach the perivascular space and subsequently the parenchyma (Reboldi et al, 2009).

Mononuclear phagocytes: origins and functions

Two fundamental phases of hematopoiesis exist during embryogenesis: primitive hematopoiesis occurring in the yolk sac is responsible for the development of erythromyeloid progenitors and definitive hematopoiesis necessary for the generation of hematopoietic stem cells (HSCs) in the aorta-gonads-mesonephros (Ginhoux et al, 2014; Perdiguero et al, 2016). Immediately after establishment of blood circulation, around embryonic day 10.0-10.5 (E10.0-10.5) of mouse development, progenitors present in the yolk sac and HSCs can migrate and colonize the fetal liver that become the main hematopoietic site after E11 (Cumano et al, 2007; Kumaravelu et al, 2002; Ginhoux et al, 2016).

Microglial cells originate from primitive yolk sac during embryogenesis. They colonize the CNS around approximately E9.5-10.5 (Ransohoff, 2016). After initial colonization of the respective organs, microglial cells cease to be produced and are then maintained by local self-renewal (Ajami et al, 2007).

HSCs give rise to progenitors and indirectly to blood monocytes. Under inflammatory conditions, depending on the stimulus provided by the local tissue microenvironment, blood monocytes (representing 4-10% of the blood nucleated cells) are able to extravasate through the endothelium into the tissues and differentiate into tissue resident macrophages, inflammatory macrophages or monocyte-derived dendritic cells (**Figure 3**). The tissue resident macrophages, inflammatory macrophages and monocyte-dendritic cells represent the mononuclear phagocyte system that was first introduced by Van Furth and Zanvil Cohn in 1968 and that is primarily accountable for antigen presentation, phagocytosis and cytokine secretion.

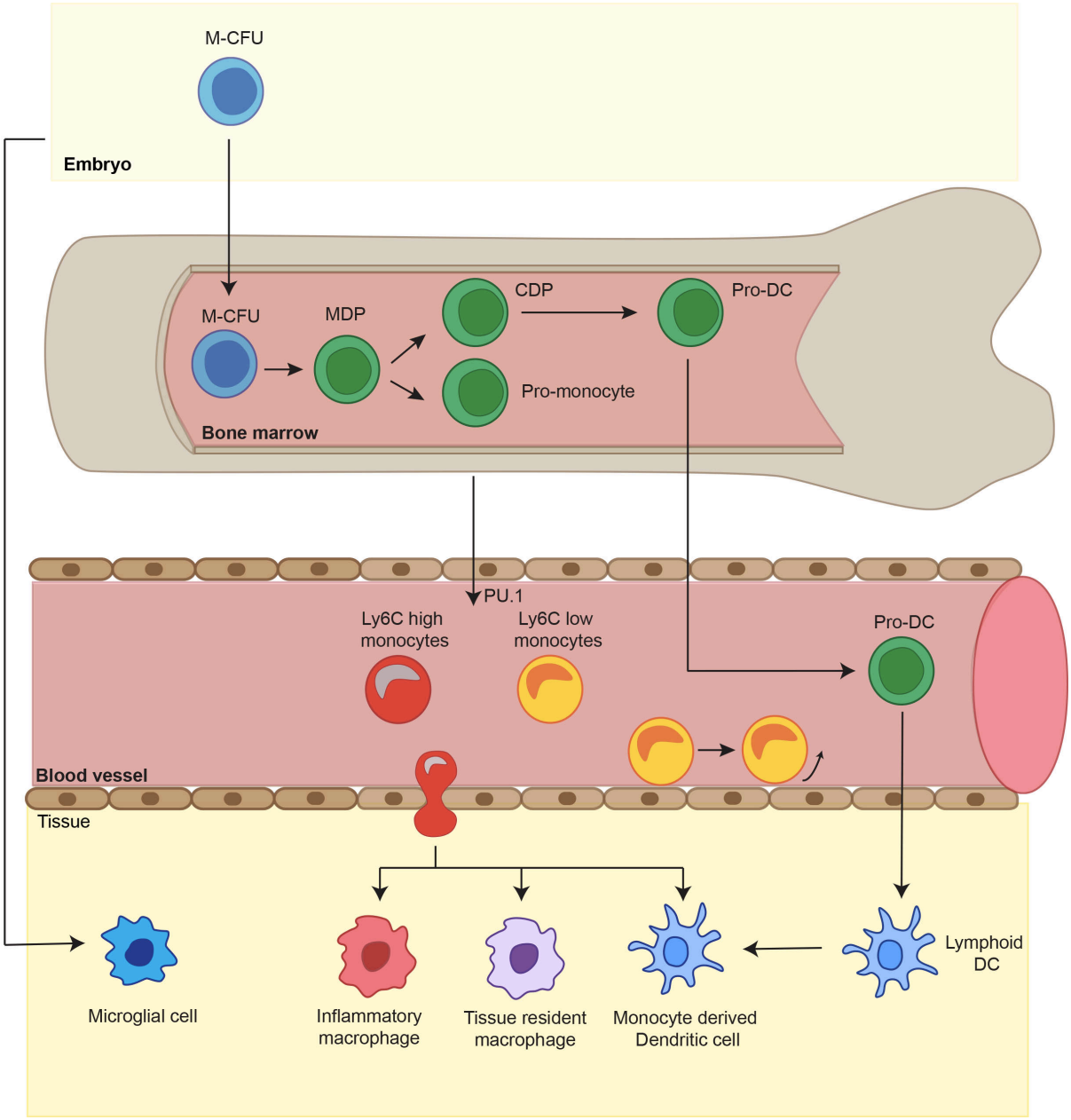

Figure 3: Mononuclear phagocyte system

Mononuclear phagocyte system (Inflammatory macrophage, tissue-resident macrophage and monocyte derived cells) arises from blood monocytes that are continuously produced during hematopoiesis and by local self-renewal. Abbreviations: M-CFU: macrophage colony forming unit, MDP: macrophage dendritic precursor, CDP: common dendritic cell progenitors, ProDC: pro dendritic cells, Lymphoid DC: Lymphoid dendritic cells. Scheme inspired from Lawrence et al, 2011; Ginhoux et al, 2014 and Mishra & Yong, 2016).

Differentiation into tissue resident macrophages is only possible due to the expression during early development of the transcription factor Runt-related transcription factor 1 (RUNX1) in HSC. This induces the expression of PU.1 and macrophage colony stimulating factor 1 receptor (CSF1R), a tyrosine kinase receptor needed for macrophage differentiation (Olson et al, 1995; Nerlov et al, 1998; Mishra & Yong, 2016; Goldman et al, 2016; Greter et al, 2013). CSF-1R has indeed a main role in the development of tissue resident macrophages. A lack of CSF-1R changed the numbers of macrophages at steady state and also during inflammation (Murray et al, 2016; Hamilton et al, 2013; Lavin et al, 2015; Auffray et al, 2009). Other cytokines also have a major role in the differentiation of monocytes into macrophages such as Macrophage Colony Stimulating Factor (M-CSF), the ligand of CSF-1 receptor, necessary for macrophage proliferation and survival (Yoshida et al, 1990).

Tissue resident macrophages have heterogeneous functions depending on their tissue location and their anatomical niche (Amit et al, 2016). They can participate in iron processing and clearance of cells debris by degrading the hemoglobin of senescent erythrocytes to perform erythropoiesis (Davies et al, 2013; Soares & Hamza, 2016).

Mononuclear phagocytes have major roles during homeostasis and pathology such as protection and defense, antigen presentation, tissue development and homeostasis, tissue reconstruction, phagocytosis of cell debris and wound healing (Campbell et al, 2013). During CNS homeostasis, a subset of macrophages located in the perivascular space is also able to detect damage-associated molecular patterns (DAMPS) and pathogen-associated molecular patterns (PAMPS). Upon inflammation, macrophages present in the perivascular space, in the meninges and in the choroid plexus can in principle regulate the entrance of immune cells (Taylor et al, 2005; Prinz & Priller, 2017).

Mononuclear phagocytes: classification

Classification of macrophages in the CNS has been for a long time a matter of debate. These cells can be separated based on different parameters: according to their location, their morphology and activation status, their chemokine receptors and ligands expression or depending on their polarization status.

CNS macrophages can be located in the parenchyma, in the perivascular space, in the meninges (both dural and leptomeningeal ones) and in the choroid plexus (Goldmann et al, 2016; Prinz & Priller, 2017). It has been shown that, depending on their position; these cells are able to play different roles in a steady state and during inflammation (Polfliet et al, 2002).

Moreover, they can also be categorized according to their morphology, which is dependent on their activation status. For instance, in a resting state, microglia appear as highly ramified cells (Ransohoff, 2016) while upon inflammation they acquire a more amoeboid morphology due to their activation.

Another way to characterize monocyte-derived macrophages is to differentiate them according to the expression of chemokines receptors and ligands (Shi & Pamer, 2011). Monocytes present in the blood can be classified into inflammatory or patrolling monocytes depending on the expression levels of two key receptors: the CC-chemokine receptor (CCR) 2 (CCR2) and the CX_3C-chemokine receptor 1 (CX_3CR1). Among other markers, both subsets of monocytes express CD11b (also called integrin alpha M), F4/80, CD68 and CD115 (M-CSF receptor necessary for macrophage differentiation). In mouse, circulating monocytes are $CCR2^{low}$ $CX_3CR1^{\mathbf{high}}$ $Ly6C^{low}$ and patrol the lumen of blood vessels while the inflammatory monocytes are $CCR2^{\mathbf{high}}$ CX_3CR1^{low} $Ly6C^{\mathbf{high}}$ and constitute approximately 2-5% of circulating leukocytes (Shi & Pamer, 2011). It has been shown that in case of CCR2 deficiency, the proportion of $Ly6C^{high}$ decreases in the inflamed tissue demonstrating a major

role of CCR2 in the trafficking of monocytes (Kurihara et al, 1997; Ajami et al, 2011). Notably, in steady-state Ly6c^{high} monocytes can re-enter the bone marrow and change their lineage phenotype becoming patrolling monocytes (Shi & Pamer, 2011; Gundra et al, 2017). The recruitment of Ly6C^{high} inflammatory monocytes is possible via two specific ligands CC-chemokine ligand (CCL) 2 and CCL7 that are both induced during inflammation (e.g. bacterial infections). Depleting either CCL2 or CCL7 strongly affects CCR2 monocytes recruitment thus showing a crucial role for these chemokines in monocyte trafficking (Jia et al, 2008). Interestingly, some of the chemokines receptors expressed by inflammatory monocytes such as CCR1 and CCR5 have also been shown to be involved in inflammatory diseases such as MS or atherosclerosis respectively (Charo et al, 2006). Otherwise, the recruitment of patrolling monocytes is mediated via the CX_3-C chemokine ligand (CX_3CL1, also called fractalkine). The absence of CX_3CR1 leads to a reduced numbers of blood circulating monocytes but also leads to a diminished recruitment of inflammatory monocytes (Auffray et al, 2009). Patrolling monocytes can in principle move toward to the site of infection and activate the inflammatory monocytes via the release of Tumour Necrosis Factor (TNF) and chemokines (Auffray et al, 2007).

Human monocytes express a different set of markers and are usually classified depending on the expression of CD14 and CD16. In mouse, blood-circulating monocyte are CCR2^{low} $CX_3CR1^{\mathbf{high}}$ Ly6C^{low} and correspond to CD14^{++} CD16^{+} intermediate monocytes and CD14^{+} CD16^{++} non-classical monocytes in humans. Inflammatory monocytes in mouse are CCR2^{high} $CX_3CR1^{\mathbf{low}}$ Ly6C^{high} and correspond to CD14^{++} CD16^{-} classical monocytes in humans (Shi & Pamer, 2011). Even though the interleukins (IL) are different between mice and human, their functions in the immune system as inflammatory and patrolling monocyte are assumed to be rather comparable in between species (Belge et al, 2002; Shi & Pamer, 2011).

Monocyte movement: Rolling, attachment, crawling and diapedesis

The function of the immune system necessitates blood leukocytes and in particular monocytes to constantly traffic throughout the circulation and cross the endothelium by extravasation, a process called diapedesis. Monocyte extravasation out of the circulation and recruitment to the CNS are tightly controlled, multistep processes requiring different adhesion molecules to roll, adhere and transmigrate. More specifically, in order to roll and attach to the endothelium $Ly6C^{hi}$ monocytes need L-selectin, P-selectin glycoprotein ligand 1 (PSGL1) (Leon et al, 2008), macrophage receptor 1 (MAC1), lymphocyte function associated antigen 1 (LFA1), platelet endothelial cell adhesion molecule (PECAM1) and very late antigen 4 (VLA4) (Shi et Pamer, 2011). While $Ly6C^{low}$ monocytes require LFA1 in order to adhere and crawl into the vascular endothelium. Transmigration of leukocytes through the endothelium is possible via the extension of pseudopodia -membrane projections- in order to pass through endothelium gaps thanks to the interaction of PECAM proteins with the endothelial cells.

M1-M2 polarization of phagocytes

Once activated, mononuclear phagocytes can be classified depending on their polarization status. An established bipolar dogma categorizes activated phagocytes in pro- or anti-inflammatory cells (also called M1 or M2, respectively) (Mills et al, 2000; Martinez et al, 2015; Murray & Wynn, 2011; Lawrence & Natoli, 2011; Martinez & Gordon, 2014). While M1 cells have been associated with the initiation of the disease or injury, M2 macrophages have been linked to the resolution of an inflammation (Kigerl et al, 2009; Sica et al, 2015; Kroner et al, 2014; Arnold et al, 2007).

Many studies have so far relied on this dichotomy, either based on human data at a fixed time point or on *in vitro* and *in situ* studies. However this classification has to be considered

carefully since it denotes a static view of the mononuclear phagocyte polarization, which does not depict the intrinsic heterogeneity of the macrophage populations. The final polarization of these cells derives from an elaborate integration of molecular signals derived from the local microenvironment; also, the presence of exogenous pathogens such as bacteria, several danger signals and epigenetic modulations have been shown to be involved in the complex mechanism of macrophage polarization (Murray et al, 2017; Mikita et al, 2011).

Pro-inflammatory macrophages or classically activated macrophages, induced *in vitro* by the presence of lipopolysaccharides (LPS) or interferon gamma (IFNγ) are described in the literature as M1 macrophages (**Figure 4**). M1 macrophages have a high capacity of presenting antigen associated with increased MHC-II expression and high microbicidal activity with the production of reactive oxygen species (e.g. nitric oxide NO). M1 macrophages take their names from their implication in the activation of T helper 1 (Th1) cells while anti-inflammatory macrophages activate T helper 2 (Th2) cells and express low amount of pro-inflammatory cytokines (e.g. IL-1, IL-6 and TNF) (Mantovani et al, 2004) and promote e.g. parasite clearance and tissue remodeling. However so far no study has shown the *in vivo* dynamics underlying the pro- and anti- inflammatory phenotype. Several types of anti-inflammatory macrophages have been described: M2a (or alternatively activated macrophages) induced by the presence of IL-4 or IL-13, M2b or type 2 activated macrophages induced by LPS and M2c or de-activated macrophages induced by IL-10 or Transforming growth factor β (TGFβ) (Stein et al, 1992) (**Figure 4**).

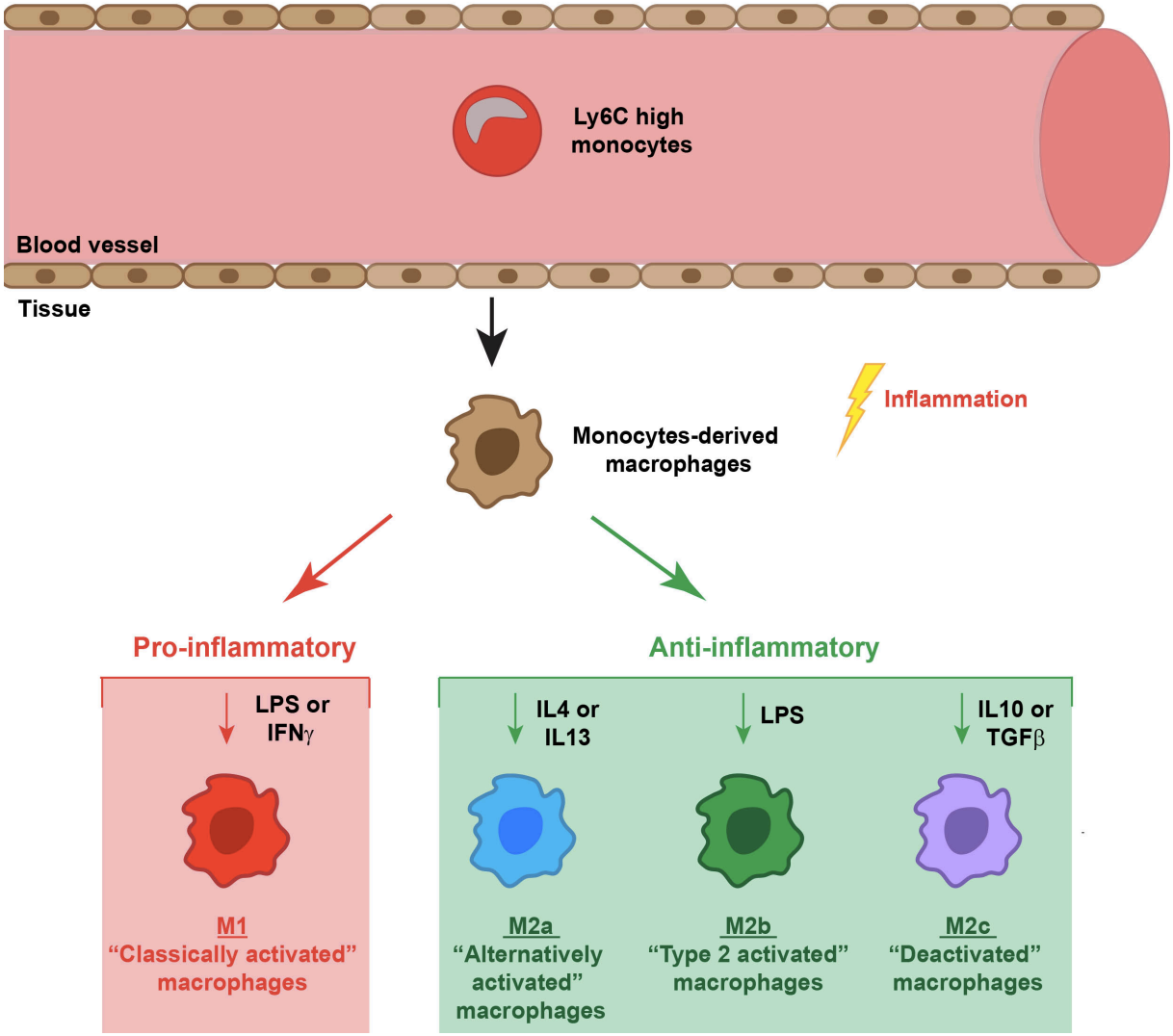

Figure 4: Pro- and anti-inflammatory macrophages fate

Pro-inflammatory macrophages are described as classically activated macrophages or M1 induced by lipopolysaccharide (LPS) or interferons γ (IFNγ). Anti-inflammatory macrophages are classified as alternatively activated macrophages or M2a induced by interleukin 4 (IL-4) and interleukin 13 (IL-13); Type 2 activated macrophages or M2b induced by LPS and deactivated macrophages or M2c induced by IL-10 and transforming growth factor β (TGFβ). Scheme inspired from Martinez et al, 2014.

This classification has encountered a lot of criticism (Ransohoff, 2016; Davies et al, 2013), as it oversimplifies the *in vivo* situation; conversely, many have proposed that the M1/M2 dichotomy can only represent the extreme phenotypes of a large, highly heterogeneous macrophages polarization spectrum (Biswas & Mantovani, 2010; Mosser et al, 2008; Murray et al, 2014).

Pro-inflammatory macrophages and anti-inflammatory macrophages shared common macrophages markers such as the adhesion molecule F4/80, CD11b, Iba1, but also possess specific markers differently regulated in each type of phagocyte phenotype. On the one hand, pro-inflammatory macrophages express specific markers described in *in vitro*, *in situ* and in both rodents and humans such as inducible nitric oxide synthase (iNOS), p22phox a subunit of the enzyme NADPH oxidase involved in the formation of reactive oxygen species, Interferon γ (INFγ), Interleukin 1 receptor (IL-1R), Tumor necrosis factor (TNF) (Kroner et al, 2014), STAT1, NFκB that activates Toll Like receptors (TLRs), the transcription factor IRF5, high production of IL-12, IL-23 (Verreck et al, 2004) and Granulocyte macrophage colony stimulating factor (GM-CSF) (Spath et al, 2017) (**Figure 5**).

On the other hand, specific markers of the anti-inflammatory macrophages include arginase-1, YM1 (chitinase-like 3); a mannose receptor expressed by non-parenchymal macrophages CD206 (also known as Mrc1; Galea et al, 2005; Goldmann et al, 2016), activin A (Ogawa et al, 2006; Ahn et al, 2012; Miron et al, 2013), resistin-like-α (Retnla), transcription factors such as STAT6 inducing the expression of Peroxisome proliferator-activated receptor, (PPAR) γ PPARγ, PPARδ, IRF4, the histone demethylase JMJD3 (regulating arginase-1, YM1, IRF4 and Retnla expression) and C/EPBβ (controlling arginase-1 expression); cytokines IL-4, IL-13 (Guglielmetti et al, 2016); IL-4 receptor (IL-4R); Lysosomal acid lipase (Lipa) involved in the lipid metabolism and lysosomal adaptor protein Lamtor1 associated with lysosomal vacuolar type H^+ ATPase (Kimura et al, 2016). Also, it

has been demonstrated that anti-inflammatory macrophages produce IL-10 in a higher amount compared to pro-inflammatory macrophages thus leading to stronger anti-inflammatory cell skewing (Lang et al, 2002; Murray et al, 2016). Moreover, it has been shown that in order to have an anti-inflammatory macrophage, the presence of glutamine is crucial while it is not necessary for a pro-inflammatory phenotype (Jha et al, 2015; Murray et al, 2016). Finally, a lipoprotein lipase CD36 has been considered as an M2 marker that affects the metabolism of fatty acid uptake, the involvement of mitochondrial oxidative phosphorylation and the activation of IL-4 pathway (Huang et al, 2014) (**Figure 5**).

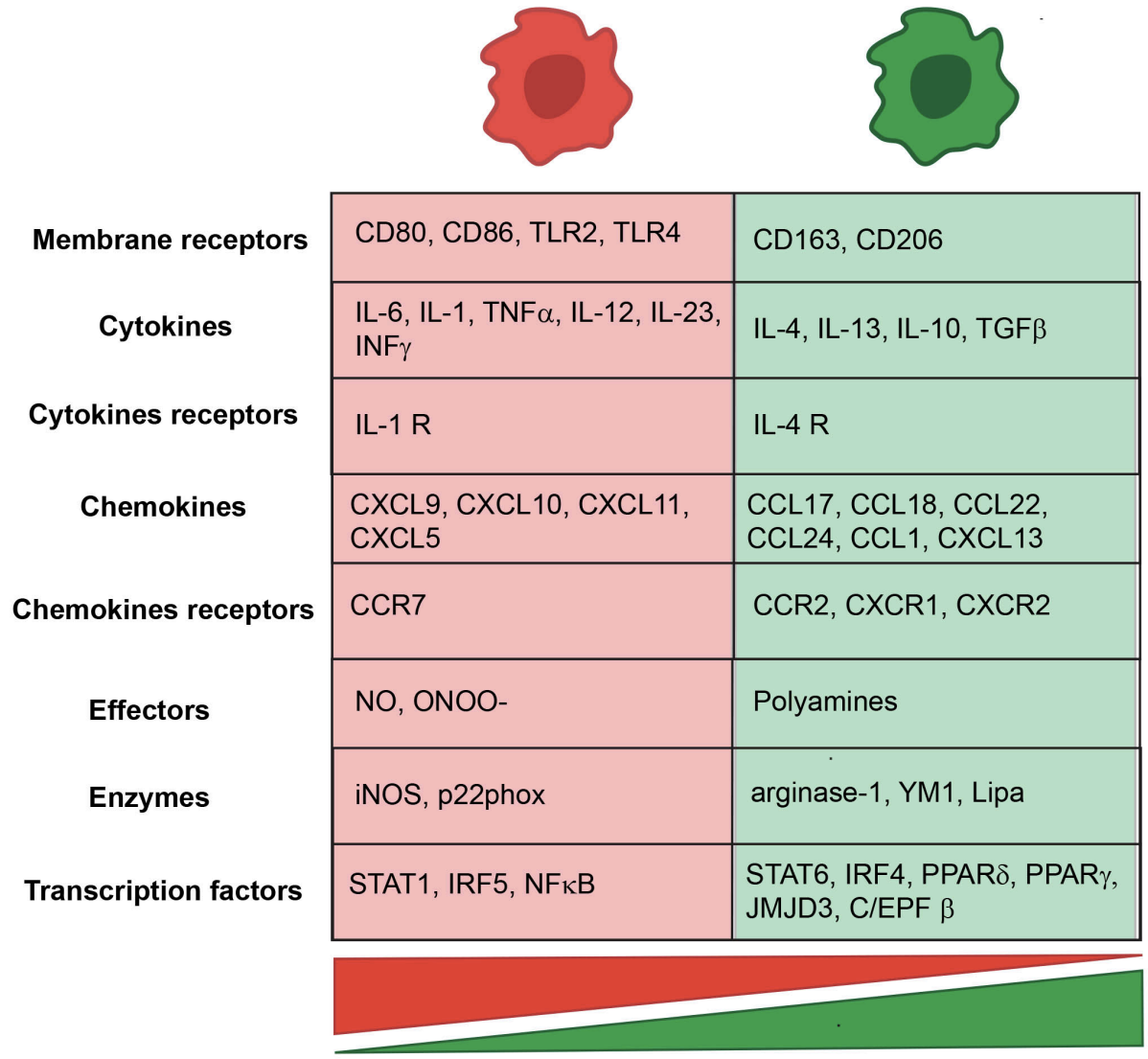

Figure 5: M1-M2 dichotomy

Figure 5: M1-M2 dichotomy

Pro- and anti- inflammatory macrophages are depicted in red and green respectively according to the M1-M2 paradigm. Can be found above: membrane receptors, cytokines, cytokines receptors, chemokines, chemokines receptors, effectors molecules, enzymes and transcriptions factors involved in this dichotomy. Scheme inspired by Murray et al, 2014.

Among the different M1/M2 marker genes, iNOS and arginase-1 deserve a particular attention. These signature enzymes for pro-inflammatory or anti-inflammatory phagocytes, respectively, compete for the same substrate, the essential amino acid L-arginine (Bronte et al, 2005). When iNOS is present, L-arginine is converted into L-citrulline and induces the production of reactive oxygen and nitrogen species with peroxynitrites (ONOO-) produced as a by-product of NO and $O2^-$, whereas when arginase-1 is produced, it triggers the expression of urea and L-ornithine that will ultimately lead thanks to the ornithine decarboxylase to the production of polyamines and L-proline involved in cell growth, collagen and extracellular matrix production respectively (Bronte et al, 2005; Kreider et al, 2007; Bogdan, 2015) (**Figure 6)**.

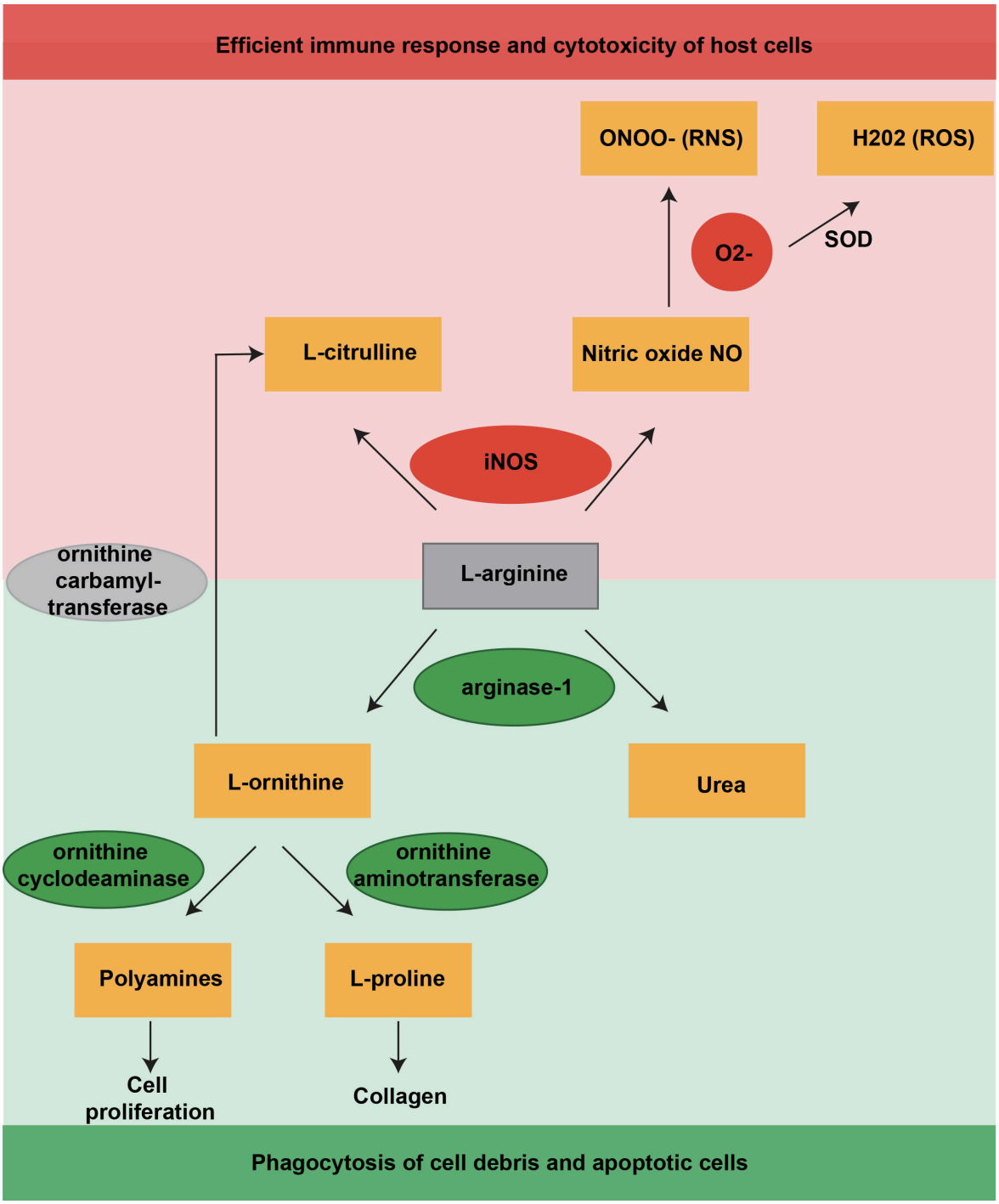

Figure 6: L-Arginine pathway

Arginase-1 and inducible nitric oxide (INOS) are two enzymes competing for the same substrate, the essential amino-acid, L-arginine. When arginase-1 is expressed, urea and L-ornithine are produced. This last induces the formation via ornithine cyclodeaminase of polyamines responsible for cell proliferation and via ornithine aminotransferase the formation of L-proline involved in collagen and extracellular matrix formation. In contrast, when iNOS

is expressed, it induces the expression of L-citrulline and nitric oxide (NO) that generates peroxynitrites (ONOO-) produced as a by-product of NO and $O2^{-}$. Scheme inspired from Bronte et al, 2005.

Involvement of mononuclear phagocytes in neurological diseases

Mononuclear phagocytes play a major role in many neurological disorders such as Alzheimer´s disease, frontotemporal dementia, Parkinson's disease, and ischemic stroke. Alzheimer's disease is a progressive neurodegenerative disorder characterized by the aggregation of amyloid β protein, neurofibrillary tangles or aggregates of phosphorylated tau protein leading to memory impairment; while frontotemporal dementia (FTD) is a progressive rare disorder defined by neuronal loss mainly in the frontal and temporal lobes of the brain, leading to dementia. Genome-wide association (GWAS) studies on Alzheimer's and FTD patients revealed several risk variants in loci associated with an increase susceptibility of developing the diseases. These risk variants were associated with the transmembrane receptor of myeloid cells CD33 -also called Siglec-3- and the tyrosine kinase binding protein (TYROBP) -also called DAP12-, both found in myeloid and lymphoid cells (Raj et al, 2014; Haure-Mirande et al, 2017). TYROBP protein has been shown to be essential for macrophage programming to induce a fusion competent state. (Helming et al, 2008). TYROBP is also able to form a complex with Triggering Receptor Expressed on Myeloid cells (TREM2) that has an important role in the degradation of tissue debris and amyloid plaques phagocytosis in Alzheimer´s disease. Also, TREM2 mutations (e.g. TREM2 T66M missense mutation) have been linked to an increase susceptibility of developing Alzheimer's disease and FTD (Yaghmoor et al, 2014).

Furthermore, IL-12 and IL-23 pro-inflammatory cytokines production can have an impact on the severity of Alzheimer´s disease. In its corresponding mouse model, the absence of both IL-12 and IL-23 induced a decrease of the disease pathology with a lower clinical impairment (Vom Berg et al, 2012). Thus, macrophages have major implications in Alzheimer's disease severity due to one of the transmembrane receptor involved in the clearance of amyloid plaques and the generation of pro-inflammatory cytokines aggravating the disease course.

Parkinson is a neurodegenerative disorder affecting the CNS that leads to severe motor defects (e.g. walking and movement impairment). The main characteristics of the disease are: death of dopaminergic neurons located in the substantia nigra and presence of Lewi bodies corresponding to the accumulation of alpha-synuclein proteins. Moreover, abnormal accumulation of iron has been observed in the CNS of Parkinson's patients but also in Alzheimer's patients. The CNS iron overload has been hypothesized to accelerate free radicals formation and neuronal death (Logroscino et al, 1997).

As mentioned previously, macrophages have a crucial role in iron processing and more specifically in its recycling during homeostasis. In steady state, this mechanism is tightly regulated to prevent an iron overload that will increase the ROS production and may directly have consequences on the CNS. Thus, macrophages may have an implication in the abnormal accumulation of iron observed in the CNS of patients suffering from Alzheimer's disease and Parkinson's disease.

In ischemic stroke (that accounts for the majority of strokes), the role of inflammatory cells, in particular microglia and peripheral monocytes/macrophages, has been extensively studied. Indeed, after an ischemic event, the level of reactive nitrogen species produced by macrophages is highly increased and contributes to the disruption of the BBB.

Importantly, macrophages generate pro-inflammatory cytokines such as interleukin-1 β and Tumor necrosis factor (TNF) alpha TNFα, that together increases the disease severity (Clausen et al, 2008; Prinz & Priller, 2017).

Multiple sclerosis

Multiple sclerosis (MS) is a chronic inflammatory disease of the CNS presumably discovered by St Lidwina of Schiedam in the 14th century and described for the first time anatomically by Jean-Martin Charcot in the 19th century. MS is a disorder that affects more than two million individuals worldwide, with a higher prevalence in young adults between the ages of 20 to 35. Women are two to three times more affected than men. The chronic inflammation in MS leads to major neurological deficits such as sensory, cognitive and motor defects (Hauser & Oksenberg, 2006; Hemmer et al, 2002; Compston & Cole, 2008). The hallmark of MS is the inflammatory plaque that is histopathologically characterized by demyelination, axonal degeneration and infiltrating immune cells in the brain and/or the spinal cord with BBB leakage. Even though MS has been first characterized by the presence of lesions located in white matter of the CNS of MS patients, it has also been shown recently -thanks to the advances of magnetic resonance imaging (MRI)- that disease also induces diffuse grey matter pathology in many patients, which is associated with worsened severity and clinical outcome. MS can take different clinical forms: Clinically isolated syndromes describing patients with a single relapse in whom dissemination over time and space have not been demonstrated; Relapsing-Remitting MS (RRMS) that affects nearly 85% of the patients and is defined by recurrent neurological followed by partial or complete clinical recovery; Primary Progressive MS (PPMS) associated with a constant progression and no period of recovery affecting 10-15% of patients; Progressive-Relapsing MS (PRMS) characterized by a continuous evolution of the disease with acute attacks with or without subsequent recovery. PRMS is associated

with worsened neurological functions and disability. In a large proportion of patients with RRMS, the disease progresses into a secondary progressive phase (SPMS) and defined by a constant progression of neurological symptoms. While focal inflammation occurs at every stage of the disease, this appears less prominently in chronic stages.

The true etiology of MS remains unknown; however, over the years many potential causative factors have been discovered. MS is a multifactorial disease thought to depend on the interaction between a genetic susceptible background, timed activation of the immune system and several environmental factors.

More than 200 candidate genes have been identified with genome wide association studies of MS susceptibility. These include certain HLA loci, Tumour necrosis factor receptor 1 (TNFR1), IL-12, interferons and Nuclear factor κ B (NFκB) (Taşan et al, 2015; Dendrou et al, 2015). The genetic data obtained have been used to create a human interactome network representing the map of biologically pertinent molecular interactions in order to facilitate cellular representation (Menche et al, 2015; Dendrou et al, 2015). To be more accurate, an interactome depicts a network of all molecular interactions (e.g. protein-protein interaction) in a single cell that can be used to infer indirect interaction among genes. Candidate genes were selected due to their functional relevance and their polymorphism associated with the disease. Two genes have been identified with a very high association to MS: HLA-A*02:01 and HLA-DRB1*15:01 variants (Hartmann et al, 2014; Dendrou et al, 2009).

Among all the environmental risk factors, one of the most studied is the Epstein-Barr virus (EBV). An increased level of antibodies against EBV has been shown to be associated with a higher risk a developing MS. Hypothetically, infection by EBV may trigger the citrullination of proteins or peptides such as myelin basic protein (MBP) during antigen processing (Yang et al, 2016); alternatively, EBV is thought to activate myelin-reactive $CD4^{+}$T cells through a mechanism called cross-reactivity. Interestingly, the absence of EBV infection has been

shown to be associated with a low risk or even an absence of MS development (Pakpoor et al, 2013; t'Hart et al, 2016).

In addition several other environmental factors have been argued to be involved in the pathogenesis of MS. Among these are low levels of the protective vitamin D, smoking (Hedstrom et al, 2009) and a former cytomegalovirus infection (Vanheusden et al, 2015; Vanheusden et al, 2017).

One of the central unresolved questions regarding the pathogenesis of MS is whether the disease derives from an initial neurodegenerative mechanism (inside-out theory) or from a peripheral inflammation leading to autoimmune CNS damage (outside-in theory). In the inside-out hypothesis, the first event to take place appears to be the death of oligodendrocytes followed by activation of macrophages and microglia. In addition, antigens leakage makes their recognition possible bystander activated autoreactive T or B cells (Locatelli et al, 2012; Peterson et al, 2007). This process will involve the mimicry of self-antigens that corresponds to the similarity/homology of a structure (e.g. same amino acid sequence) or functions between a self-antigen of the host and a pathogen that may trigger an immune cross-reaction response against the self-antigen. Damaged axons and myelin are phagocytosed and antigens presented to autoreactive T and B cells leading to a secondary autoimmune response against myelin sheath. The alternative theory of outside-in corresponds to first an activation in the periphery of the immune system followed by an invasion of immune cells into the CNS.

Histological hallmarks of MS

Oligodendrocytes and their insulating myelin sheaths are the main targets of the chronic inflammation observed in MS patients. Myelin is a lipid-enriched biological membrane surrounding neuronal axons and allowing fast saltatory conduction of the axon potential. The

process of myelination occurs both in the CNS and in the peripheral nervous system (PNS), with myelin being generated by oligodendrocytes and Schwann cells respectively (Nave et al, 2014). In MS, demyelination can occur both in the white and grey matters and lesions can vary in size, shape, location and are often associated with different degrees of oligodendrocytes loss. As stated previously, demyelinating lesions in the grey matter are associated with a poor disease prognosis.

Axonal degeneration is another important histological hallmark of MS. Recent studies have suggested that release of reactive oxygen and nitrogen species (ROS/RNS) by macrophages and microglia during lesion formation brings about focal axonal damages followed by axonal degeneration and mitochondrial fragmentation. This mechanism has been referred to as focal axonal degeneration (FAD) and has been described both in a mouse model of MS as well as in acute lesions from MS patients (Nikic et al, 2011). This study also reveals that demyelination is not necessary for axonal degeneration. In addition, axonal damage can be reversible. In this model, extrinsic application of ROS/RNS on the spinal cord triggers focal axonal degeneration, and removal of these reactive species can conversely induce axonal recovery. Although in steady state, physiological levels of reactive species are needed for several biological processes, in experimental autoimmune encephalomyelitis (EAE) and in MS, high concentrations of ROS and RNS can be responsible for the induction of an oxidative stress and also lead to oligodendrocyte damage at an early phage of MS (Haider et al, 2011). The main reactive species released by activated macrophages and microglia are nitric oxide (NO) produced by iNOS and superoxide (0_2^-) produced by NADPH oxidase. Former studies revealed that treating EAE with iNOS inhibitors ameliorate the course of the disease and neurological symptoms (Okuda et al, 1998). The extent of axonal damage is correlated with an increase of macrophages, microglia and $CD8^+$ T cells but however not with TNFα and iNOS mRNA in biopsies of MS patients (Bitsch et al, 2000; Selmaj et al, 1988; Mitrovic et al,

1994). It has also been postulated that an important amount of mitochondrial DNA mutations could lead to mitochondrial injury and increased production of reactive species (Campbell et al, 2012, Haider et al, 2011). This would account for an energy production failure and misfolding of proteins in the endoplasmic reticulum (ER) (Dendrou et al, 2015).

T lymphocytes

Finally, the most important pathological hallmark of MS is inflammation in the form of infiltrating immune cells associated with leakage of the BBB. It has been extensively demonstrated that autoreactive T cells are able to target CNS auto-antigens and more precisely myelin proteins (Fletcher et al, 2010). T cells can target several myelin proteins including myelin oligodendrocyte glycoprotein (MOG), proteolipid protein (PLP) or Myelin Basic Protein (MBP). These autoreactive T cells can be found in the CNS at every stage of the disease. The balance between Th1 and Th2 cells play a major role in the development of MS pathology and EAE. While Th1 cells have been associated with the initiation of lesions, Th2 cells have been linked to disease recovery. Indeed, Th1 cells are able to release pro-inflammatory cytokines such as INFγ and TNFα. In MS lesions and in patients CSF, increased level of TNFα has been found. Moreover, recent studies have reported an altered number of regulatory T cells ($CD4^+$ T_{reg} and $CD8^+$ T_{reg}) in the periphery of patients with MS compared to controls (Feger et al, 2007; Dendrou et al, 2015).

B lymphocytes

In contrast to T cells, the numbers of B cells infiltrating the CNS fluctuate over the disease course and are located in the CSF, meninges and the parenchyma. Besides, the antibodies produced can be found in the CSF and reach the deep cervical lymph nodes. Due to the recent

advances of high throughput sequencing, different clones of B cells could be characterized in the CSF of MS patients (Obermeier et al, 2012). Furthermore, autoantibodies have been shown to participate in the formation of lesions with the presence of IgG in lesions (Lucchinetti et al, 1996).

Macrophages and microglia

While, it has been established that CNS autoreactive T cells trigger inflammation, demyelinated lesions and focal axonal degeneration, the role of myeloid cells has for a long time not been clearly appreciated in the pathology of MS, even though monocyte-derived macrophages and microglia play a major role in the initiation and development of the disease.

Macrophages can be considered as a double edge sword, as two types of macrophages exist: one the one hand pro-inflammatory macrophages activating Th1 cells and found during relapses and on the other hand anti-inflammatory monocytes-derived macrophages activating Th2 cells and present during remission.

Macrophages and microglia are the main cellular infiltrates in MS lesions and in EAE; and the main producers of reactive oxygen species in MS lesions (Bjartmar et al, 2003; Trapp et al, 1998; Hauser et al, 2006; van Waesberghe et al, 1999).

As mentioned previously, reactive species can lead to axonal degeneration, mitochondrial and oligodendrocyte damage in MS and in EAE (Nikic et al, 2011; Haider et al, 2011). The main reactive species released by activated macrophages and microglia are NO and superoxide (0_2^-) produced by iNOS and NADPH oxidase respectively.

Moreover, studies have shown that macrophages promote T cell recruitment into the CNS via an increase expression of matrix metalloproteinases necessary for T cell infiltration in MS and

EAE (Toft-Hansen et al, 2004) and via the expression of CD40, CD86 and MHCII on their cell surface (Edwards et al, 2006).

While pro-inflammatory macrophages can have harmful consequences, anti-inflammatory macrophages are able to promote tissue repair thanks to the production of anti-inflammatory cytokines. Anti-inflammatory macrophages have also been shown to participate into the differentiation of oligodendrocytes increasing subsequently remyelination (Miron et al, 2013).

Understanding the equilibrium between pro- and anti- inflammatory macrophages is an important prerequisite for the development of therapeutic strategies that can limit tissue damage and improve recovery of neuroinflammatory lesions.

MS treatments

MS pathogenesis is associated with immune cells infiltration. These latter can be targeted to affect different aspects of the disease such as the reduction of relapses occurrences and severity or the delay of disease progression. Despite the lack of cure for MS, a wide range of treatments approved by the food and drug administration (FDA) exist on the market: for clinical isolated syndromes (CIS): interferons β, glatiramer acetate and teriflunomide; for patients afflicted with the RRMS: in addition alemtuzumab, fingolimob, natalizumab, dimethyl fumarate or mitoxantrone and for patients with SPMS: interferons β and mitoxantrone. These drug therapies are generally considered for their consequences on T cells and B cells, however their effects on myeloid cells is often neglected (Mishra et al 2016).

Interferons-β (IFNβ), is the most prescribed drug to treat RRMS and its application leads to the reduction of proliferating T cells, decrease of TNFα production and modification of adhesion molecules necessary for the immune cells passage through the BBB. This treatment also affects myeloid cells and in particular monocytes/macrophages. Indeed, IFNβ treatment

on cultured monocytes from MS patients triggered a reduction of metalloproteases productions (e.g. MMP2) and a decrease migratory phenotype (Galboiz et al, 2002). Moreover, patients treated with IFNβ produced reduced levels of pro-inflammatory cytokines (Hussien et al, 2004), reduced ROS production (Lucas et al, 2003) and higher level of anti-inflammatory cytokines (e.g. IL-10) (Liu et al, 2001) compared to non-treated patients with IFNβ.

Glatiramer acetate (Copaxone), is an immuno-modulatory drug constituted of four amino acids (glutamic acid, alanine, lysine and tyrosine) that resembles MPB protein. Glatiramer acetate bins MHC molecules recognized by T cells through their TCR thus inhibiting T cell activation (Ziemssen et al, 2007). The main drug effect is the generation of Th2 cells that produce IL-4, IL-10 and TGFβ. Moreover, glatiramer acetate administration in EAE has been shown to be associated with the development of anti-inflammatory monocytes-derived macrophages (M2; Weber et al, 2007), inducing the activation of regulatory T cells and ameliorating the disease course. Blood monocytes from MS patients exhibit increased phagocytosis (Pul et al, 2012), an inhibition of NO production (Iarlori et al, 2008) and a decrease IL-12 cytokine production (Kim et al, 2004) thus revealing the effect of glatiramer acetate on myeloid cells.

Fingolimob (FTY720) is a drug that mimics sphingosine-1-phosphate receptors (S1P-R) located on both lymphocytes and myeloid cells surfaces, responsible for lymphocytes escape from the lymph nodes. With fingolimob treatment, lymphocytes are then sequestrated in the lymph nodes and their access to the CNS is prevented which inhibits lesion formation.

Dimethyl fumarate, is a compound absorbed via the small intestine reducing the oxidative stress and the production of pro-inflammatory T cells (Mishra et al, 2016). This drug has been shown to prevent the production of NO and pro-inflammatory cytokines (IL-1β, TNFα and IL-6) in microglial and astrocytic cell cultures of rat (Wilms et al, 2010).

Alemtuzumab is a humanized monoclonal antibody targeting a glycoprotein CD52 present on the cell surface of a subset of leukocytes (lymphocytes and monocytes). Alemtuzumab treatment triggers a depletion of T lymphocytes, B lymphocytes and NK cells.

Teriflunomide, is a reversible inhibitor of the enzyme dihydro-orotate dehydrogenase, a key mitochondrial enzyme responsible for the synthesis of pyrimidine during proliferation. Teriflunomide treatment has been shown to significantly reduced the release of IL-6 from human peripheral blood mononuclear cell cultures stimulated with LPS (Bar-Or et al, 2014).

Natalizumab, is a monoclonal antibody developed against α4β1 integrin (Very Late Antigen 4 VLA-4) expressed on the surface of leukocytes membranes (e.g. T cell). The integrin VLA-4 is fundamental for the CNS infiltration of T cells via the passage of the BBB. Thus natalizumab treatment prevents the entrance of T cells into the brain and thus limits CNS inflammation.

Mitoxantrone is an immunosuppressive, antineoplastic compound first developed for chemotherapy that can now be prescribed for RRMS and SPMS. Mitoxantrone prevents cells division and has the capacity to intercalate into the DNA. However its use is associated with a higher risk to develop leukemia and heart damage.

Experimental models of Multiple Sclerosis

Multiple sclerosis is a disorder that only affects human beings. Despite the fact that no animal model of MS is able to reproduce and describe perfectly all the hallmarks of the disease, they are very useful to better understand the process of neuroinflammation and demyelination occurring in the disease (Pachner, 2011). Thus, the choice of the model has to be done carefully depending on the different working questions. For instance, attempts of investigating initial MS etiology in animal models need to take into account the peculiar microbiological

conditions and the homogeneous genetic backgrounds of laboratory animals compared to the complex influence of pathogens and environment that shape the immune system of MS patients (Adams et al, 2003; t‘ Hart et al, 2011).

Several kind of experimental models of MS have been developed over the years. Some are virally induced, such as Theiler´s encephalomyelitis, some induced by chemical agents, such as lysophosphatidyl choline (lysolecithin), ethidium bromide and cuprizone; lastly some are induced by immunizations against CNS antigens, such as experimental autoimmune encephalomyelitis (EAE).

In the Theiler’s murine encephalomyelitis virus (TMEV) model an intra-cerebral injection of the picorna Theiler’s virus induces two separate phases of disease. First, an acute phase associated with encephalitis with mostly neurons being infected. Secondly, a chronic phase leading to demyelination, inflammation, axonal disturbances and subsequent remyelination. This induced disease is very useful to model the production of IgG in the CNS over time as also observed in MS patients; however, a major downfall of this model is the timing of clinical paralysis, which can take up to several months.

Lysolecithin is a lipid generated by phospholipase A2. The model relies on the local stereo-tactical injection of LPC either in the corpus callosum or in the spinal cord, where its accumulation triggers demyelination. A single injection is sufficient to induce a focal demyelinating lesion followed by a remission. This model is commonly used to study demyelination and re-myelination.

The Ethidium Bromide model has been extensively used in rats and is induced quite similar to the Lysolecithin model with the direct focal intracerebral or intraventricular microinjection of this compound leading to neural cell degeneration and demyelination. Spontaneous remyelination occurs consequently to the injections. This model is used to study inflammation, demyelination and remyelination processes.

Among the chemically induced MS models, cuprizone administration has been widely used to study demyelination since the 1960s and has been characterized in different mice strains such as Swiss, CDI, ICI, BALB/c, SJL and C57BL/6 mice. Cuprizone (bis-(cyclohexanone) oxaldihydrazone), a neurotoxic compound, is given to adult mice mixed with the rodent chow. This drug is a copper chelator that induces a copper deficiency, alters oligodendrocytes survival thus triggering demyelination of the CNS. The demyelination starts in the corpus callosum after three weeks of treatment and is complete at five weeks. For the neocortex, the demyelination is complete at little bit later c.a. at six weeks (Skripuletz et al, 2011). This model can be useful to study reproducible demyelination in the CNS but not to study the inflammatory component of MS, as it does not lead to sustained neuroinflammation.

Several Experimental autoimmune encephalomyelitis (EAE) models exist including both active and passive induction. In both cases, EAE is triggered by the stimulation of T cells reactive against myelin sheath antigens leading to a demyelination, CNS inflammation, axonal injury and neurological deficits, which are shared characteristics of MS (Rangachari et al, 2013, Lassmann et al, 2017). Passive EAE models are induced by the adoptive transfer of myelin reactive T cells isolated from mice that were formerly primed with myelin antigens, into naïve mice (Stromnes et al, 2006). Commonly, Th1 cells are transferred against myelin peptides or proteins recognizing MOG, MBP or PLP.

Active Experimental autoimmune encephalomyelitis (EAE) is one the most widely used experimental models of MS, in which vertebrates (most commonly rodents) are immunized against an encephalitogenic CNS-specific myelin antigen, such as MOG, PLP or MBP emulsified in Complete Freund`s adjuvant (CFA, heat inactivated mycobacteria with mineral oil) with another bacterial adjuvant such as Pertussis Toxin (produced by the bacteria *Bordetella pertussis*) injected at 0 and 2 days after immunization (Bruckener et al, 2003). The

use of adjuvants is crucial as these activate the innate immune response and exacerbate the antigen specific immune response.

Every mouse strain possesses immune-dominant peptides i.e. a selective preference for loading specific peptides in the context of MHC-II and for lymphocytes to recognize such presented peptides. For example, C57BL/6 mouse strain is more susceptible to induction of EAE with MOG 35-55 peptide (Pachner, 2011).

Inflammation is one of the hallmarks of EAE that affects principally the spinal cord and is already occurring post-immunization before the clinical symptoms. The disease course of EAE in C57BL/6 mice begins usually with a weight loss around 11 days post immunization, which corresponds usually to one day prior to clinical onset, followed by a progressive weakness of the tail and the hindlimbs. The peak of the disease appears few days later and generally corresponds to a complete flaccid paralysis of the hindlimbs. A remission phase occurs progressively after the peak of the disease correlated with an improvement of neurological deficits. Throughout the entire course of the disease, the animal is scored daily in order to assess neurological deficits according to an established EAE scoring scale starting from 0 to 5 (0: being no clinical sign of the disease or weakness, 1: paralysis of the tail, 1.5-2: paresthesia, 2.5: dragging of at least one foot, 3: complete paralysis of the hindlimbs, 3.5 same as score 3 plus a weakness of the forelimbs, 4: complete limb paralysis and 5:death).

What happens following immunization has been widely studied (Engelhardt et al, 2009). During the first week after injection of myelin peptides and adjuvants, dendritic cells, macrophages are recruited to the immunization depot and start processing the antigens. Afterwards, lymph nodes drain the inflammation site. Activate lymphocytes are able to pass through the disrupted BBB and enter the CNS.

Numerous investigations are focusing on cytokines (i.e. TNFα) released by T cells and their impact on the disease course of EAE. Indeed, blocking TNFα ameliorates the severity of EAE (Ruddle et al, 1990; Selmaj et al, 1991). In EAE, the pathways the most considered involved Th1, Th17 and Th2 cells with a particular interest on IL-23, IL-1 β, TGFβ inducing Th17 cells and on IL-22 and IL-17 cytokines produced by Th17.

Moreover, it has been demonstrated in EAE that antigen-presenting cells (APC) - including B cells, macrophages and dendritic cells- are able to present thanks to MHC on their surface that will be recognized by TCR. In the particular case of MHCII interacting with $CD4^+$T cells, monocytes are recruited towards the CNS. (Dendrou et al, 2015).

EAE presents distinct advantages compared to other experimental models of MS. One of them is the apparition of the weakness that occurs between one to two weeks post immunization compared to e.g. the TMEV model that may require several months. Also, several current common treatments in MS were successfully initiated in EAE and transferred to MS, such as glatiramer acetate, Mitoxantrome, Fingolimod (FTY720) and Natalizumab (blocking α4β1 integrin necessary for the adhesion of leukocytes).

One of the main drawbacks of comparing EAE model to MS concerns the induction of the disease that requires the administration of an extensive amount of adjuvants in order to elicit the development of the disease. Moreover, EAE is dominated by a large amount of $CD4^+$ T cell in comparison to a dominant infiltration of $CD8^+$ T cells present in both grey and white matter lesions in MS patients (Frisher et al, 2009; Dendrou et al, 2015).

Questions and specific aims

Where do polarized phagocytes originate?

It has been widely accepted that in MS and in its animal model EAE, pro- and anti-inflammatory macrophages are present during different stages of the disease. While pro-inflammatory macrophages have been associated with the initiation of the disease, anti-inflammatory macrophages have been linked to the resolution of inflammation. Knowing in which compartment macrophages start to express their pro-inflammatory arsenal would increase the available knowledge about the initiation of lesions formation. However, no study has shown so far when and where the polarization of pro-inflammatory macrophages arises in the different CNS compartments *in vivo.*

Can CNS microenvironments influence phagocyte phenotype?

Whether the location of a phagocyte influence its phenotype is still unclear. Is the presence of cytokines, pro- or anti- inflammatory molecules present in the CNS milieu able to influence the phagocyte phenotype?

Do the CNS compartment such as meninges, pia/parenchyma and deep parenchyma have a major role on the proportion of pro- and anti- inflammatory macrophages?

This question is very relevant for many therapeutic aspects. If we could modify the milieu of CNS microenvironment to influence the macrophage fate, we would be able to modulate the state of neuroinflammatory lesions to a resolution/remission fate.

Does the position relative to the meninges, vasculature and core of the lesion in spinal EAE lesions influence the pattern of lesion expansion?

Knowing where the mononuclear phagocytes start to polarize into a M^{iNOS} phenotype could present clues on the molecules, effectors, cytokines present in the CNS milieu that can influence their polarization.

Are phagocyte phenotypes stable or can they display plasticity?

We used an *in vivo* spinal imaging approach to follow the phenotype of macrophages populations and phenotypes in different CNS microenvironments and address the following question: Are there consecutive waves of phagocytes with a different phenotype over the course of EAE, or are individual macrophages able to modify their polarization during the passage from the formation to the resolution of neuroinflammatory lesions? In summary: is it a population exchange or rather a phenotype switch?

3. Material and Methods

Mouse strains and genotyping

C57BL/6 mice were purchased from Janvier Labs (Saint Berthevin Cedex, France). The subsequent genetically modified mouse lines were used: *Arginase-YFP* mice (C.129S4/(B6)-Arg1^{tm1Lky}/j) (Reese et al, 2007), *CD68-GFP* mice (C57BL/6-Tg(CD68-EGFP)1Drg/j) (Iqbal et al, 2014) and *Rosa26-Stp-fl-YFP* mice (B6.Cg-Gt(Rosa)26Sor<tm3(CAG-EYFP)Hze>/J), *CCR2-RFP* mice (B6.129(Cg)-Ccr2$^{tm2.1Ifc}$/J) and *CX3CR1-GFP* mice (B6.129P-Cx3cr1^{tm1Litt}/J) were obtained from The Jackson laboratory (Bar Harbor, Maine). The *iNOS-tdTomato-cre* mouse line was obtained from Alain Bessis´ laboratory (Paris, France) (Bechade et al, Glia 2014).

The genotyping of the mice were assessed from tails DNA extraction with the following PCR pairs of primers for *iNOS-tdTomato-cre*, *cre* forward GCA TTA CCG GTC GAT GCA ACG AGT GAT GAG, *cre* reverse GAG TGA ACG AAC CTG GTC GAA ATC AGT GCG; for *Arginase-YFP* and *Rosa26-stop-fl-YFP*, *YFP* forward ATC TTC TTC AAG GAC GAC GGC AAC TAC AAG, *YFP* reverse AGA GTG ATC CCG GCG GCG GTC ACG AAC TCC; for *CD68-GFP*, *GFP* forward GCA CGA CTT CTT CAA GTC CGC CAT GCC, *GFP* reverse GCG GAT CTT GAA GTT CAC CTT GAT GCC.

For all the experiments, adult mice of minimum 6 weeks of age from both sexes were used in compliance with the animal welfare regulations and animal handling guiding principles.

Active EAE induction

Adult mice were immunized by the injection of 400µg of purified recombinant MOG (N1-125) emulsified in complete Freund's adjuvant (containing 10mg/ml heat inactivated *Mycobacterium tuberculosis* H37 Ra mixed with mineral oil, Sigma-Aldrich). In order to

elicit an immune reaction, 400ng of pertussis toxin (Sigma-Aldrich) was inoculated intraperitoneally (i.p) at day 0 and day 2 post immunization. The weight of the animals was followed daily and a score was attributed according to the neurological behavior test results as follow: EAE score 0, no clinical signs; 0.5, partial weakness of the tail; 1, tail paralysis; 1.5, gait instability or impaired righting ability; 2, hind limb paresis; 2.5, hind limb paresis with dragging of at least one foot; 3, complete flaccid hind limb paralysis; 3.5, hind limb paralysis and weakness of at least one fore limb; 4, hind limb and fore limb paralysis; 5, death. Mice were analyzed at several time points during the disease course: the first time point was the weight loss characterized by a loss of weight, onset defined as the first day of clinical symptoms, peak as 2-3 days after the onset, remission as 7 days following the apparition of the symptoms.

Bone marrow-derived macrophage culture

Arginase-YFP, *iNOS-tdTomato-cre* and C57BL/6 control mice were sacrificed with Isoflurane and the bones of the pelvis and hindlimbs were extracted (Hips, Tibia, Fibula, Femur) in order to expose the bone marrow cavity for a further bone marrow preparation. The bone marrow was flushed out with ice-cold RPMI-1640 (Sigma-Aldrich) supplemented with 10% fetal calf serum (Sigma-Aldrich), 100U/ml penicillin/streptomycin and filtered with 70µm nylon mesh cell strainers (Falcon) followed by a lysis step with Ammonium chloride ACK buffer for 5' on ice. Cells were resuspended in RPMI-1640 (Sigma-Aldrich) supplemented with 10% fetal calf serum (Sigma-Aldrich), 100U/ml Penicillin/streptomycin, 5ng/ml of macrophage colony stimulating factor (mCSF, R&D Systems) and transferred to 8-wells Nunc Lab-Tek chamber slides (Sigma-Aldrich) at a concentration of 2.5 million of cells/mL. The medium was changed every 3 days with RPMI-1640 (Sigma-Aldrich) supplemented with 10% fetal calf serum (Sigma-Aldrich), 100U/ml Penicillin/streptomycin, 5ng/ml of macrophage colony

stimulating factor (mCSF, R&D Systems) and after 7 days in culture *in vitro*, the medium was substituted for the non-polarized control by mCSF-supplemented phenol red-free RPMI-1640 (Sigma-Aldrich) medium, for the pro-inflammatory polarization with lipopolysaccharide (100ng/ml) and IFNγ (10ng/ml)-supplemented medium and for the anti-inflammatory polarization with recombinant IL-4 (10ng/ml) and IL-13 (10ng/ml)-supplemented medium.

Immunocytochemistry

After 48hrs of culture in the respective conditions (non-activation, pro-inflammatory and anti-inflammatory), bone-marrow derived macrophages were fixed with 4% paraformaldehyde (PFA) for 10' on ice and blocked for 1hr at room temperature with 10% goat serum in PBS, 0.5% Triton.

For the cells derived from the bone-marrow of *iNOS-tdTomato-cre* and C57BL/6 control mice, the following stainings were performed for 1hr in PBS 1x supplemented with 1% Goat serum and 0.5% Triton against the antigens: iNOS (ABN26, Millipore), I-A/I-E (M5/114.15.2, BD Pharmingen), p22-phox (sc-20781, Santa Cruz), and tdTomato (16D7, Kerafast) and for the cells derived from the bone-marrow of *Arginase-YFP* and C57BL/6 control mice against the antigens: iNOS (ABN26, Millipore), YM1 (01404, StemCell Technologies), CD206 (MR5D3, BioLegend) and GFP (ab13970, Abcam). Detection was assessed by the use of Alexa Fluor-coupled secondary antibodies (Life Technologies) for 1hr at room temperature in PBS 1x supplemented 1% Goat serum and 0.5% Triton. A nuclear staining using DAPI (Thermo Fisher) was performed for 10' at room temperature. Sections were mounted with Vectashield (Vector Laboratories) and coverslips fixed by nail polish.

Samples were acquired with an upright confocal microscopy system (FV1000 Olympus) equipped with 20x/0.85 oil immersion objective, zoom 3.5x and image size 1024x1024.

Images were scanned using standard filter sets, processed with Fiji for quantification and Adobe Photoshop software (Adobe) for image representation with a Despeckle filter.

The values of antibody-specific fluorescent intensities were calculated after the subtraction of the background signal and isotype control-fluorescence. YFP and tdTomato-specific fluorescent intensities were determined after subtraction of the background signal and staining intensity detected in control C57BL/6 mice.

Flow cytometry

Mice were sacrificed with Isoflurane and perfused with PBS. After CNS isolation and transfer in ice-cold PBS (Sigma-Aldrich), tissue was cut in pieces and digested for 30´ at 37°C in RPMI containing 2% fetal calf serum (Sigma-Aldrich), 25mM HEPES (Sigma-Aldrich), DNase I (10ng/ml, StemCell Technologies) and Collagenase D (0.8mg/ml, Roche). The reaction was interrupted by the addition of 0.5M EDTA 1:100 dilution (Sigma-Aldrich), filtered through 70µm nylon mesh cell strainers (Falcon) and resuspended in a 30% solution of Percoll (Sigma-Aldrich). The suspension was centrifuged for 30´ with a gradient of 10.800 r.p.m. and after the removal of the top (myelin) and lower (red cells) layers, the remaining solution was filtered through 70µm nylon mesh cell strainers (Falcon).

For analysis of cell populations from the blood: blood collection was performed from the heart or the submandibular vein in heparin-coated tubes followed by erythrocytes removal with an incubation for 10’ on ice with FACS Lysing solution (BD Biosciences).

For analysis of cell populations in the lymph nodes: inguinal and axillary lymph nodes were isolated, dissociated in ice-cold PBS (Sigma-Aldrich) using glass slides and filtered through 70µm nylon mesh cell strainers (Falcon).

After Fc-receptor blockade (CD16/32, 1µl/million cells, clone 2.4G2, BD Biosciences) and using LIVE/DEAD staining (Invitrogen), the following stainings were performed in ice-cold PBS: CD45 (clone 30-F11, BioLegend), CD11b (clone M1/70, BD Biosciences), CD11c (clone N418, Abcam), F4/80 (clone BM8, eBiosciences), Ly6C (clone AL21, BD Biosciences), Ly6G (clone 1A8, Biolegend). Samples were acquired on a LSR-Fortessa cytometer (BD Biosciences) and results analyzed with FlowJo software.

RNA sequencing analysis

The following experiments were performed by Marta Joana Costa Jordão and analyzed by Ori Staszewski and Dr. Giuseppe Locatelli as follows:

Cells were isolated from the CNS of *iNOS-tdTomato-cre* x *Arginase-YFP* mice as described above, co-stained with LIVE/DEAD (eBioscience), CD45 (clone 30-F11, eBioscience), CD11b (clone M1/70, eBioscience), CD64 (clone X54-5/7.1, BD), and sorted through a FACS Aria III (Becton Dickinson) based on the YFP and tdTomato fluorescent reporter proteins expressions. Extraction of total RNA was performed from cells stabilized in RNAprotect buffer using the RNeasy Plus Micro Kit protocol (QIAGEN). Cells were stocked and shipped in RNAprotect buffer at 2-8°C. After pellet formation, the RNAprotect buffer was replaced by RLT Plus. The samples were homogenized by vortexing for 30" and gDNA Eliminator spin columns were used to remove Genomic DNA contamination. After application of ethanol, the samples were applied to RNeasy MinElute spin columns followed by subsequent washing steps. Total RNA was eluted in 12µl of nuclease-free water and purity was assessed on the Agilent 2100 Bioanalyzer with the RNA 6000 Pico LabChip reagent set (Agilent). In order to generate first strand cDNA from 100-500pg total RNA, the SMARTer Ultra Low Input RNA Kit for Sequencing v4 (Clontech Laboratories, Inc.) was used and double stranded cDNA was amplified by LD PCR (13 or 14 cycles) and purified via magnetic

beads. Library was prepared as described in the Illumina Nextera XT Sample Preparation Guide (Illumina, Inc.) and 150pg of input cDNA were tagged and separated by the Nextera XT transposome. In order to generate the multiplexed sequencing libraries, products were purified and amplified via a limited-cycle PCR program (PCR step 1:5 dilutions of index 1 (i7) and index 2 (i5) primers were used). The libraries were quantified using the KAPA SYBR FAST ABI Prism Library Quantification Kit (Kapa Biosystems, Inc.). Equal molar amounts of each library were combined and used for cluster generation on the cBot with the Illumina TruSeq SR Cluster Kit v3. The sequencing was accomplished on a HiSeq 1000 using the indexed, 50 cycles single-read (SR) protocol and the TruSeq SBS v3 reagents. Image analysis and base calling produced .bcl files that were converted into .fastq files using the software CASAVA1.8.2. Isolation of the RNA, preparation of the library and RNAseq were performed at the Genomics Core Facility "KFB - Center of Excellence for Fluorescent Bioanalytics" (University of Regensburg, Regensburg, Germany). Fastq files were quality controlled using FastQC and reads were mapped to the GRCm38 mouse genome using the Star aligner (Dobin et al, 2013). Read counts were acquired by the featureCounts package and the analysis of differential gene expression was achieved using the limma/voom pipeline in R (Ritchie et al, 2015). Statistically-significant differentially expressed genes were defined using a cutoff of $\log_2(|\text{fold-change}|)$ and adjusted p-value <0.05 following the suggestions by the SEQC consortium. PCA analysis was performed using the prcomp package within the R stats library. VennDiagrams were created using the R library VennDiagram.

Immunohistochemistry and *in situ* confocal microscopy

Mice were sacrificed with Isoflurane and perfused transcardially with PBS-Heparine 1:1000 followed by 4% of PFA. Dissection of the CNS was followed by a 12hrs post fixation with

4% PFA, cryo-protected with PBS1x supplemented with 30% Sucrose (Sigma-Aldrich), embedded in Tissue-Tek (Sakura Finetek Europe B.V.) and frozen at -20°C.

Tissue sections were cut sagitally with a thickness of 30-50µm using a Leica cryostat. A pre-treatment of the sections was performed using antigen retrieval in a sodium citrate buffer (pH 8.5) for 30' at 85°C, followed by a blocking for 30´ in PBS supplemented with 10% goat serum, 0.1% Triton and stained overnight at 4°C in PBS supplemented with 2% Goat serum, 0.1% Triton against the following antigens: iNOS (ABN26, Millipore), arginase-1 (sc-20150, Santa Cruz), tdTomato (16D7, Kerafast), GFP (ab13970, Abcam), Iba-1 (019-19741, Wako), Olig2 (AB9610, Chemicon International), GFAP (G9269, Sigma-Aldrich) and CD3 (CD3-12, Serotec). Detection was assessed by incubation with Alexa Fluor-coupled secondary antibodies (Life Technologies/Abcam) for 3hrs at room temperature in PBS supplemented with 2% Goat serum and 0.1% Triton.

For the Iba-1 immunohistochemistry performed at steady-state, sections were blocked for 1hr with PBS supplemented with 10% Goat serum, 0.5% Triton; incubated overnight at 4°C with Iba-1-specific antibody (019-19741, Wako) in PBS supplemented with 1% Goat serum, 0.5% Triton and detection was assessed by the incubation for 3hrs at room temperature with Alexa Fluor 647-coupled secondary antibody (Life Technologies) in PBS supplemented with 1% Goat serum 0.5% Triton.

For the laminin immunostaining, sections were blocked for 1hr with 10% Goat serum and 0.4% Triton in 0.1M PB solution, incubated overnight at 4°C with a laminin-specific antibody (ab11575, Abcam) in 0.1M PB supplemented with 5% Goat serum and 0.4% Triton and detection was assessed by the incubation for 2hrs at room temperature with a Alexa Fluor 647-coupled secondary antibody (Life Technologies) in 0.1M PB supplemented with 5% Goat serum 0.4% Triton.

A nuclear staining using DAPI (Thermo Fisher) was performed for 10' at room temperature. Sections were mounted with Vectashield (Vector Laboratories) and coverslips fixed by nail polish.

Samples were acquired with an upright confocal microscopy system (FV1000 Olympus) equipped with 10x/0.4 air, 20x/0.85 and 60x/1.42 oil immersion objectives. Images were scanned using standard filter sets, processed with Fiji software for quantification and Adobe Photoshop software (Adobe) for image representation with a Despeckle filter. For laminin-specific staining, Iba-1 staining performed at steady state and stainings from *iNOS-tdTomato-cre x Rosa26-Stp-fl-YFP* mice; pictures have been processed with a Dust and scratches filter.

Quantitative analysis of *in situ* images

Co-localization of tdTomato and YFP reporter proteins with the cell-type markers Iba-1, CD3, Olig2, GFAP was visually determined in *iNOS-tdTomato-cre* and *Arginase-YFP* single transgenic mice perfused at peak of EAE. Co-localization of tdTomato and YFP reporter proteins with iNOS- and arginase-1-immunoreactivity was determined in *iNOS-tdTomato-cre* and *Arginase-YFP* mice single transgenics as follows. Control C57BL/6 sections were used to assess the background of tdTomato and YFP intensities. After background correction, cells with tdTomato and YFP intensities higher than the signal detected in C57BL/6 control (average fluorescent intensity + 3 standard deviations) were included in the analysis. A rabbit isotype control was used to determine the background of iNOS and Arginase antibodies. Among tdTomato and YFP positive cells, background-corrected iNOS- and arginase-1-intensities were measured and considered positive if their intensities were higher than the signal detected in isotype control from the same mice (average fluorescent intensity + 3 standard deviations).

To determine the relative proportion of M^{iNOS}, $M^{iNOS/Arginase}$ and $M^{Arginase}$ cells over the EAE course, intensities of background-corrected tdTomato and YFP reporter proteins were measured in *iNOS-tdTomato-cre* x *Arginase-YFP* mice (Experiment performed by Dr. Giuseppe Locatelli).

The signals from tdTomato and YFP intensities were considered positive if higher than the respective signal (average fluorescent intensity + 3 standard deviation) detected in *Arginase-YFP* (for tdTomato signals) and *iNOS-tdTomato-cre* (for YFP signals) single transgenic mice at the same time point of EAE (n=5 mice per group). To determine the polarization of mononuclear phagocytes over the disease course, we calculated the ratio of YFP/tdTomato intensities. When the ratio was higher than 5, cells were categorized as $M^{Arginase}$ and when the ratio was less than 0.2, cells were classified as M^{iNOS}. Cells that had ratios between these values were classified as $M^{iNOS/Arginase}$.

To assess the proportion of polarized phagocytes over the disease course, we stained the sections with the phagocyte marker Iba-1 in *iNOS-tdTomato-cre* x *Arginase-YFP*. In an EAE lesion, the identification of Iba-1^+ cells was visually assessed and the intensities of tdTomato and YFP were measured in these cells as described previously. Non-polarized cell were considered to have both tdTomato and YFP intensities below the respective signals (average + 3 standard deviations) detected in *Arginase-YFP* (for tdTomato signals) and *iNOS-tdTomato-cre* (for YFP signals) mice at the same EAE time point (n=5 or 6 *iNOS-tdTomato* x *Arginase-YFP* mice and n=3 for single transgenics at each timepoint).

To evaluate the spatial distribution of polarized cells in EAE lesions at disease onset, cell intensities were measured for YFP and tdTomato in *iNOS-tdTomato-cre* x *Arginase-YFP* mice as described above. A squared grid of 400μm^2 was overlayed on the acquired image of EAE lesions using Fiji software and the proportion of M^{iNOS}, $M^{iNOS/Arginase}$ and $M^{Arginase}$ cells was calculated per square. Single squares were gathered to form combined structured in order to

analyze either joined bands starting from the pial surface, concentric squares starting from the core of the lesion and parallel bands starting from the main vessel (counterstained with Laminin) in EAE lesions.

Fate tracking experiment of mononuclear phagocytes expressing arginase-1 was realized in *iNOS-tdTomato-cre x Rosa26-Stp-fl-YFP* mice at peak of EAE as the following: The backgrounds of tdTomato and YFP intensities and arginase-1 antibody were background-subtracted. The intensities of tdTomato and YFP were considered positive if higher than the respective signal (average + 3 standard deviation) detected in *Rosa26-Stp-fl-YFP* control mice at the same EAE time point. Arginase-1 co-staining was evaluated positive if its fluorescence intensity was higher than the signal detected in its rabbit isotype-control from EAE lesions of the same mice (average + 3 standard deviations).

In vivo imaging method, processing and quantifications

Mice were anesthetized with ketamine (87mg/kg), xylazine (13mg/kg) and placed on a heating pad for 15'. Tracheotomy and intubation were achieved in order to decrease breathing artifacts. A laminectomy was performed to expose the dorsal spinal cord superfused with artificial cerebrospinal fluid and clamped as previously described (Nikic, et al, 2011). Images were acquired with an Olympus FV1200 MPE microscope equipped with a 25×/1.25 water immersion objective (Olympus), using 488nm and 568nm single-photon excitation, zoom 1x-1.4x, step size 1.9-2.2µm and image sizes of 800x800-1024x1024 pixels. The vasculature was revealed by i.p. injection of 200µg of Dextran-AF647 (Life Technologies). For image representation, pictures have been gamma-adjusted and processed with a Dust and scratches filter using Photoshop (Adobe).

The expression of tdTomato and YFP was visually assessed based on the fluorescence intensities in the 488nm and 568nm channels in *iNOS-tdTomato-cre* x *Arginase-YFP* mice to determine the different mononuclear phagocyte polarization phenotypes (Experiment performed by Dr Giuseppe Locatelli). Cells expressing a detectable intensity amount in both 488nm and 568nm channels corresponding to YFP and tdTomato respectively were categorized as $M^{iNOS/Arginase}$.

To determine the proportion of polarized cells in *iNOS-tdTomato-cre* x *Arginase-YFP* mice in the different CNS microenvironments (Experiment performed by Dr Giuseppe Locatelli), EAE lesions were initially imaged starting from the dural surface. Lesion volume was re-acquired following the surgical removal of the upper meninges as previously described (Romanelli et al, 2013). The location of the cells was assessed as follow: Upper meninges if the cells were located in the upper part of the image stack present before and absent after dura removal; pia/parenchyma interface or in the parenchymal compartment based on their relative depth from the upper pia surface (assessment following dura mater removal). The top 2 cell layers from the pia layer (i.e. up to ~10µm from the tissue surface of the tissue) were assessed to be at the interface of pia/parenchyma, while all polarized cells below the 3rd cellular layer from the tissue surface were judged to belong to the parenchymal compartment.

For timelapse *in vivo* imaging of *iNOS-tdTomato-cre* x *Arginase-YFP* mice (Experiment performed by Dr Giuseppe Locatelli), spinal cord EAE lesions were acquired for 6hrs with an interval of 2hrs. Over the 6hrs imaging, single cells could be followed based on their morphology, their location and the pattern of polarization of adjacent cells. Mononuclear phagocytes phenotypes were assessed *in vivo* for all time point as described above. In order to confirm the visual assessment of phenotype switching, we quantified the YFP fluorescence intensity (after background-subtraction) at 0 and 6hrs in M^{iNOS} changing cells compared to M^{iNOS} cells that did not undergo a phenotype switch over time and that were laying at a comparable tissue depth. Localization of polarized cells switching their phenotype in the

upper meninges, pia/parenchyma or parenchyma was determined based on respective cells positions in the stack and in relation to reflectance of dura and pia mater.

For the *in vivo* bleaching experiment in *iNOS-tdTomato-cre* x *Arginase-YFP* mice (Experiment performed by Dr. Giuseppe Locatelli), spinal EAE lesions were first imaged with a low magnification (1.3x). Bleaching of the fluorescence signal was achieved by exposing the center of the lesion area (higher magnification, 4.3x, Kalman filter=2) to 80% (488nm) and 50% (568nm) laser power. Promptly after bleaching the tdTomato and YFP fluorescence intensity, the entire lesion area was re-acquired ("bleached" image, magnification 1.3x) and after 5hrs. The intensity of the tdTomato and YFP fluorescence signal in polarized cells was background-subtracted and quantified before bleaching, after bleaching and after 5hrs, both in the bleached area and in the surrounding non-affected tissue. The iNOS and arginase-1 promoters were evaluated active if the tdTomato and YFP fluorescence (respectively) were increased by at least 30% in comparison to the average fluorescent change in unbleached cells in the same time frame at 5hrs compared to the immediate values post-bleaching.

For time-lapse *in vivo* imaging of *iNOS-tdTomato-cre* x *CD68-GFP* mice at onset of EAE, an injection of Dextran-AF647 revealed the vasculature (as described previously). Spinal cord lesions imaging were performed during 6hrs with a 3hr intervals. The assessment of the proportions of GFP^+ mononuclear phagocytes expressing tdTomato was attributed visually at the initial imaging timepoint. Cell localization in upper meninges, pia/parenchyma, perivascular, vascular or parenchyma was based visually on the cell position in the stack, the cell position relative to the vasculature and the tissue reflectance. In order to detect the polarization of GFP+ cells that lack tdTomato fluorescence signal at 0hr and that became GFP^+M^{iNOS} over the 6hrs, the tdTomato signal was visually assessed.

Statistical analysis

Data sets were analyzed using 1-way ANOVA followed by Bonferroni's multiple comparison tests. Statistical analyses were performed with GraphPad Prism software.

4. Results

Characterization of *iNOS-tdTomato-cre* and *Arginase YFP* mouse lines

To follow the plasticity of mononuclear phagocytes phenotype from the formation to the resolution of neuroinflammatory lesions over the course of EAE, we used two transgenic mouse lines, *iNOS-tdTomato-cre* and *Arginase-YFP* mice to study the expression of iNOS and arginase-1 signatures enzymes, respectively. As previously mentioned, iNOS and arginase-1 enzymes are competing for the same substrate, the essential amino-acid L-arginine and are in consequence suitable markers to investigate the pro- and anti-inflammatory polarization states of phagocytes. Both *iNOS-tdTomato-cre* and *Arginase-YFP* mouse lines carry in their genetic construction a fluorescent reporter protein under the control of iNOS or arginase-1, respectively. While the *iNOS-tdTomato-cre* mouse line (Bechade et al, 2014) expresses under iNOS promoter the tdTomato red fluorescent protein together with a Cre recombinase, the *Arginase-YFP* mouse line (Reese et al, 2007) expresses the yellow fluorescent protein (YFP) under the arginase-1 promoter.

First, we wanted to confirm that both single-transgenic mouse lines actually expressed the reporter proteins under defined conditions. We thus isolated bone marrow-derived macrophages from both *iNOS-tdTomato-cre* and *Arginase-YFP* mice. The cells were cultured *in vitro* under several conditions with mCSF for 48hrs as follow: non-activation (Ø), medium supplemented with LPS and IFNγ to induce a pro-inflammatory (M1) phenotype and medium supplemented with IL-4 and IL-13 to induce an anti inflammatory (M2) phenotype. We found that tdTomato expression was specifically induced under pro-inflammatory conditions (**Figure 7a**) and correlated with the expression of other pro-inflammatory markers such as iNOS, MHC-II and p22phox in *iNOS-tdTomato-cre mice* (**Figure 7b**, n=5 mice, number of cells analyzed for tdTomato: MØ=1,381, M(LPS+IFNγ)=2,082, M(IL4+IL13)=1,415; for

MHC-II: MØ=822 M(LPS+IFNγ)=451, M(IL4+IL13)=607; for iNOS: MØ=639, M(LPS+IFNγ)=1,154, M(IL4+IL13)=583; for p22phox: MØ=742, M(LPS+IFNγ)=928, M(IL4+IL13)=832. ***, P<0.0001, 1-way-Anova with Bonferroni post-hoc correction).

Conversely, YFP expression was selectively induced under anti-inflammatory conditions (**Figure 8a**) and associated with the expression of other anti-inflammatory markers such as YM1 and CD206 in *Arginase-YFP* mice (**Figure 8b**, n=5 mice, number of cells analyzed for YFP: MØ=948, M(LPS+IFNγ)=702, M(IL4+IL13)=1,141; for YM1: MØ=203, M(LPS+IFNγ)=176, M(IL4+IL13)=342; for iNOS: MØ=237, M(LPS+IFNγ)=236, M(IL4+IL13)=241; for CD206: MØ=280, M(LPS+IFNγ)=129, M(IL4+IL13)=309. ***, P<0.0001, 1-way-Anova with Bonferroni post-hoc correction).

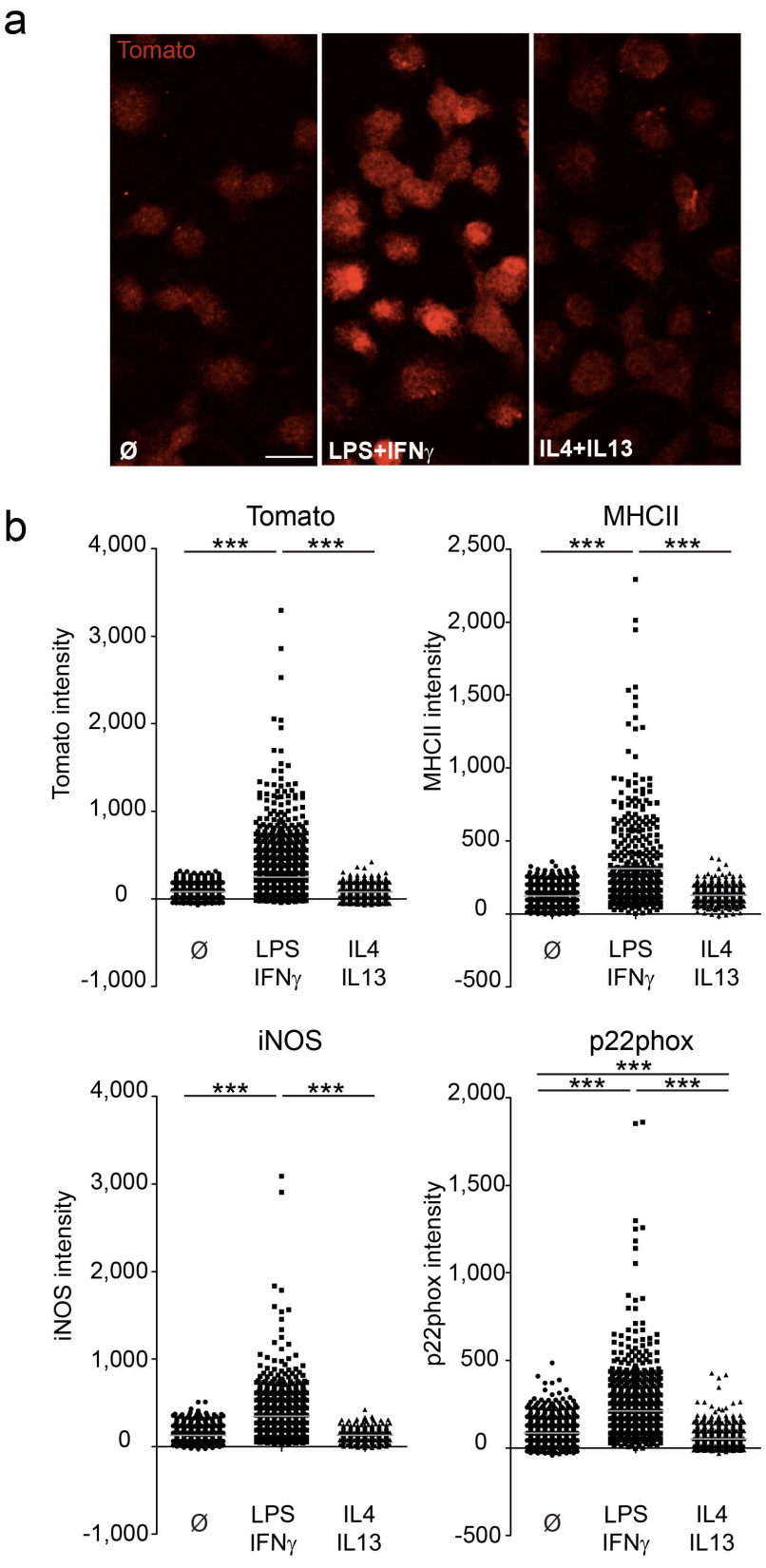

Figure 7: Bone marrow-derived macrophages culture *in vitro* isolated from *iNOS-tdTomato-cre* mice.

Figure 7: Bone marrow-derived macrophages culture *in vitro* isolated from *iNOS-tdTomato-cre* mice.

Culture for 48hrs with mCSF: (Ø), LPS+IFNγ or IL4+IL13, n=5 mice. (a) Confocal images of tdTomato expression (red) revealed by immunohistochemistry. (b) quantifications of fluoresence intensity signals from tdTomato-, MHCII-, iNOS- and p22phox- revealed by immunohistochemistry. Scale bar, 20µm. ***, P<0.0001, 1-way-Anova with Bonferroni post-hoc correction. ***Figure from Locatelli, Theodorou et al, submitted in Nature Neuroscience.***

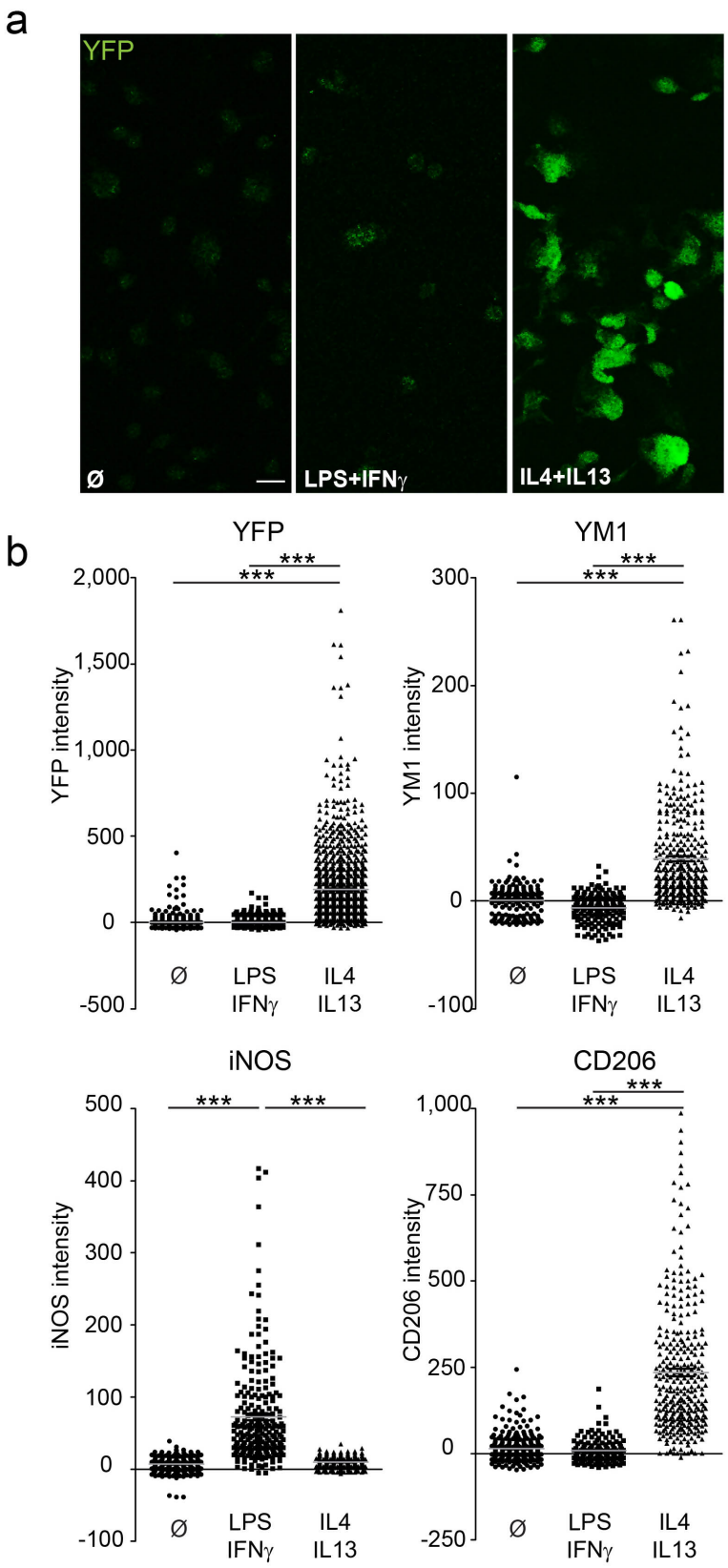

Figure 8: Bone marrow-derived macrophages culture *in vitro* isolated from *Arginase-YFP* mice.

Figure 8: Bone marrow-derived macrophages culture *in vitro* isolated from *Arginase-YFP* mice.

Culture for 48hrs with mCSF: (Ø), LPS+IFNγ or IL4+IL13, n=5 mice. (a) Confocal images of YFP expression (green) revealed by immunohistochemistry. (b) quantifications of fluoresence signals from YFP-, YM1-, iNOS- and CD206-, revealed by immunohistochemistry. Scale bar, 20µm. ***, P<0.0001, 1-way-Anova with Bonferroni post-hoc correction. ***Figure from Locatelli, Theodorou et al, submitted in Nature Neuroscience.***

Absence of iNOS/arginase-1 expression in the healthy spinal cord

Then, we wanted to determine whether such reporter protein expression could be detected under homeostatic conditions in transgenic mice using several approaches: *in vivo* imaging, confocal microscopy and flow cytometry. We first generated double transgenic *iNOS-tdTomato-cre x Arginase-YFP* reporter mice by crossing single transgenic mice. In the resulting mouse line, we could not detect any reporter protein expressions in the CNS in the steady state either by means of *in vivo* spinal imaging with the vasculature revealed by injection of Dextran (Experiment performed by Dr Giuseppe Locatelli, **Figure 9a**), by using fixed tissue sections co-stained with a phagocytic marker Iba-1 and imaged with confocal microscopy (**Figure 9b,** n=3 mice) and finally by flow-cytometric analysis of CNS-isolated mononuclear phagocytes ($CD45^{int}$ $CD11b^{high}$) (**Figure 9c**, average percentage of polarized cells (± s.e.m.) was 0.27 ± 0.1 for M^{iNOS}, 0.0 for $M^{Arginase}$ and 0.0 for $M^{iNOS/Arginase}$ cells, n=4 mice).

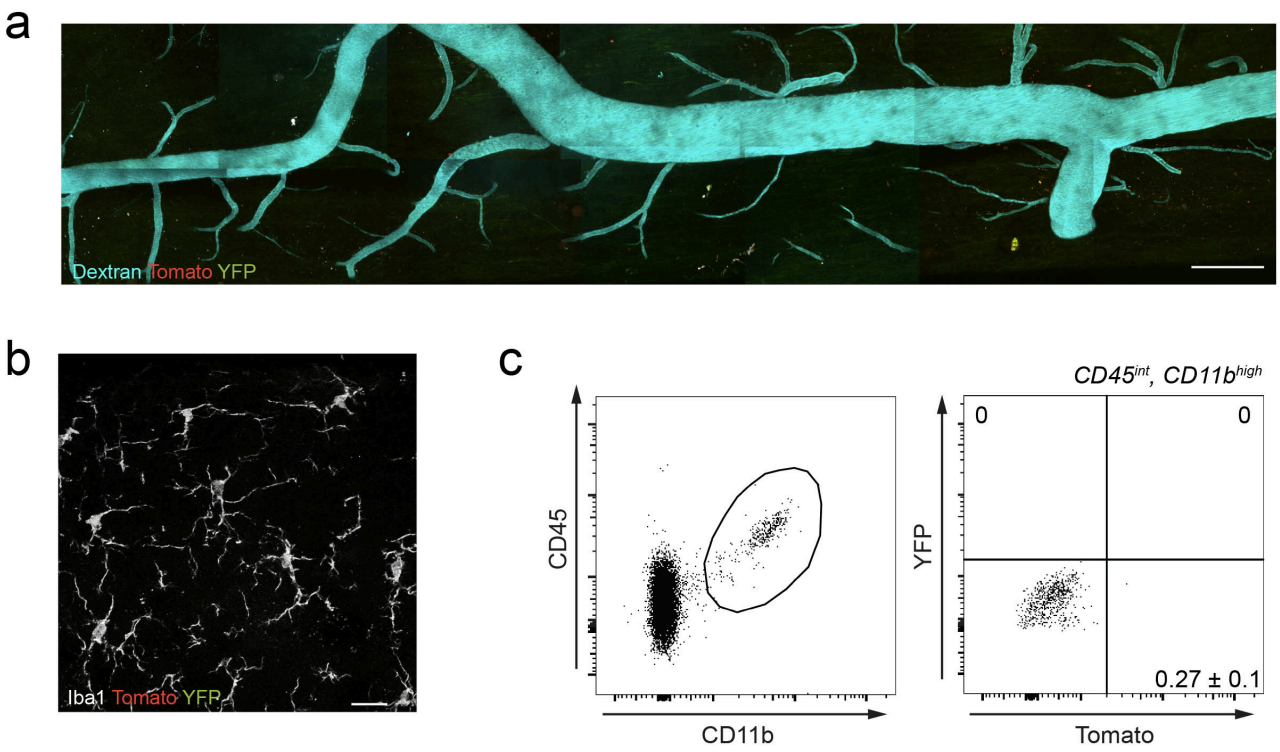

Figure 9: Absence of iNOS and arginase-1 expression under homeostasis in the CNS of *iNOS-tdTomato-cre x Arginase-YFP* mouse.

(a) Acquisitions from *in vivo* imaging of the spinal cord of *iNOS-tdTomato-cre x Arginase-YFP* mouse during homeostasis (tdTomato in red; YFP in green; vasculature revealed by Dextran-AF647 injection in cyan). (b) Confocal image of the spinal cord of *iNOS-tdTomato-cre x Arginase-YFP* mouse during homeostasis (tdTomato in red; YFP in green; Iba-1-immunostaining in gray). Scale bar, 20µm. (c) Flow cytometric analysis of cells isolated from the CNS of *iNOS-tdTomato x Arginase-YFP* mice during homeostasis and gated on $CD45^{int}$ $CD11b^{high}$. ***Figure from Locatelli, Theodorou et al, submitted in Nature Neuroscience.***

In situ colocalization of iNOS and arginase-1 with a phagocyte marker in the CNS

To study the role of activated phagocytes in the context of neuroinflammation, active EAE was induced in *iNOS-tdTomato-cre* x *Arginase-YFP* mice by immunization with recombinant MOG. This triggered the presence of fluorescently labeled cells in the CNS. In both single transgenic *iNOS-tdTomato-cre* and *Arginase-YFP* mice, more than 90% of the fluorescently labeled cells co-stained with a macrophage/microglia marker Iba-1 (Average percentage of colocalization between tdTomato and Iba-1 was 93.7 ± 2.5 s.e.m. and between YFP and Iba-1 was 95.3 ± 1.5 s.e.m. (For the analysis of tdTomato and Iba-1: n=3 mice and 447 cells analyzed; for the analysis of YFP and Iba-1: n=3 mice and 601 cells analyzed). No colocalization of fluorescent cells with CD3, Olig2, Glial fibrillary acidic protein (GFAP) representing T cells, oligodendrocytes and astrocytes respectively, was observed in the spinal cord at peak of EAE (**Figure 10**).

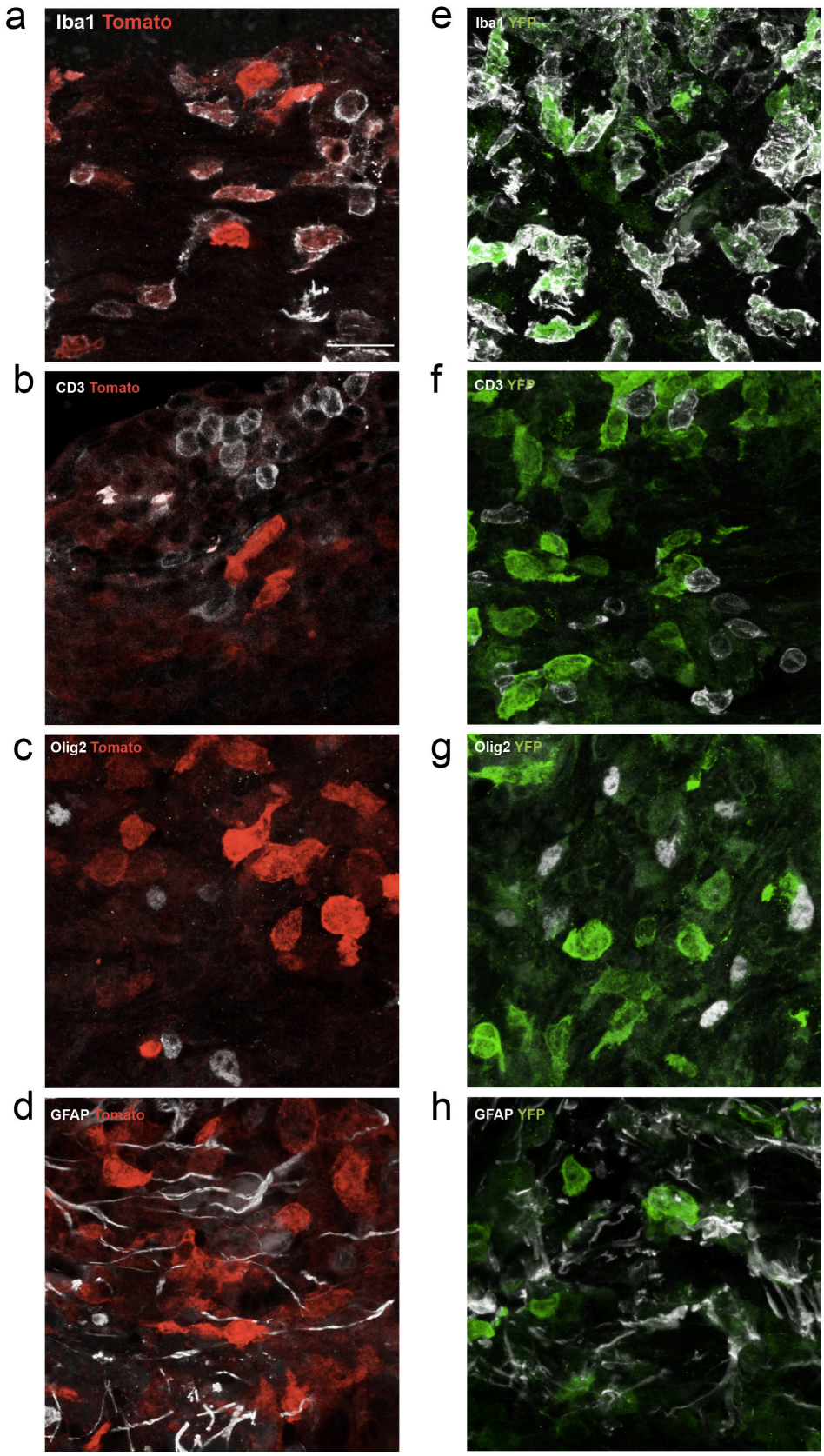

Figure 10: *In situ* colocalization of tdTomato and YFP reporter proteins with cellular markers in the CNS.

Figure 10: *In situ* colocalization of tdTomato and YFP reporter proteins with cellular markers in the CNS.

(a-d) Confocal images of spinal lesions in *iNOS-tdTomato-cre* mouse perfused at peak of EAE (tdTomato in red); (e-h) confocal images of spinal lesions in *Arginase-YFP* mice perfused at peak of EAE (YFP in green); (a-h) co-staining with phagocytes (**a**,**e**; Iba-1, gray), T cells (**b**,**f**; CD3, gray), oligodendrocytes (**c**,**g**; Olig2, gray) and astrocytes (**d**,**h**; GFAP, gray). Scale bar 20µm. ***Figure derived from Locatelli, Theodorou et al, submitted in Nature Neuroscience.***

In situ colocalization of iNOS/arginase-1 with reporter proteins in the CNS

Next, we confirmed that tdTomato fluorescent signal in *iNOS-tdTomato-cre* mice was associated with the expression of iNOS detected by immunohistochemistry at weight loss (**Figure 11a**). Indeed 98.6 ± 1.2% of tdTomato$^+$ cells were co-stained with iNOS at this timepoint (Average ± s.e.m.; n=5 mice and 732 cells analyzed) (**Figure 11b**); while the YFP fluorescent signal in *Arginase-YFP* mice was correlated with the expression of arginase-1 by immunohistochemistry (**Figure 11a**) with 99.8 ± 0.2% of YFP$^+$ cells that were also arginase-1$^+$ (Average ± s.e.m.; n=5 mice and 658 cells analyzed at the remission stage) (**Figure 11b**).

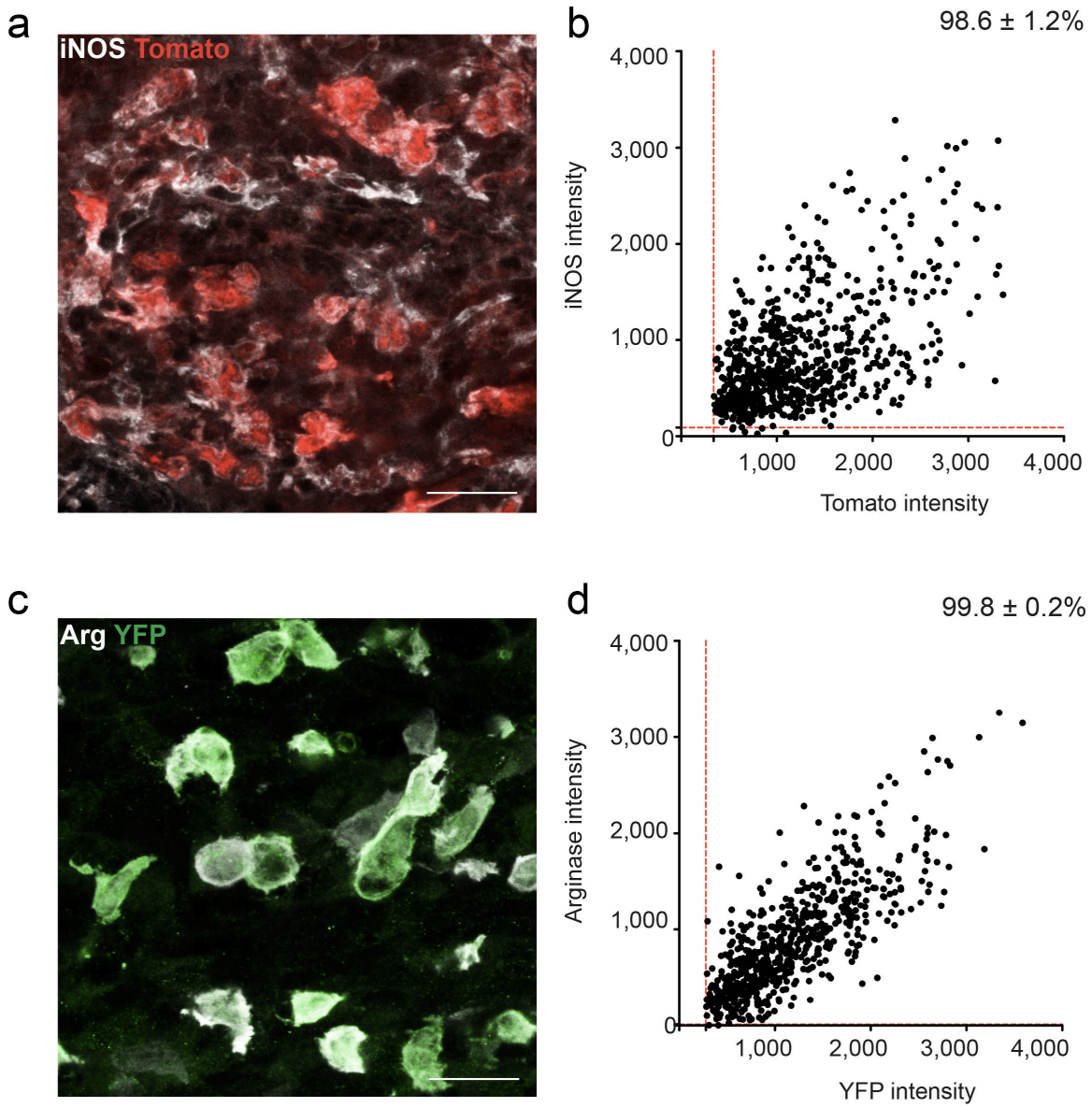

Figure 11: *In situ* colocalization of iNOS and arginase-1 with the respective reporter proteins in the CNS.

(a) Confocal image of a spinal cord lesion in *iNOS-tdTomato-cre* mouse at weight loss (tdTomato in red; iNOS in gray). Scale bar, 20µm. (b) tdTomato- and iNOS-fluorescence intensities were analyzed in cells located in spinal lesions of *iNOS-tdTomato-cre* mice at EAE weight loss. iNOS was expressed in 98.6 ± 1.2% of tdTomato^{+} cells (average ± s.e.m.; n=5 mice and 732 cells analyzed). (c) Confocal image of a spinal cord lesion in *Arginase-YFP*

mouse at remission (YFP in green; arginase-1 in gray). Scale bar, 20μm. (d) YFP- and arginase-1-fluorescence intensities were analyzed in cells located in spinal lesions of *Arginase-YFP* mice at remission. Arginase-1 was expressed in 99.8 ± 0.2% of YFP^+ cells (average ± s.e.m.; n=5 mice and 658 cells analyzed). ***Figure from Locatelli, Theodorou et al, submitted in Nature Neuroscience.***

Determination of the proportion of resident cells expressing iNOS and arginase-1 signature enzymes

Besides, during neuroinflammation, activated phagocytes can derive either by the activation of resident microglia or by the invasion of activated macrophages/microglia. Thus, we wanted to provide an estimate of the relative contribution of resident microglia to the mononuclear phagocytes expressing iNOS and arginase-1 signature enzymes. We therefore used the *CCR2-RFP* mouse line crossed with *CX_3CR1-GFP* transgenic mouse line to distinguish monocyte-derived ($CCR2^{high}$ CX_3CR1^{low}) and microglia-derived ($CCR2^{low}$ CX_3CR1^{high}) phagocytes, as depicted in the overview of the **figure 12**.

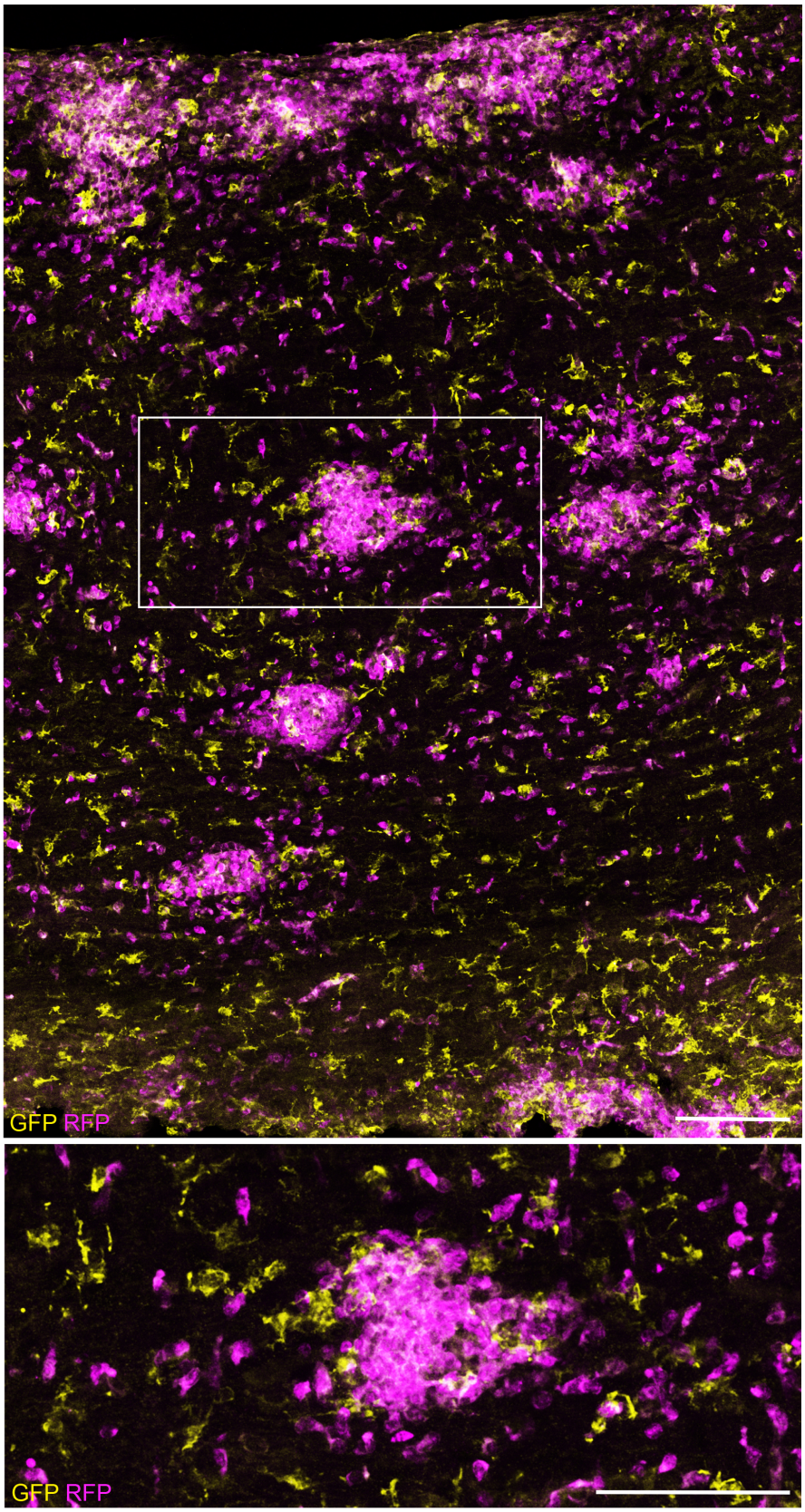

Figure 12: Overview of spinal lesions in *CCR2-RFP x CX$_3$CR1-GFP* transgenic mouse peak of EAE

Figure 12: Overview of spinal lesions in *CCR2-RFP x CX$_3$CR1-GFP* transgenic mouse peak of EAE

Confocal images representing spinal cord lesions overview (upper panel, GFP in yellow, RFP in magenta) and magnified inset depicting one lesion (lower panel) in *CCR2-RFP x CX$_3$CR1-GFP* transgenic mouse line perfused at peak of EAE. Scale bars 100µm.

By achieving an iNOS and arginase-1 immunostaining at peak of EAE, we could assess the proportion of resident microglia cells in spinal lesions expressing these pro- and anti-inflammatory enzymes respectively. Our data showed that more than 90% of the cells present in a spinal lesion of *CCR2-RFP* x *CX$_3$CR1-GFP* at peak of EAE are derived from invading monocytes (n=4 mice, for the iNOS co-staining: 448 cells analyzed with 8.2 ± 2.1% of resident cells and 91.8 ± 2.1% of invading cells; for the arginase-1 co-staining: 516 cells analyzed with 2.1 ± 0.5% of resident cells and 97.9 ± 0.5% of invading cells) (**Figure 13**).

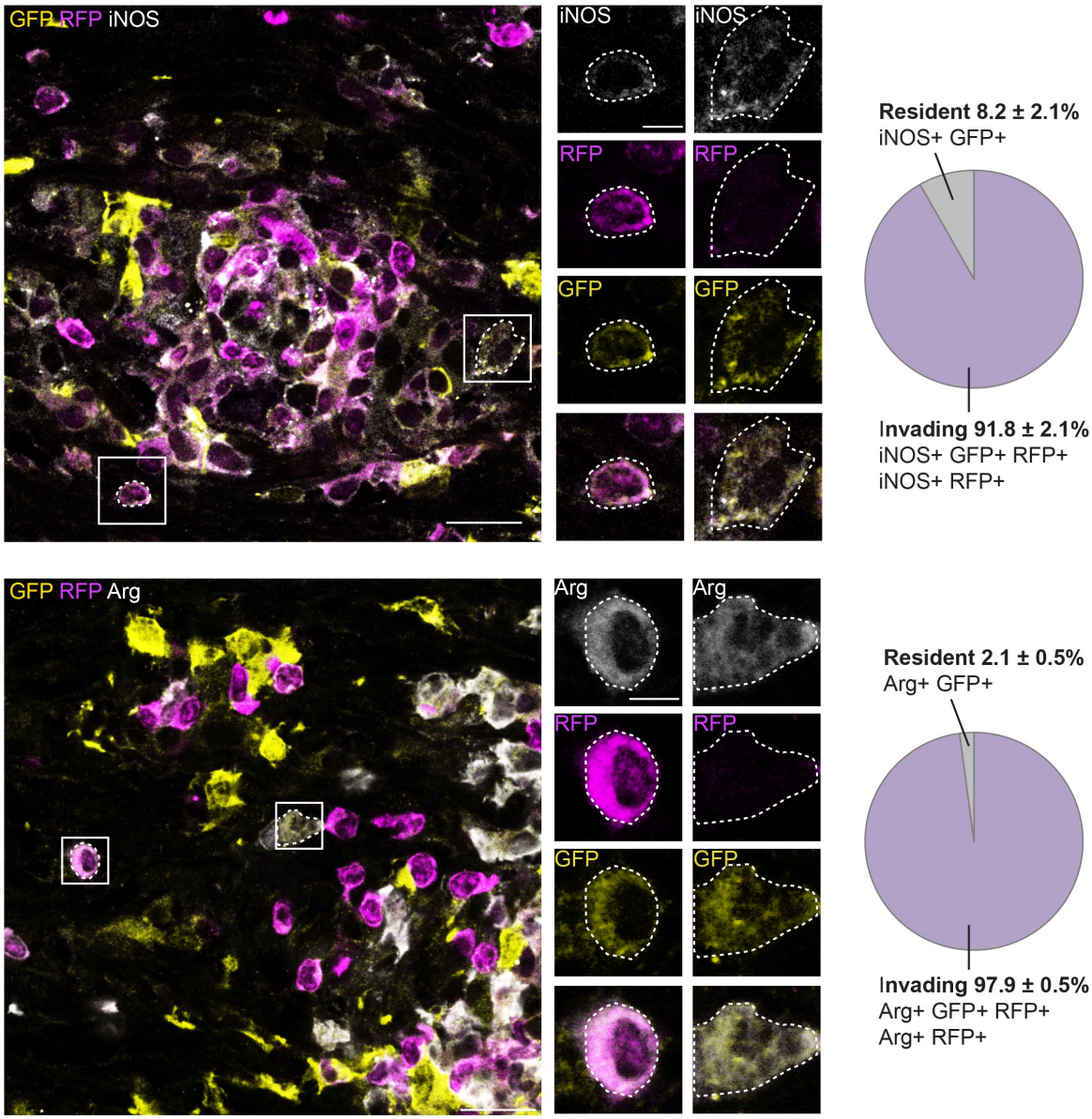

Figure 13: Proportion of resident versus invading cells in *CCR2-RFP x CX$_3$CR1-GFP* mouse line at peak of EAE.

(a) Confocal image of a spinal lesion in *CCR2-RFP x CX$_3$CR1-GFP* transgenic mouse line perfused at peak of EAE (GFP in yellow, RFP in magenta, iNOS co-staining in gray). Scale bar 20µm. Magnified insets represent on the right column a resident cell ($iNOS^+GFP^+$) and on the left column, an invading cell ($iNOS^+$ RFP^+ GFP^+), scale bar 5µm. Quantitative analysis of the proportion of resident cells ($iNOS^+GFP^+$) and invading cells ($iNOS^+$ RFP^+ GFP^+ and

iNOS^{+} RFP^{+}) in spinal lesions of *CCR2-RFP x CX$_3$CR1-GFP* mice, perfused at peak of EAE. Data are shown as average expression ± s.e.m.

(b) Confocal images of spinal lesion in *CCR2-RFP x CX$_3$CR1-GFP* transgenic mouse line perfused at peak of EAE (GFP in yellow, RFP in magenta, arginase co-staining in gray). Scale bar 20µm. Magnified insets represent on the right column, a resident cell (Arginase^{+}GFP^{+}) and on the left column, an invading cell (Arginase^{+} RFP^{+} GFP^{+}), scale bar 5µm. Quantitative analysis of the proportion of resident cells (Arg^{+}GFP^{+}) and invading cells (Arg^{+} RFP^{+} GFP^{+} and Arg^{+} RFP^{+}) in spinal lesions of *CCR2-RFP x CX$_3$CR1-GFP* mice, perfused at peak of EAE. Data are shown as average expression ± s.e.m.

The progression of reporter protein expression correlates with the pro- and anti-inflammatory phagocyte phenotypes

After validation of the single transgenic mice, we performed an EAE time course experiment in double transgenic *iNOS-tdTomato-cre* x *Arginase-YFP* mice to analyze neuroinflammatory lesions. We noticed the presence of several phagocytes populations: M^{iNOS} expressing tdTomato only, M^{Arginase} expressing YFP only and M^{iNOS}M^{Arginase} cells expressing both fluorescent reporter proteins (**Figure 14a**). The time points chosen for analysis were: weight loss, clinical onset, peak (2-3 days after onset) and remission (7 days after EAE onset).

We measured the fluorescence intensity of both tdTomato and YFP signals over the EAE time course and quantified the relative proportion of YFP vs. tdTomato expression. This analysis revealed that M^{iNOS} phagocytic cells dominated early lesions (i.e. weight loss), whereas M^{Arginase} prevailed at a later time point including remission (Analysis performed by Dr. Giuseppe Locatelli, **Figure 14b**). We could likewise observe a large proportion of macrophages expressing both markers over the entire course of the disease suggesting the

presence of intermediary phenotypes and the existence of a rather continuous phagocyte phenotype spectrum. In addition, the proportion of M^{iNOS} phagocytic cells decreased over the EAE course while the proportion of $M^{Arginase}$ became predominant towards the resolution of neuroinflammatory lesions (**Figure 14b**, n=6 mice at weight loss, n=10 at onset, n=7 at peak, n=5 at remission).

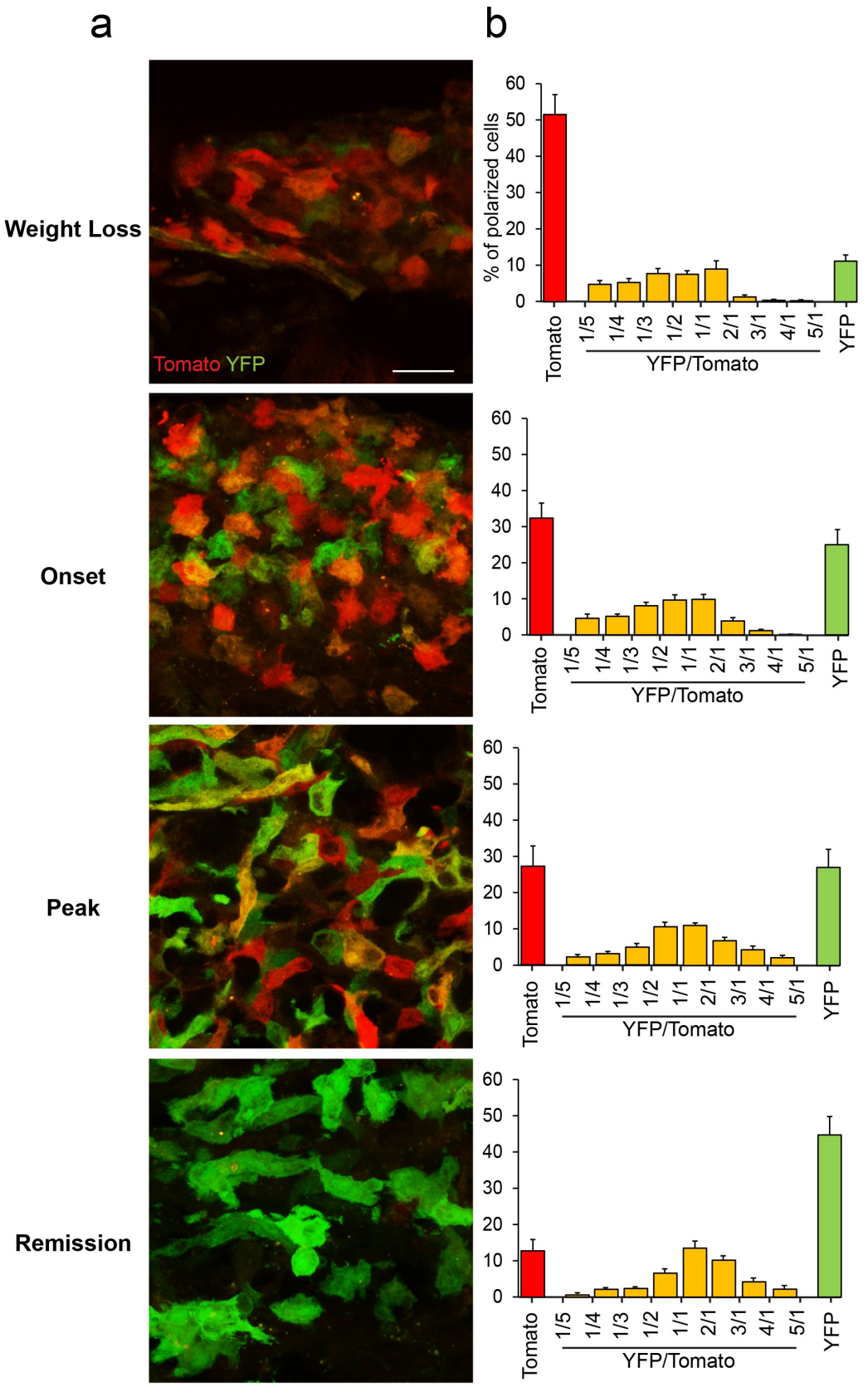

Figure 14: Progression of the reporter protein expression correlate with the pro- and anti- inflammatory phagocyte phenotype

Figure 14: Progression of the reporter protein expression correlate with the pro- and anti- inflammatory phagocyte phenotype.

(a) Confocal images of spinal cord lesions at the indicated stages of EAE in *iNOS-tdTomato-cre x Arginase-YFP* mouse (tdTomato in red, YFP in green), Scale bar, 20µm. (b) Quantitative analysis of M^{iNOS}, $M^{iNOS/Arginase}$ $M^{Arginase}$ cell populations located in spinal cord lesions at the indicated stages of EAE in *iNOS-tdTomato-cre x Arginase-YFP* mouse (M^{iNOS} in red, $M^{iNOS/Arginase}$ in yellow, $M^{Arginase}$ in green). ***Figure derived from Locatelli, Theodorou et al, submitted in Nature Neuroscience.***

To estimate the proportion of all phagocytes that are polarized, we performed immunohistochemistry for the phagocyte marker Iba-1 on tissue sections derived from *iNOS-tdTomato-cre* x *Arginase-YFP* mice during an EAE time course (**Figure 15**, n=5 or 6 animals). We observed a proportion of non-polarized cells over the course of EAE: at weight loss 32.8 ± 3.8% (Average ± s.e.m.), cells analyzed=1,425; at onset: 22.3 ± 1.3% (Average ± s.e.m.), cells analyzed=1,690; at EAE peak: 9.1 ± 1.2% (Average ± s.e.m.), cells analyzed=1,913; at remission: 24.0 ± 9.8% (Average ± s.e.m.), cells analyzed=1,926.

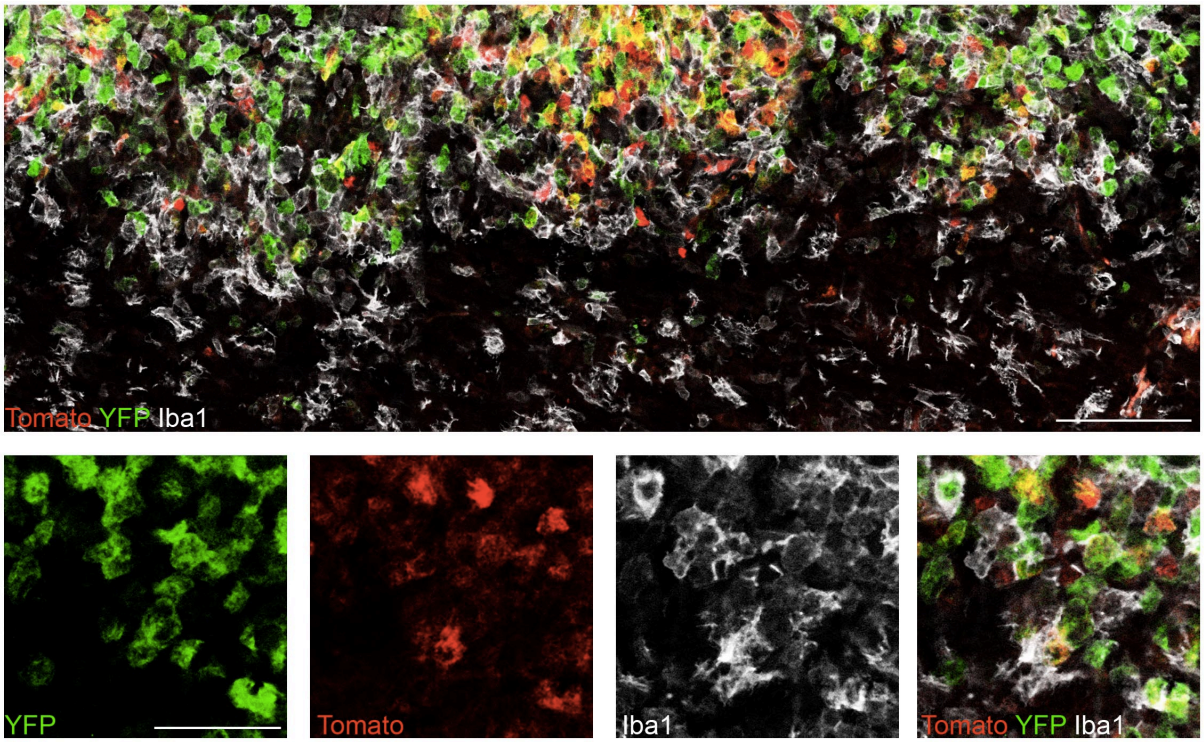

Figure 15: Overview of macrophages polarization state at peak of EAE in *iNOS-tdTomato-cre x Arginase-YFP* mice

Confocal images of an overview of spinal lesions (YFP in green, tdTomato in red, iba-1 co-staining in gray) in *iNOS-tdTomato-cre x Arginase-YFP* mice perfused at peak of EAE (Upper panel, scale bar 100µm**)** and magnified insets (lower panel, scale bar 50 µm).

Transcriptional analysis of macrophages populations isolated from the CNS

Further analyses on the reporter protein expressions were realized on CNS-isolated cell populations from *iNOS-tdTomato-cre* x *Arginase-YFP* mice at peak of EAE using flow cytometry. The $CD11b^{high}$ $CD45^{high}$ gate contained the majority of polarized cells and revealed three distinct cells populations, likewise observed by immunohistochemistry and *in vivo* imaging: M^{iNOS}, $M^{iNOS/Arginase}$ and $M^{Arginase}$ cells (**Figure 16a**). A significantly higher proportion of these phagocyte population expressed $F4/80^{high}$ and $CD11c^{high}$ than the unpolarized cell population from the same $CD11b^{high}$ $CD45^{high}$ gate. However, it is important

to mention that all these cell populations shared similarities such as the high expression of Ly6c, characteristic marker of inflammatory monocytes/macrophages (**Figure 16b**, n=6 mice).

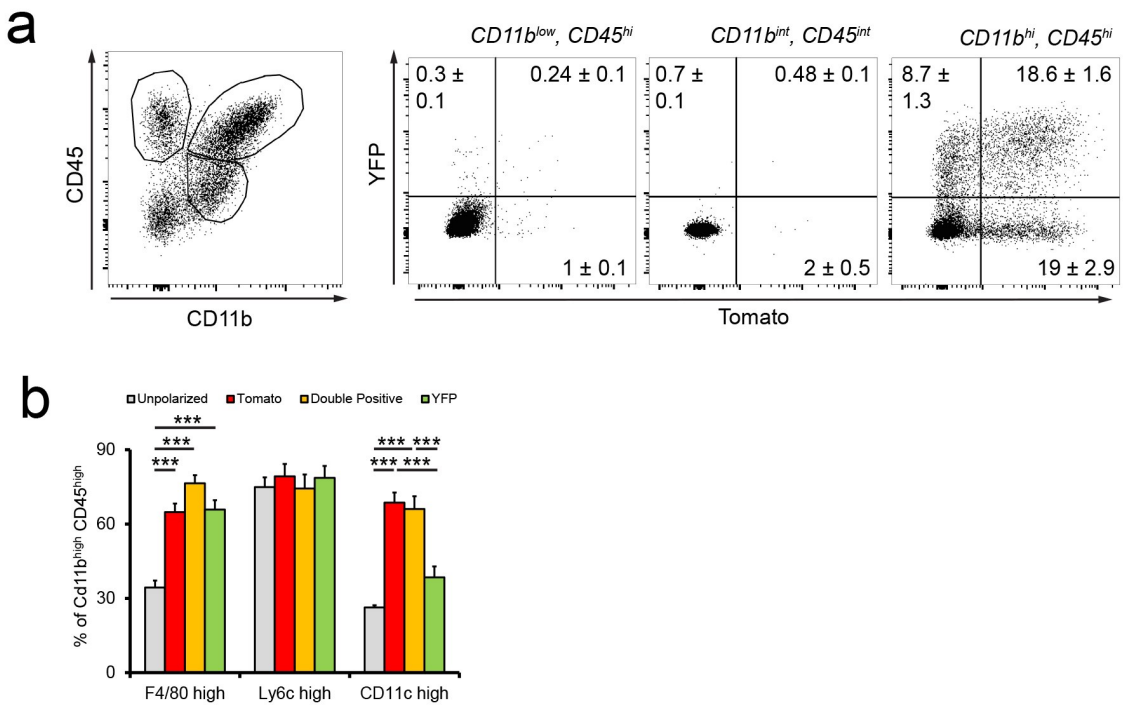

Figure 16: Flow cytometric analysis of tdTomato and YFP expression in cells isolated from *iNOS-tdTomato-cre x Arginase-YFP mice*.

(a) Gating strategy based on CD11b and CD45 revealing M^{iNOS}, $M^{iNOS/Arginase}$ and $M^{Arginase}$ cell populations in $CD11b^{high}$ $CD45^{high}$. (b) Analysis of the expression of F4/80, Ly6C and CD11c in unpolarized and polarized $CD45^{high}$-$CD11b^{high}$ cells. ***Figure from Locatelli, Theodorou et al, submitted in Nature Neuroscience.***

To better define the transcriptional make-up of different polarized macrophages, $CD11b^{high}$ $CD45^{high}$ $CD64^{positive}$ cells were isolated from the spinal cords of *iNOS-tdTomato-cre* x

Arginase-YFP mice at weight loss and analyzed via RNA sequencing (Experiment performed by Marta Joana Costa Jordão and analyzed by Ori Staszewski and Dr. Giuseppe Locatelli). The principal component analysis of the transcriptional profile of these macrophage populations in the inflamed CNS revealed M^{iNOS}, $M^{iNOS/Arginase}$ and $M^{Arginase}$ cells as distinct populations (**Figure 17a**, n=4 mice), however with a strongly overlapping transcriptome that is distinct from the classic M1-M2 phenotype observed in *in vitro* experiments (**Figure 17b**, n=4 mice). In addition, these cell populations were closely related to unpolarized $CD11b^{high}$ $CD45^{high}$ $CD64^{positive}$ cells from the inflamed CNS. The iNOS expression was significantly higher in M^{iNOS} cells ($tdTomato^{+}$ only) compared to the other populations ($M^{iNOS/Arginase}$, $M^{Arginase}$, $M^{unpolarized}$) while the arginase-1 expression was significantly higher in the $M^{iNOS/Arginase}$ and $M^{Arginase}$ cells populations presumably due to the start of arginase-1 translation (**Figure 17c**, n=4 mice).

The transcript analysis of M^{iNOS}, $M^{iNOS/Arginase}$ and $M^{Arginase}$ cell populations showed that many genes were differently up- or down regulated; among these, receptors or surface molecules, secreted molecules, C1q molecules, chemokines, enzymes or signaling molecules (**Figure 17d**, n=4 mice). We also observed that glycolysis and lipid processing pathways were significantly upregulated in M^{iNOS}, $M^{iNOS/Arginase}$ and $M^{Arginase}$ cell populations compared to unpolarized (e.g. Aldoa, GDPD1 for glycolysis and Pla2g7 for lipid processing) (**Figure 17d,** n=4 mice).

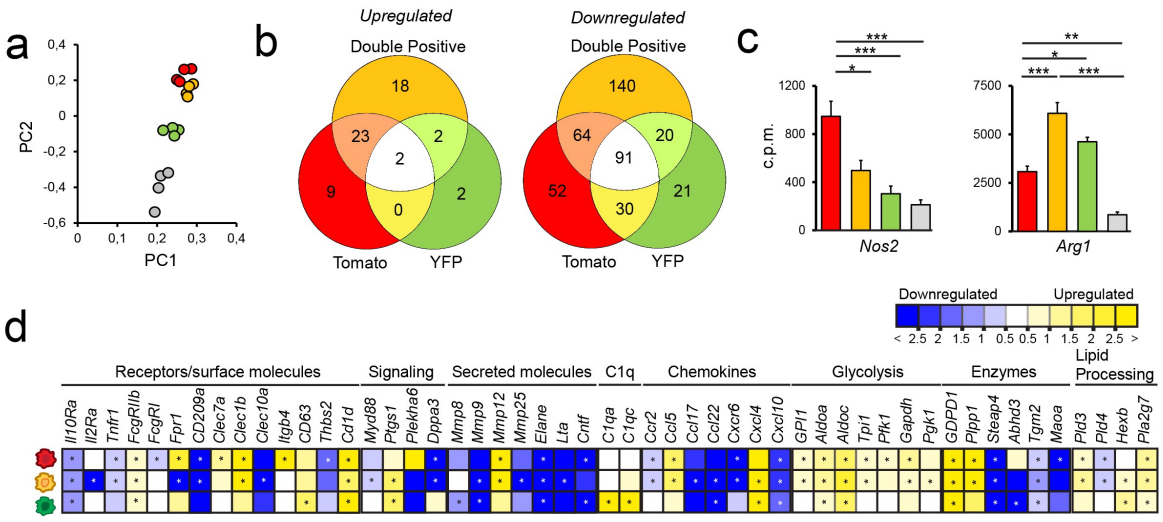

Figure 17: RNA sequencing analysis of CD45^{high}-CD11b^{high}-CD64^{positive} cells isolated from the CNS of *iNOS-tdTomato-cre x Arginase-YFP* mice at weight loss.

(a) Principal component analysis of M^{iNOS}, M$^{iNOS/Arginase}$, M^{Arginase} and M^{unpolarized} cell populations. (b) Venn diagrams represent significantly regulated genes in polarized cells compared to unpolarized cells. (c) Count-per-million expression of Nos2 and Arg1. (d) Selection of differentially regulated genes in polarized cells compared to unpolarized cells (shade of blue represent down-regulated genes, shades of yellow represent up-regulated genes, expression fold-change; *, P<0.05). Data are shown as average expression ± s.e.m.; *, P<0.05, **, P<0.01 ***, P<0.001, 1-way-Anova with Bonferroni post-hoc correction. ***Figure from Locatelli, Theodorou et al, submitted in Nature Neuroscience.***

Importance of CNS compartmentalization for the establishment of mononuclear phagocyte phenotypes *in vivo*

In order to determine the importance of the spinal cord microenvironment for the establishment of the phagocyte phenotype, we performed *in vivo* imaging in *iNOS-tdTomato-cre* x *Arginase-YFP* mice over the time-course of EAE and analyzed the proportions of M^{iNOS},

$M^{iNOS/Arginase}$ and $M^{Arginase}$ cell in the different CNS compartments: upper meninges (dura and arachnoidea), pia mater/parenchyma border and deep parenchyma (Experiment performed by Dr Giuseppe Locatelli, **Figure 18a**).

First we acquired a spinal cord volume starting from the upper meninges until the deep parenchyma, followed by the surgically removal of the upper meninges and once again the imaging of the same volume of spinal cord tissue (**Figure 18a**). The mononuclear phagocytes that were absent following removal of the meninges were considered to be located in this compartment. The mononuclear phagocytes present at the pia/parenchyma border could be observed at the beginning of the second image acquired after removal of the upper meninges. This *in vivo* imaging approach disclosed the existence of mononuclear phagocyte phenotype gradients in the different spinal cord compartments particularly at earlier EAE time points (i.e. weight loss and onset of EAE). Indeed, the parenchyma was significantly enriched in M^{iNOS} cells in comparison to the upper meninges at both onset and peak of EAE while contrarily $M^{Arginase}$ cells were predominant in the upper meninges at both onset and peak of EAE as calculated with a 1-way-Anova with Bonferroni post-hoc correction (**Figure 18b**, n=5 at weight loss, 6 at onset, 5 at peak, 5 at remission).

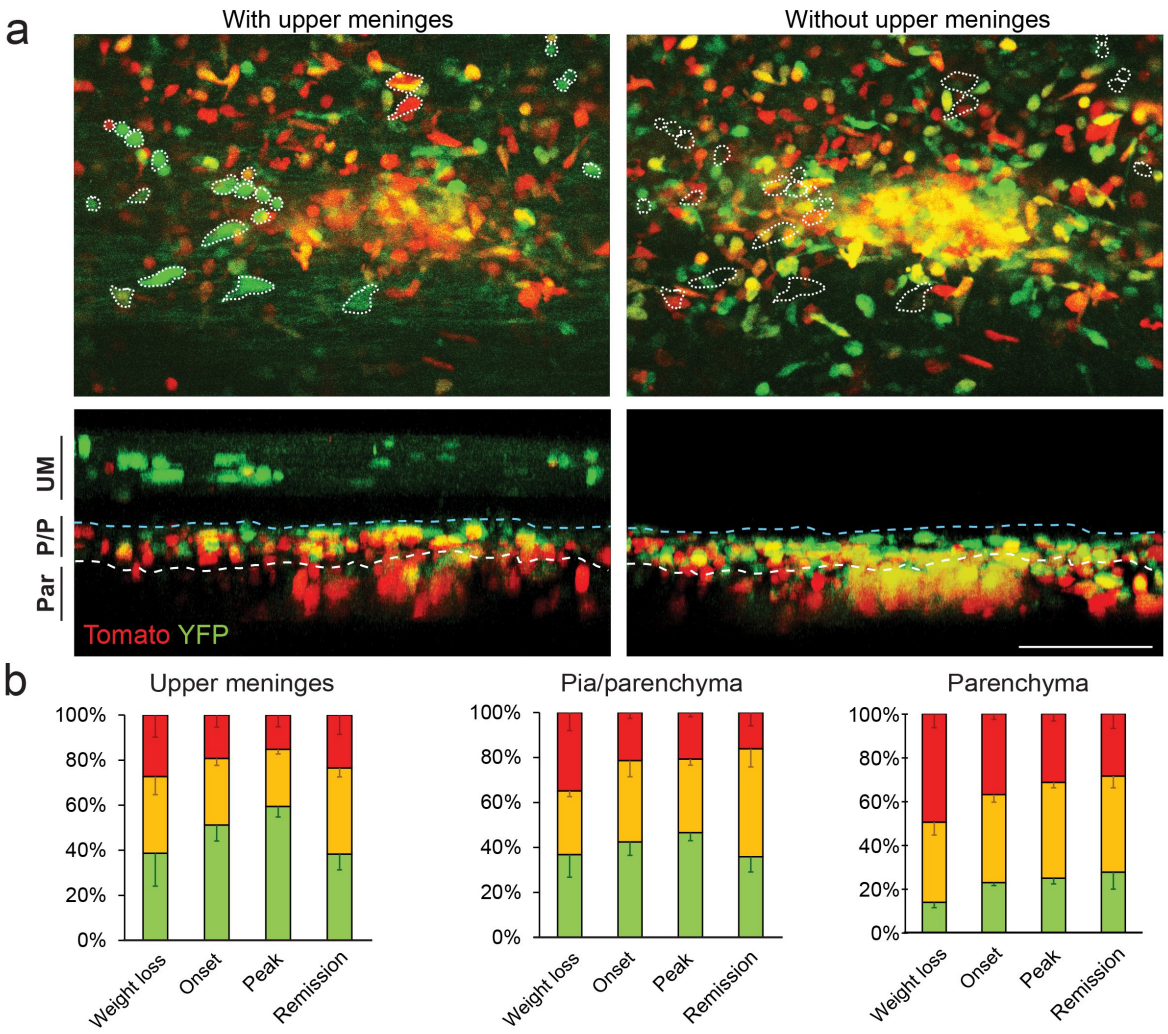

Figure 18: Importance of CNS microenvironments for the establishment of mononuclear phagocyte phenotypes in *iNOS-tdTomato-cre x Arginase-YFP* mice.

(a) *In vivo* image acquisition of a spinal lesion of *iNOS-tdTomato-cre x Arginase-YFP* mouse at EAE onset before (left) and after (right) removal of upper meninges. Lower panel represent the lateral projection in the different microenvironment of the CNS (UM=upper meninges, P/P=Pia/parenchyma interface, Par=Parenchyma). Dashed cell contours (above) indicate UM cells; dashed lines (below) indicate upper (cyan) and lower (white) P/P limits. Scale bar, 90µm. (b) Quantitative analysis of the percentage of polarized M^{iNOS}, $M^{iNOS/Arginase}$, $M^{Arginase}$ cells in the spinal cord of *iNOS-tdTomato-cre x Arginase-YFP* mice during the EAE time course. ***Figure from Locatelli, Theodorou et al, submitted in Nature Neuroscience.***

Isotropic distribution of mononuclear phagocyte phenotypes in parenchymal lesions at EAE onset *in situ*

In order to study whether a spatial gradient of mononuclear phagocyte phenotype exist in parenchymal lesions, we performed an immunohistochemistry revealing the vasculature with a Laminin staining in *iNOS-tdTomato-cre* x *Arginase-YFP* mice at onset of EAE. No specific gradient of differently polarized phagocytes was found originating from the top of the lesion, from the lesion core or starting from the blood vessels, hence demonstrating a rather isotropic distribution of mononuclear phagocyte phenotypes in neuroinflammatory lesions at onset of EAE (**Figure 19**, n=7 mice; 1,869 cells assessed for the analysis starting from the pial surface, n=7 mice and 1,894 cells assessed for the analysis from the core of the lesion, n=5 mice and 436 cells assessed for the analysis starting from the blood vessel. No significant differences were observed (1-way-Anova with Bonferroni post-hoc correction).

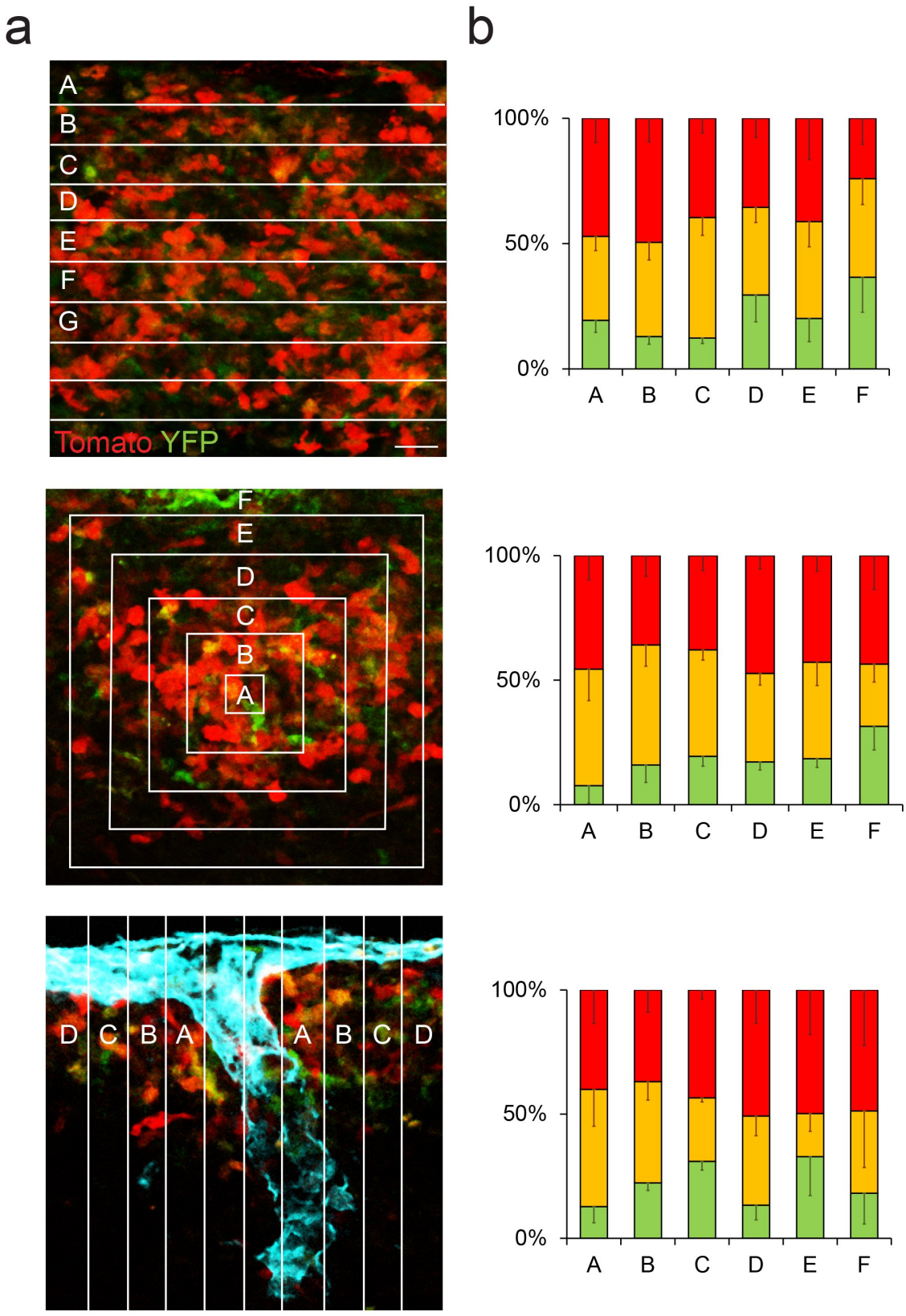

Figure 19: Isotropic distribution *in situ* of mononuclear phagocyte phenotypes in parenchymal lesions at onset of EAE in *iNOS-tdTomato-cre x Arginase-YFP* mice.

Figure 19: Isotropic distribution *in situ* of mononuclear phagocyte phenotypes in parenchymal lesions at onset of EAE in *iNOS-tdTomato-cre x Arginase-YFP* mice.

(a) Confocal images of spinal lesions of *iNOS-tdTomato-cre x Arginase-YFP* mice perfused at onset of EAE (tdTomato in red, YFP in green). Bands of 20µm of thickness depict the spatial distribution of polarized cells emanating from pia surface (top panel), concentric squares starting from the core of the lesion (middle panel) or parallel to the main blood vessel revealed by Laminin co-staining (cyan, lower panel). Scale bar 20µm. (b) Quantitative analysis of the proportion of M^{iNOS}, $M^{iNOS/Arginase}$ and $M^{Arginase}$ cells as indicated in (a). ***Figure derived from Locatelli, Theodorou et al, submitted in Nature Neuroscience.***

Mononuclear phagocyte polarization is initiated after CNS entry

To understand in which CNS compartment mononuclear phagocytes established a M^{iNOS} pro-inflammatory phenotype, we made use of the *iNOS-tdTomato-cre* mouse line crossed with *CD68-GFP* mouse line, in which all mononuclear phagocytes are associated with a green fluorescent protein (GFP) (Iqbal et al, 2014). We used an *in vivo* spinal imaging in *iNOS-tdTomato-cre x CD68-GFP* mice at onset of EAE to first understand, in which location M^{iNOS} cells were present (**Figure 20a,c**, n=7 mice). No polarized mononuclear phagocytes were located in the vasculature revealed by Dextran, while considerable proportions of cells expressing tdTomato were found in the perivascular space, parenchyma, pia/parenchyma border and upper meninges **(Figure 20a,c**, n=7 mice, 4,355 cells analyzed at the pia/parenchyma border, 2,727 cells in the upper meninges, 142 in the vasculature, 268 in the perivascular space and 1,778 cells in the parenchyma).

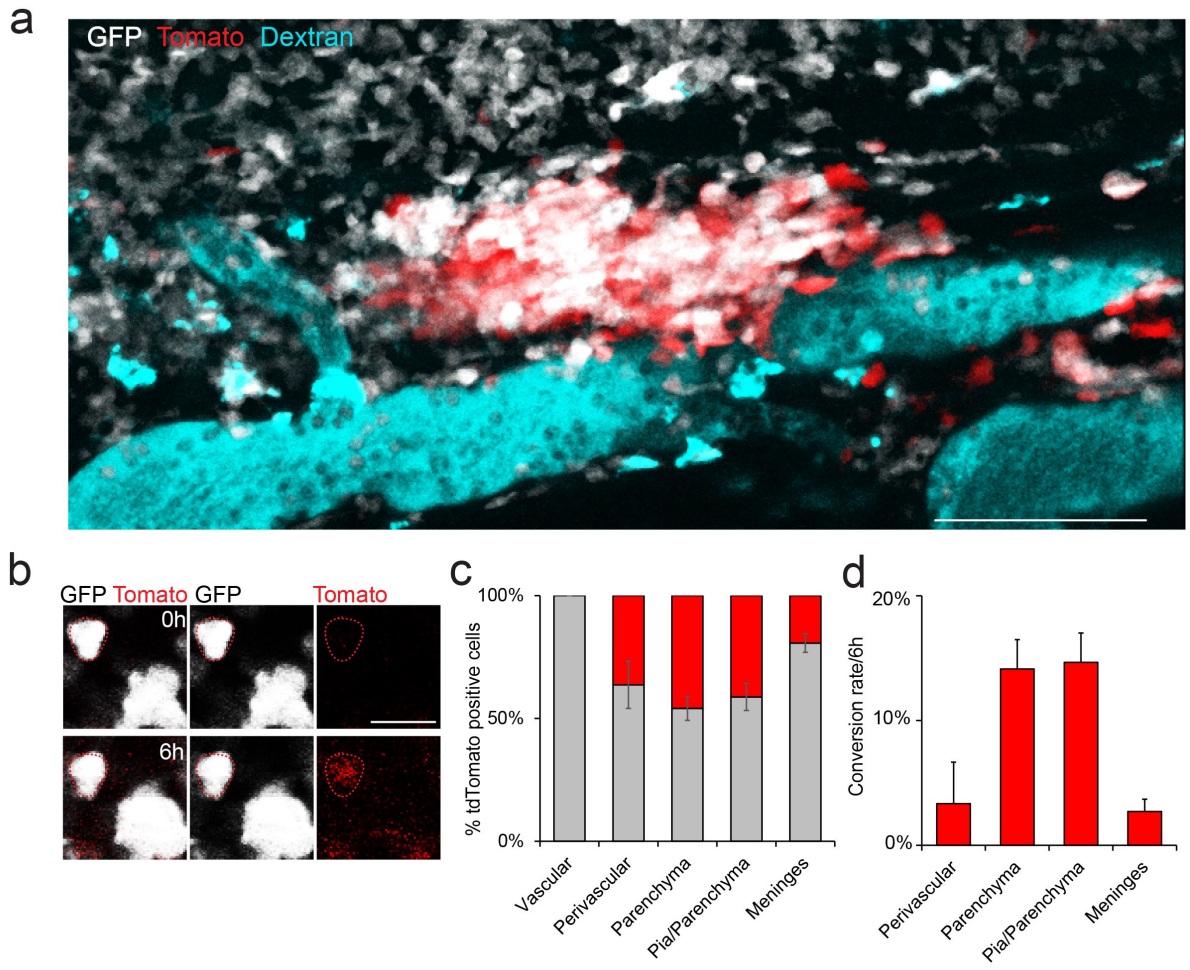

Figure 20: M^{iNOS} phagocyte phenotype is initiated after CNS entry in *iNOS-tdTomato-cre x CD68-GFP mice* at onset of EAE.

(a) *In vivo* image acquisition of a spinal lesion in *iNOS-tdTomato-cre x CD68-GFP* mice at EAE onset (GFP in gray, tdTomato in red, Dextran-647 in cyan, scale bar 100µm), (b) *in vivo* time-lapse imaging of *iNOS-tdTomato-cre x CD68-GFP* mice at EAE onset (scale bar 20µm). Dashed cell contours represent an unpolarised GFP^+ cell converting into a GFP^+M^{iNOS} after 6hrs. (c,d) Quantitative analysis of the proportion of GFP^+M^{iNOS} (red) and unpolarized GFP^+ cells at initial time point of imaging (c) and conversion rate of unpolarised GFP^+ (gray) to GFP^+M^{iNOS} (red) cells (d) in the different CNS microenvironments of *iNOS-tdTomato-cre x CD68-GFP* mice at EAE onset. Data are shown as average expression ± s.e.m. ***Figure from Locatelli, Theodorou et al, submitted in Nature Neuroscience.***

These results corroborated the findings obtained by flow cytometry in *iNOS-tdTomato-cre* x *Arginase-YFP* mice during EAE with the absence of reporter proteins expression in phagocytes isolated from peripheral compartments such as the blood circulation and lymph nodes (**Figure 21**, for the cells isolated from the blood: n=5 mice, populations were gated based on CD45 and CD11b expression. Average percentage of polarized cells (± s.e.m.) was 0.002 ± 0.002 for M^{iNOS} and 0.0 for $M^{Arginase}$ cells in the $CD45^{high}$-$CD11b^{neg}$ population, 0.01 ± 0.01 for M^{iNOS} and 0.0 for $M^{Arginase}$ cells in the $CD45^{high}$-$CD11b^{high}$ population, 0.0 for M^{iNOS} and 0.001 ± 0.001 for $M^{Arginase}$ cells in the $CD45^{neg}$-$CD11b^{neg}$ population, 0.0 for M^{iNOS} and $M^{Arginase}$ cells in the $CD45^{int}$-$CD11b^{int}$ population. No $M^{iNOS/Arginase}$ cells were observed; for the lymph nodes: n=8 mice, populations were gated based on CD45 and CD11b expression. Average percentage of polarized cells (± s.e.m.) was 0.007 ± 0.003 for M^{iNOS} and 0.003 ± 0.002 for $M^{Arginase}$ cells in the $CD45^{high}$-$CD11b^{neg}$ population, 0.0003 ± 0.0003 for M^{iNOS} and 0.0 for $M^{Arginase}$ cells in the $CD45^{neg}$-$CD11b^{neg}$ population, 0.09 ± 0.03 for M^{iNOS} and 0.0 for $M^{Arginase}$ cells in the $CD45^{high}$-$CD11b^{high}$ population. No $M^{iNOS/Arginase}$ cells were observed). Overall, our data suggest that macrophages enter the CNS unpolarized via the blood circulation and afterwards start to express iNOS either in the perivascular space, in the meninges or directly in the parenchyma.

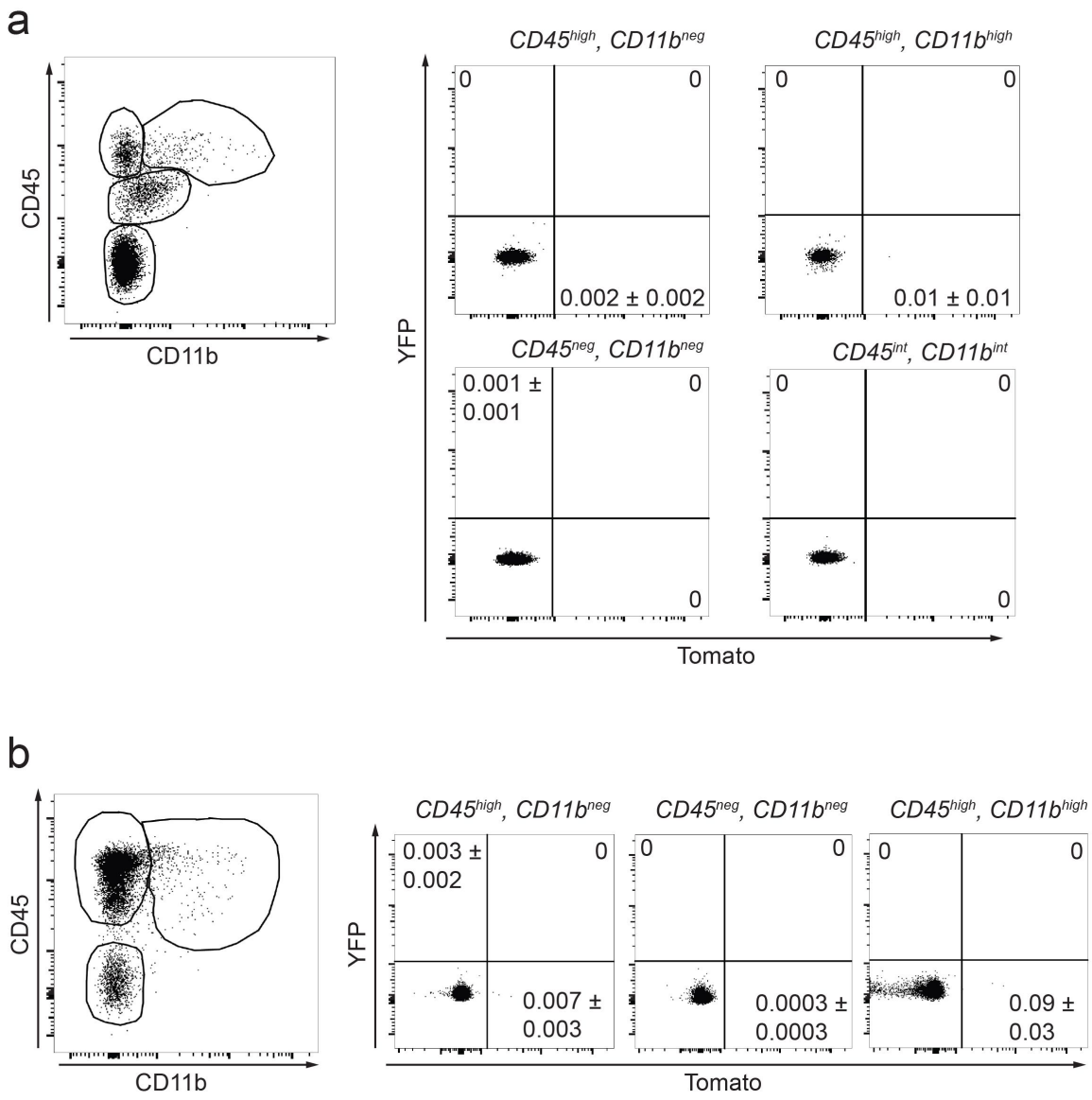

Figure 21: Absence of reporter protein expression in mononuclear phagocytes located in blood and lymph nodes in *iNOS-tdTomato-cre x Arginase-YFP* mice during EAE.

(a) Flow cytometric analysis of cells isolated from blood in *iNOS-tdTomato-cre x Arginase-YFP* mice at peak of EAE (n=5 mice). (b) Flow cytometric analysis of cells isolated from lymph nodes in *iNOS-tdTomato-cre x Arginase-YFP* mice at peak of EAE (n=8 mice). ***Figure from Locatelli, Theodorou et al, submitted in Nature Neuroscience.***

In addition, we verified the previous *in vivo* visual assessment of polarized cells belonging to the perivascular space by performing a co-staining with Laminin on *iNOS-tdTomato-cre x CD68-GFP* mice at onset of EAE. We compared the percentage of perivascular cells (GFP^+ and GFP^+ $Tomato^+$) in contact with the inner line of the Laminin staining that corresponded to our criteria for *in vivo* imaging quantification and the percentage of cells present in between the two lines of the Laminin depicting the entire perivascular space. We underestimated the number of cells present in the perivascular space with the *in vivo* imaging analysis, however the percentages were comparable. With the criteria, in contact with the inner line of the Laminin we found 31.5 ± 17.7% of GFP^+ $Tomato^+$ perivascular cells and 68.5 ± 17.7 % of GFP^+ while 31.9 ± 9.1% of GFP^+ $Tomato^+$ perivascular cells and 68.1 ± 9.1 of GFP^+ perivascular cells in between the two lines of the Laminin (**Figure 22,** n=3 mice and 79 cells analyzed). These results were similar to the ones obtained with *in vivo* imaging (36.3 ± 9.6 % GFP^+ $Tomato^+$ perivascular cells and 63.7 ± 9.6 % GFP^+ perivascular cells).

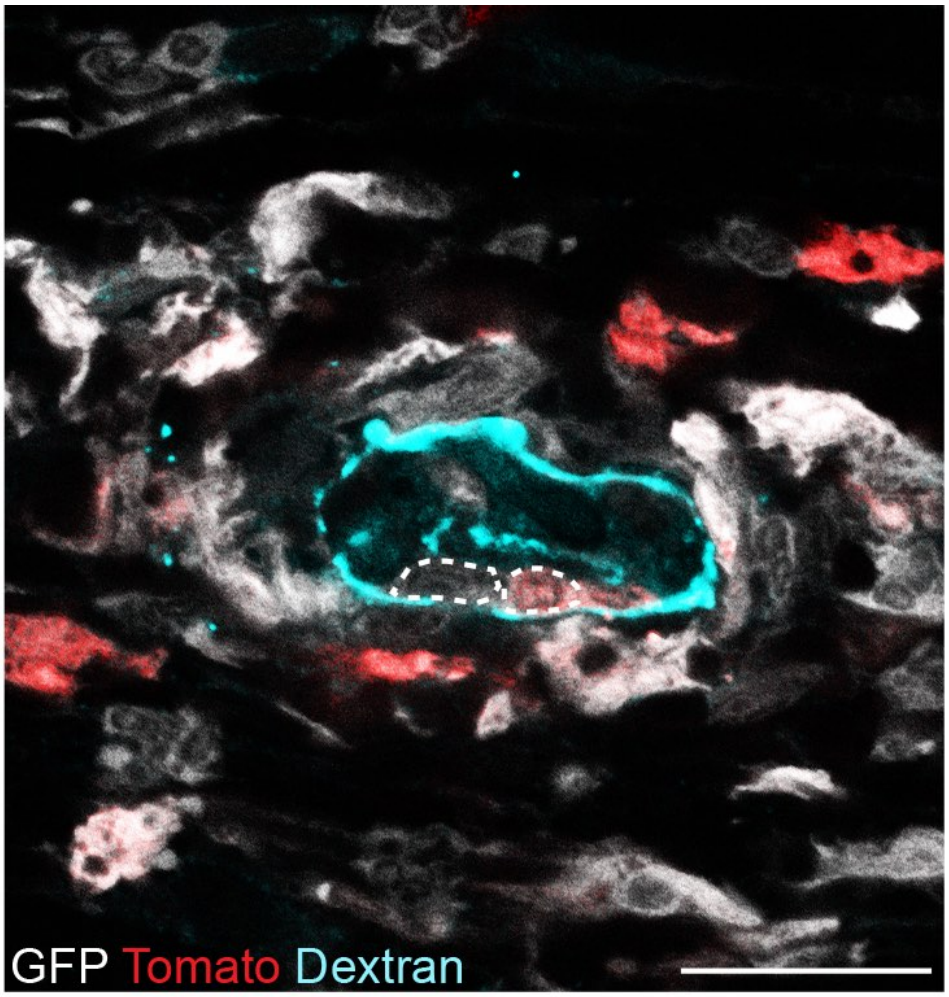

Figure 22: Determination of M^{iNOS} phagocyte phenotype in the perivascular space in *iNOS-tdTomato-cre x CD68-GFP* mouse at onset of EAE.

Confocal image of a spinal EAE lesion in *iNOS-tdTomato-cre x CD68-GFP* mouse (YFP in gray, tdTomato in red, Laminin co-staining in cyan) perfused at onset of EAE. Scale bar 20µm. Outline dashed cell represents a cell located in the perivascular space, on the left that is only GFP^+ and on the right that is GFP^+ $Tomato^+$.

Highest conversion rate of tdTomato expression in the parenchyma and at the pia/parenchymal border

Moreover, we studied the spatial and temporal distributions of the initial pro-inflammatory polarization of mononuclear phagocytes using *in vivo* imaging of the *iNOS-tdTomato-cre x CD68-GFP* mice at EAE onset. The cells imaged were assigned to a position in their respective CNS compartments: perivascular space, parenchyma, pia/parenchyma border and upper meninges. The analysis was performed over time (6hrs) by comparing the tdTomato fluorescent reporter protein expression. Thus, we could assess the M^{iNOS} polarization rate corresponding the conversion of a non-polarized GFP^+ phagocyte to a GFP^+ $tdTomato^+$ phagocyte (**Figure 20b**, n=7 mice). Tracking single cells over time was achievable as mononuclear phagocytes are relatively stable in neuroinflammatory lesions. Our data suggest that the highest probability of initiation of tdTomato expression in inflammatory phagocytes was in the parenchyma and in the pia/parenchymal border (**Figure 20d,** n=7 mice). In contrast, the conversion rate over 6hrs of tdTomato expression initiation was very low in the perivascular space and in the upper meninges (**Figure 20d**, n=7 mice). Number of cells analyzed in perivascular space: 51, in parenchyma: 197, at the pia/parenchyma border: 301 and in the upper meninges: 214.

These findings seem to suggest that during early stages of EAE, mononuclear phagocytes enter the parenchyma unpolarized via the blood circulation and that micro-environmental cues may influence the induction of a pro-inflammatory mononuclear phagocyte polarization characterized by the expression of tdTomato fluorescent reporter protein.

Progression of mononuclear phagocyte phenotypes during EAE evolution

As mentioned before, mononuclear phagocytes can be tracked over time using spinal *in vivo* imaging as depicted in the representative overview of the spinal cord during EAE (Experiment performed by Dr Giuseppe Locatelli, **Figure 23a**). In addition, we observed the presence of lesions located in the vicinity of the vasculature revealed by i.p. injection of Dextran-647 (**Figure 23a**). We could previously observe that after the initiation of M^{iNOS} polarization during early stages of the disease, the entire mononuclear phagocyte population switch to a $M^{Arginase}$ phagocyte phenotype over the course of the disease (**Figure 14b**).

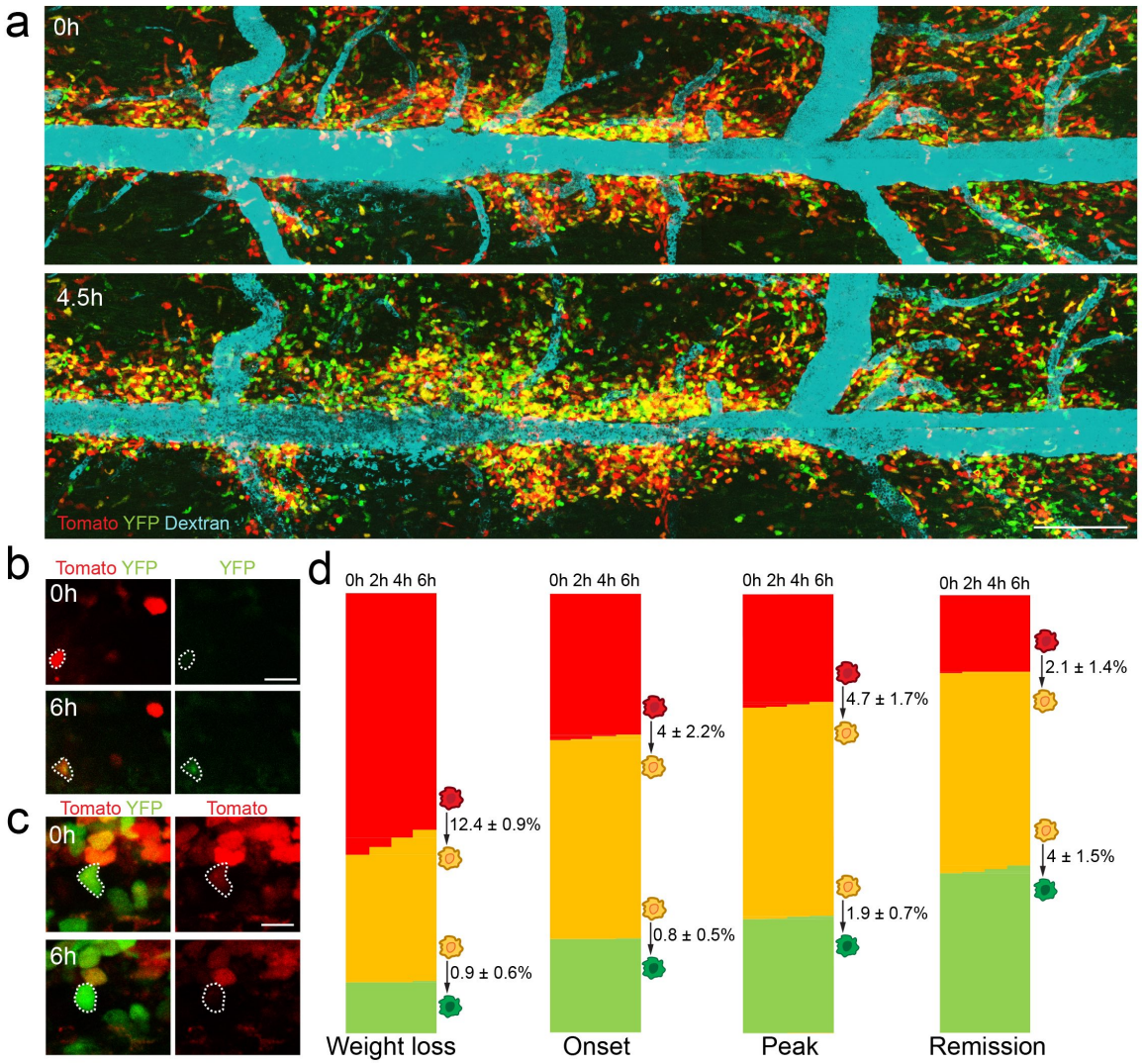

Figure 23: Progression of mononuclear phagocyte phenotype over the disease course

Figure 23: Progression of mononuclear phagocyte phenotype over the disease course (a) *In vivo* image acquisitions of spinal lesions in *iNOS-tdTomato-cre x Arginase-YFP* mice at peak of EAE, scale bar 200µm (tdTomato in red, YFP in green, Dextran-647 in cyan). (b) Representative example at weight loss of a M^{iNOS} cell (above) becoming a $M^{iNOS/Arginase}$ cell (below, scale bar 20µm). (c) Representative example at peak of EAE of a $M^{iNOS/Arginase}$ cell (above) becoming a $M^{Arginase}$ cell (below, scale bar 5µm). (d) Quantitative analysis from *in vivo* imaging of single mononuclear phagocyte located in spinal lesions in *iNOS-tdTomato-cre x Arginase-YFP mice.* Shown are proportions of M^{iNOS} cells switching to $M^{iNOS/Arginase}$ (above) and of $M^{iNOS/Arginase}$ cells switching to $M^{Arginase}$ (below) over 6hrs. ***Figure from Locatelli, Theodorou et al, submitted in Nature Neuroscience.***

Several hypotheses have been put forward concerning the existence of differentially polarized mononuclear phagocyte populations. On the one hand, M^{iNOS} cells could depart from the CNS and be replaced by the infiltration of arginase-1 expressing cells populations ($M^{iNOS/Arginase}$ or $M^{Arginase}$ cells) in EAE lesions; alternatively, single M^{iNOS} cells could switch over time their phenotype and start expressing EYFP to become either $M^{iNOS/Arginase}$ or (subsequently) $M^{Arginase}$ cells. Understanding whether several waves of incoming macrophage population or whether the same cell may adapt its phenotype could have impact for our understanding and treatment of MS pathology.

To consider these distinct hypotheses, we performed several time-lapse spinal *in vivo* imaging experiments in *iNOS-tdTomato-cre* x *Arginase-YFP* transgenic mouse lines during an EAE time course from weight loss to remission (Experiment performed by Dr Giuseppe Locatelli).

First, we wanted to determine if a single mononuclear phagocyte was able to modulate its phenotype over a 6 hour imaging in spinal EAE lesions. Among thousands of cells analyzed, we could indeed observe some polarized macrophages modifying their phenotype over the

disease course by switching from a M^{iNOS} to $M^{iNOS/Arginase}$ or by switching from a $M^{iNOS/Arginase}$ to $M^{Arginase}$ phenotype. This switch seemed to be occurring in unidirectional manner from M^{iNOS} to $M^{Arginase}$ phenotype, passing through an intermediary stage ($M^{iNOS/Arginase}$) where both reporter proteins are expressed.

These results suggest the existence of a rather continuous phenotype spectrum. It is important to note that the highest conversion rate from M^{iNOS} to $M^{iNOS/Arginase}$ was found during lesion formation (i.e. weight loss) whereas the highest conversion rate from $M^{iNOS/Arginase}$ to $M^{Arginase}$ was predominant at lesion resolution (i.e. remission or 7 days after onset). Besides, the conversion rate from M^{iNOS} to $M^{iNOS/Arginase}$ decreased over the EAE course while contrariwise the conversion rate from $M^{iNOS/Arginase}$ to $M^{Arginase}$ increased over the disease course (**Figure 23d,** 614 cells analyzed at weight loss, 1,180 at onset, 920 at peak, 612 at remission; 7 mice analyzed at weight loss, 7 mice at onset, 6 mice at peak and 5 mice at remission).

Conversions in the direction $M^{iNOS/Arginase}$ to M^{iNOS} or in the direction of $M^{iNOS/Arginase}$ to $M^{Arginase}$ were not or only very exceptionally observed. Indeed, no adaptation of mononuclear phagocyte phenotype from $M^{iNOS/Arginase}$ to M^{iNOS} were observed among 1439 $M^{iNOS/Arginase}$ cells analyzed and only one $M^{Arginase}$ cell out of 784 underwent a $M^{Arginase}$ to $M^{iNOS/Arginase}$ switch.

Mononuclear phagocytes plasticity occurs mainly in the parenchyma and at the pia/parenchyma border

Similarly to the results obtained for the M^{iNOS} polarization in the *iNOS-tdTomato-cre x CD68-GFP* mice (**Figure 19**), mononuclear phagocyte conversion in the *iNOS-tdTomato-cre* x *Arginase-YFP* transgenic mouse line happened locally in the CNS and mainly in the parenchyma and at the pia/parenchyma border (**Figure 24**). The vast majority of mononuclear

phagocyte phenotype conversions happened in these compartments throughout the formation to the resolution of EAE neuroinflammatory lesions (for the switch from M^{iNOS} to $M^{iNOS/Arginase}$, number of cells per timepoint: weight loss, n=36, onset, n=15, peak, n=11, remission, n=2; for the switch from $M^{iNOS/Arginase}$ to $M^{Arginase}$, number of cells per timepoint: weight loss, n=2, onset, n=2, peak, n=7, remission, n=10).

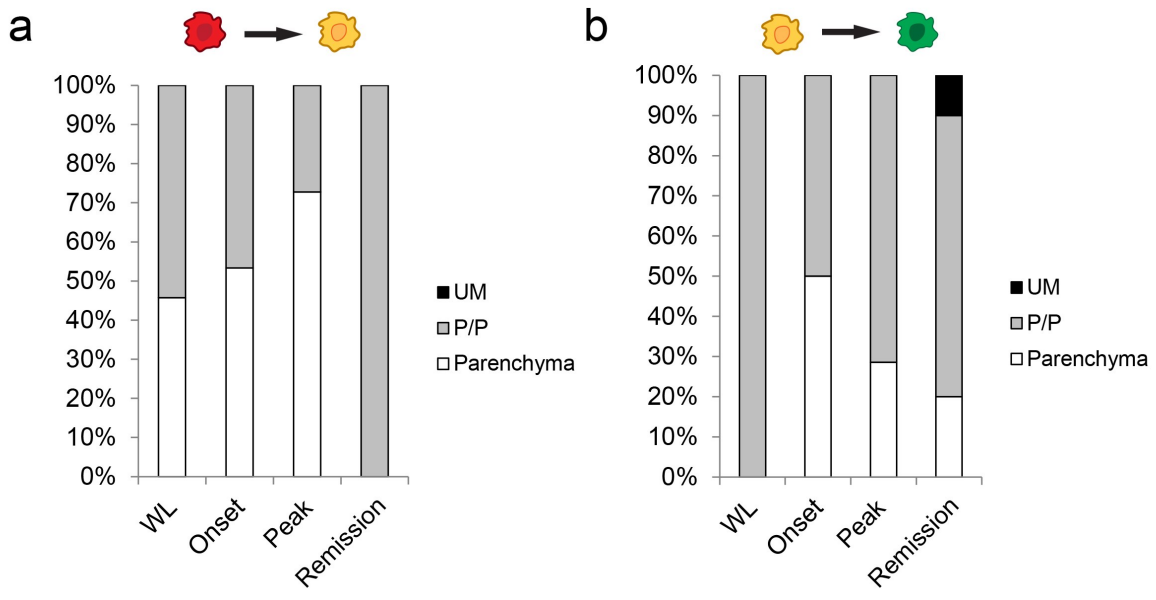

Figure 24: Distribution of switching mononuclear phagocytes during the EAE time course in *iNOS-tdTomato-cre x Arginase-YFP mice.*

(a) Quantitative analysis of mononuclear phagocytes switching over 6hrs of imaging during the course of EAE from M^{iNOS} to $M^{iNOS/Arginase}$. (b) Quantitative analysis of mononuclear phagocytes switching over 6hrs of imaging during the course of EAE from $M^{iNOS/Arginase}$ to $M^{Arginase}$. ***Figure from Locatelli, Theodorou et al, submitted in Nature Neuroscience.***

These results directly demonstrate for the first time that polarized mononuclear phagocytes can modify and adapt their phenotype locally over the disease course by switching in an unidirectional manner from M^{iNOS} to $M^{iNOS/Arginase}$ and finally $M^{Arginase}$ in spinal resolving EAE lesions.

Reporter promoters are still active over the course of EAE

Next, we wanted to investigate whether the large population of $M^{iNOS/Arginase}$ cells observed in spinal lesions over the EAE time course was indeed a real phagocyte phenotype intermediate and corresponded to the active co-expression of iNOS and arginase-1 signature enzymes. In fact, the expression of both tdTomato and YFP fluorescent reporter proteins in $M^{iNOS/Arginase}$ cells does not automatically indicates that both genes promoters are active at the same time or are still active. This is especially important for the *iNOS-tdTomato-cre* mouse line, which has been shown to have a stable tdTomato fluorescent reporter protein while the iNOS protein expression has a very short half-life (Kolodziejski et al, 2004).

In order to study the iNOS and arginase-1 promoter activity in mononuclear phagocytes in spinal lesions over the disease course, we used an *in vivo* imaging bleaching approach in *iNOS-tdTomato-cre* x *Arginase-YFP* transgenic mouse line (Experiment performed by Dr. Giuseppe Locatelli). This experiment consisted in the acquisition of fluorescence intensities of M^{iNOS}, $M^{iNOS/Arginase}$, $M^{Arginase}$ cell populations in an EAE lesion volume followed by an increase of the laser power intensity in order to bleach the reporter protein fluorescence signal -around 80% for the tdTomato and 50% for the YFP- (**Figure 25a**). We were then able to follow the fluorescence re-establishment using *in vivo* imaging over time (**Figure 25a,c**). Our data suggests that 80% of $M^{iNOS/Arginase}$ cells still have an iNOS and arginase-1 active promoter at early stages of the diseases (i.e. weight loss) while it decreased to 50% at later stages suggesting that iNOS and arginase-1 promoters activity in the CNS diminished over the

disease course (**Figure 25 b,d,** n=7 mice). However, this experiment revealed that a relevant number of $M^{iNOS/Arginase}$ cells that appeared double positive with the tdTomato and YFP expression, were not expressing any longer iNOS or arginase-1 (**Figure 25d**, n=7 mice). These findings confirm that $M^{iNOS/Arginase}$ cells are indeed a genuine intermediate phenotype population from the shift occurring from M^{iNOS} to $M^{Arginase}$ in EAE lesions (**Figure 23**).

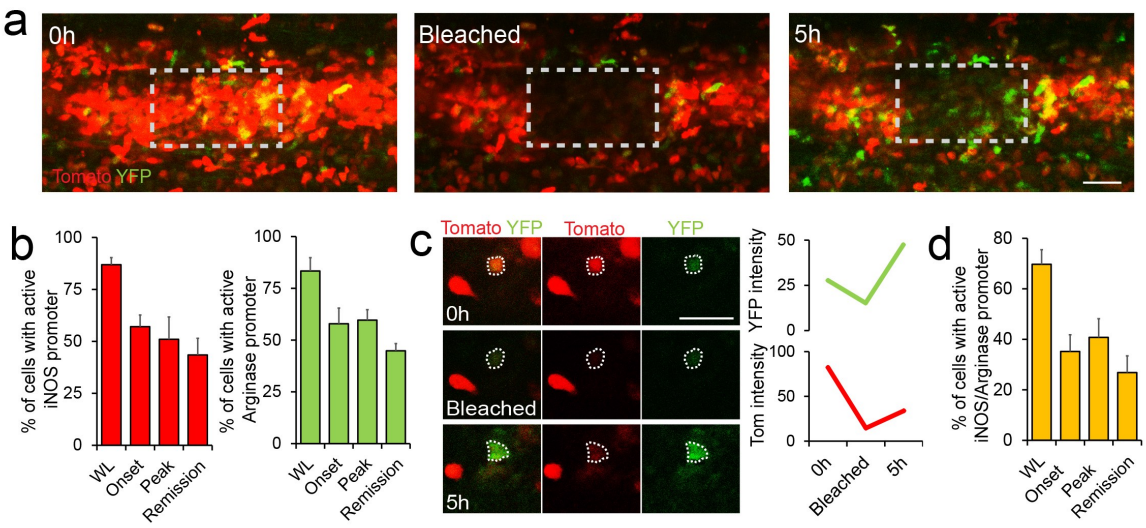

Figure 25: iNOS and arginase-1 promoters are still active over the course of EAE in *iNOS-tdTomato-cre x Arginase-YFP mice.*

(a) Reprensentative pictures of *in vivo* imaging acquisitions of spinal lesions in *iNOS-tdTomato-cre x Arginase-YFP* mouse at onset of EAE before bleaching (left), after bleaching (center) and 5hrs later (right). Scale bar, 40µm. (b) Quantitative analysis of the percentage of of M^{iNOS} (left) and $M^{Arginase}$ (right) cells with active promoter. (c) Representative examples of the fluorescence intensity of a $M^{iNOS/Arginase}$ cell (outlined) before and after bleaching using *in vivo* time-lapse. Scale bar, 25µm. (d) Quantitative analysis of the percentage of $M^{iNOS/Arginase}$ cells with active iNOS and arginase-1 promoters. ***Figure from Locatelli, Theodorou et al, submitted in Nature Neuroscience.***

Presence of a "*de novo*" macrophages population expressing $M^{Arginase}$

Lastly, we wanted to examine the origin of $M^{Arginase}$ mononuclear phagocytes in spinal EAE lesions and understand whether this phenotype exclusively came from a $M^{iNOS/Arginase}$ switch towards $M^{Arginase}$ cell populations.

In order to address this question, we made use of the Cre recombinase from the *iNOS-tdTomato-cre* mouse line and crossed it with the *Rosa26-Stp-fl-YFP* reporter mouse line, thus resulting in the specific induction of YFP in cells expressing the Cre recombinase. To track the origin of $M^{Arginase}$ cells we performed an arginase-1 immunohistochemistry in *iNOS-tdTomato-cre x Rosa26-Stp-fl-YFP* during EAE. This approach revealed that while mononuclear phagocytes that express arginase-1 and YFP have been subjected to a switch, the ones expressing arginase-1 but not YFP appeared *de novo* (**Figure 27**, n=4 mice, 344 cells analyzed).

We also observed that tdTomato and YFP reporter proteins were absent of the blood circulation in *iNOS-tdTomato-cre* x *Arginase-YFP* transgenic mouse line using flow cytometry presuming the absence of iNOS and arginase-1 expression in this compartment (**Figure 22**).

We confirmed these results in the *iNOS-tdTomato-cre x Rosa26-Stp-fl-YFP* transgenic mouse line by flow cytometry analysis of blood samples (**Figure 26,** n=5 *iNOS-tdTomato-cre* x *Rosa26-Stp-fl-YFP* mice and n=8 control *Rosa26-Stp-fl-YFP* mice, populations were gated based on CD45 and CD11b expression. Average percentage of YFP^{+} cells (± s.e.m.) was 0.016 ± 0.008 in control and 0.25 ± 0.04 in *iNOS-tdTomato-cre* x *Rosa26-Stp-fl-YFP* mice in the $CD45^{high}$-$CD11b^{neg}$ population, 0.007 ± 0.007 in control and 0.013 ± 0.013 in *iNOS-tdTomato-cre* x *Rosa26-Stp-fl-YFP* mice in the $CD45^{high}$-$CD11b^{high}$ population, 0.0006 ±

0.0004 in control and 0.0005 ± 0.0005 in *iNOS-tdTomato-cre* x *Rosa26-Stp-fl-YFP* mice in the $CD45^{neg}$-$CD11b^{neg}$ population).

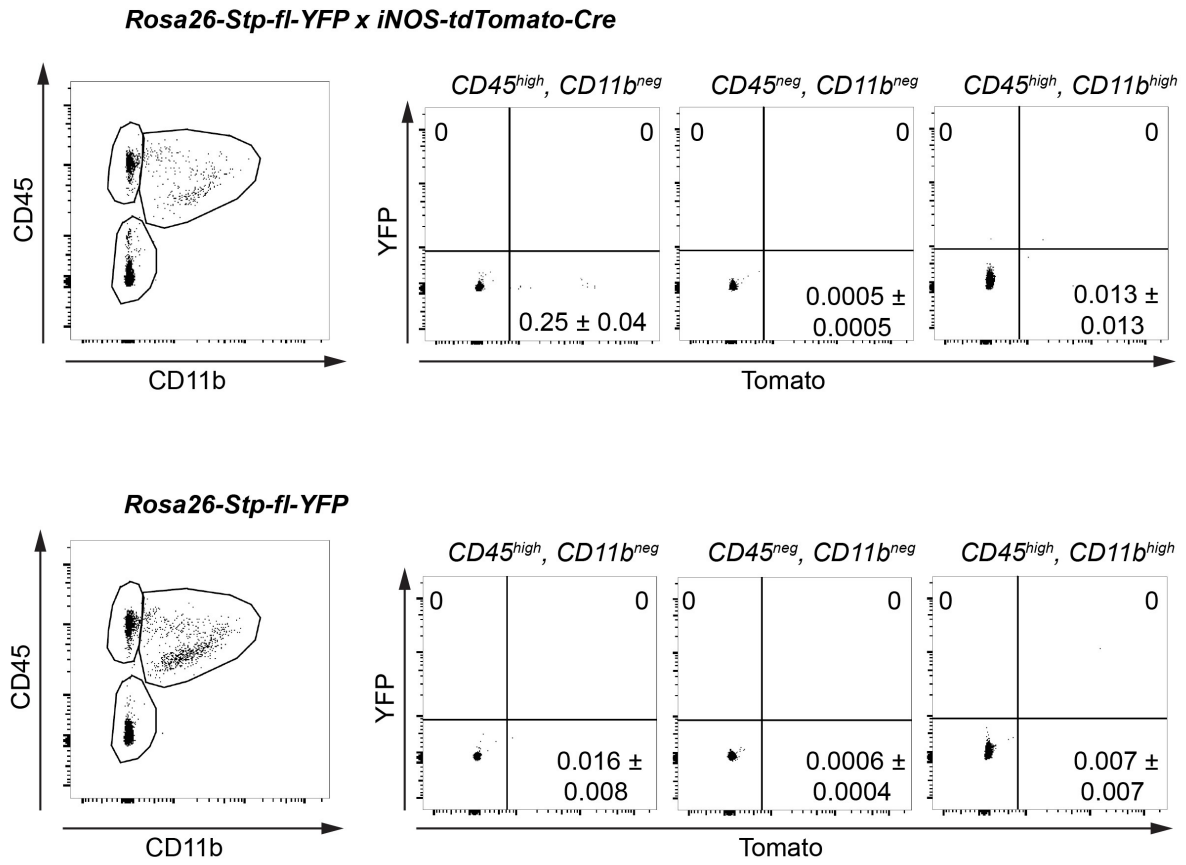

Figure 26: Absence of YFP expression in mononuclear phagocytes isolated from the blood of *iNOS-tdTomato-cre x Rosa26-Stp-fl-YFP* mice and *Rosa26-Stp-fl-YFP* mice during EAE.

Flow cytometric analysis of mononuclear phagocytes isolated from the blood of *iNOS-tdTomato-cre x Rosa26-Stp-fl-YFP* mice and *Rosa26-Stp-fl-YFP* mice at peak of EAE (n=5 and n=8 respectively). ***Figure from Locatelli, Theodorou et al, submitted in Nature Neuroscience.***

Furthermore, we verified the efficiency of the Cre recombinase expression in *iNOS-tdTomato-cre* by studying the proportion of mononuclear phagocytes expressing both YFP and tdTomato. We found 84.7 ± 3.7% of co-expression in tdTomato positive cells present in the EAE lesions (n= 344 cells analyzed from 4 mice). This fate tracking approach showed that roughly 2/3 of all $M^{Arginase}$ result from a phenotypic switch while 1/3 of arginase-1 expressing-macrophages appear *de novo*, thus revealing two different origins of anti-inflammatory macrophages (**Figure 27**, n=4 mice).

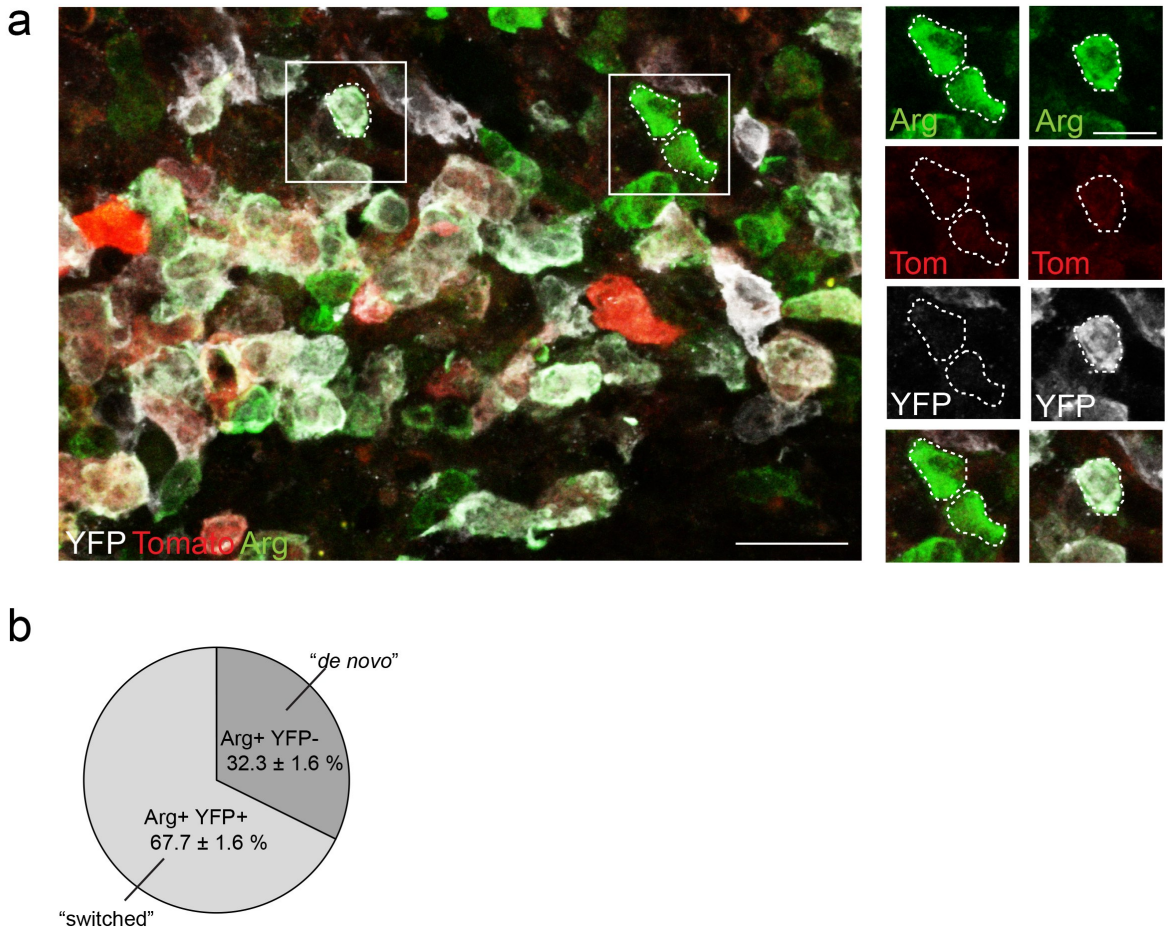

Figure 27: Existence of "*de novo*" mononuclear phagocyte population expressing $M^{Arginase}$.

(a) Confocal image of a spinal lesion in *iNOS-tdTomato-cre x Rosa26-Stp-fl-YFP* mouse perfused one/two days after EAE onset (YFP in gray, tdTomato in red, arginase co-staining in

green, scale bar 20μm, magnified insets represent *de novo* $YFP^{negative}M^{Arginase}$ cells, left, and a switched $YFP^{positive}M^{Arginase}$ cell, right, scale bar 10μm. (b) quantitative analysis of the proportion of *de novo* $YFP^{negative}M^{Arginase}$ and switched $YFP^{positive}M^{Arginase}$ cells in spinal lesions of *iNOS-tdTomato-cre x Rosa26-Stp-fl-YFP mice*. Data are shown as average expression ± s.e.m. ***Figure from Locatelli, Theodorou et al, submitted in Nature Neuroscience.***

5. Discussion

In our study, we used two transgenic mouse lines that translated the induction of the phenotype signature enzymes iNOS and arginase-1 into the expression of the reporter fluorescent proteins tdTomato and EYFP, respectively. We investigated the plasticity of phagocyte phenotypes in the context of neuroinflammation, by inducing the common multiple sclerosis model EAE in double transgenic reporter mice. Our results showed that phagocyte phenotypes evolved over time, from the formation to the resolution of spinal neuroinflammatory lesions. While phagocytes expressing iNOS dominated lesions at early stages of the disease, arginase-1 expressing phagocytes prevailed at later time points. Moreover, a substantial proportion of macrophages expressed both reporter proteins over the entire disease course. Transcriptional profiling of these mononuclear phagocytes revealed M^{iNOS}, $M^{iNOS/Arginase}$ and $M^{Arginase}$ cells as distinct populations in the inflamed CNS, nevertheless with a strongly overlapping transcriptome. As shown in experimental models of autoimmune CNS inflammation, mononuclear phagocytes can arise from infiltrating monocytes-derived macrophages or from resident microglia (London et al, 2013). We assessed the relative contribution of resident microglia in our transgenic reporter mice and detected a small proportion of $iNOS^+$ cells (8.2 ± 2.1%) and $arginase\text{-}1^+$ cells (2.1 ± 0.5%) that were derived from the resident microglia pool. Then, we used a spinal *in vivo* imaging in order to determine the evolution of macrophage phenotypes at the level of single cells, over time and space. We found that the spinal cord microenvironment has a crucial role in the establishment of mononuclear phagocytes phenotypes in neuroinflammatory lesions. Indeed the parenchyma was enriched in M^{iNOS} cells, in comparison to the upper meninges where $M^{Arginase}$ cells were predominant. However, no specific pattern of mononuclear phagocytes distribution within parenchymal lesions could be described. Then, we investigated the location of the initial M^{iNOS} cells phenotype in different compartments and found that

macrophages enter the CNS unpolarized and start expressing iNOS either in the upper meninges, in the perivascular space or in the parenchyma with the highest polarization rate into pro-inflammatory state in the two latter microenvironments. More importantly, we noticed that polarized macrophages could adjust their phenotype over the course of EAE from a pro- to an anti-inflammatory state (M^{iNOS} to $M^{Arginase}$). A transitional stage existed where both reporter proteins are expressed indicating a rather continuous phenotype spectrum. The *in vivo* bleaching of the respective reporter proteins for M^{iNOS} and $M^{Arginase}$ cells revealed that both reporter proteins were still active in most polarized cells over the course of EAE, thus suggesting that the $M^{iNOS/Arginase}$ phenotype was indeed a genuine phagocyte phenotype intermediate. Furthermore, an iNOS-expression fate tracking experiment showed that approximately 1/3 of arginase-1 expressing macrophages appeared *de novo,* interestingly implying two different origins of anti-inflammatory macrophages.

Limitations

One indisputable caveat of our study is the difference between human and murine species. Are the differences observed in mice between pro- and anti-inflammatory macrophages markers (e.g. CNS compartmentalization influence) also valid in human? Undoubtedly, not all findings in mice are necessarily also applicable in humans. Still, EAE has been legitimated as an animal model to study inflammatory processes in MS, as several current therapeutic interventions for MS were successfully initiated through EAE studies e.g. glatiramer acetate, Mitoxantrome, Fingolimod and Natalizumab.

Moreover, our transgenic mouse lines present some limitations concerning the timing of the initiation of iNOS or arginase-1 expressions. Indeed, the iNOS expression has been shown to have a shorter half-life than the tdTomato fluorescent protein (Kolodziejski et al, 2004). Thus,

our experimental detection of fluorescent protein signal did not necessarily imply that the endogenous reporter proteins were still expressed. However, we verified that both reporter proteins were actually still expressed over the entire course of the disease with the bleaching approach experiment. Even if we could established the location of the initial polarization of M^{iNOS} cells, the iNOS expression may have been set up earlier due to the time required to fold the tdTomato protein. Most probably, the switching had already happened.

Challenging the M1-M2 concept

How can macrophages exert both beneficial and detrimental effects in the context of CNS inflammation?

This assumption is supported by the bipolar dogma referring to pro- and anti-inflammatory macrophages as M1-M2 macrophages introduced by Charles Mills in 2000 and inspired from the Th1-Th2 concept (Mills et al, 2000). However, this concept has been principally based on results obtained from *in vitro* cell cultures experiments relying on defined stimulations of macrophages (e.g. for iNOS: Corradin et al, 1993). Yet, this classification might be an oversimplification and not depict correctly the *in vivo* situation. Another classification of macrophages relied on the type of stimuli encountered by macrophages (e.g. LPS or IL-4) (Murray et al, 2014). Still, this classification remains reductionist, as it does not describe the origin of the cell and its complex microenvironment (Nahrendorf et al, 2016). Over time, this concept has driven the classification of several specific cell markers into one group or the other (M1-M2), with dynamics of phagocyte phenotype switching that have only been formerly inferred through artificial *in vitro* paradigms. Nevertheless, our data rather favor the concept of phagocyte phenotype spectrum along which phagocytes are able to adapt their phenotypes in EAE lesions in an unidirectional manner (M^{iNOS} to $M^{Arginase}$) with an

intermediate stage. The RNA sequencing analysis revealed that M^{iNOS}, $M^{Arginase}$ and $M^{iNOS/Arginase}$ cell populations also showed distinct genes regulations. Interestingly, numerous classical genes formerly identified *in vitro* from cell cultures experiments, as belonging to M1 or M2 cells, were not differentially regulated *in vivo* in between M^{iNOS}, $M^{iNOS/Arginase}$, $M^{Arginase}$ cell populations. These results strongly suggest that the *in vivo* situation is more intricated than expected from mere *in vitro* experimental scenarios. Overall, the classification into M1 or M2 macrophages is certainly not optimal and should be taken with precaution. Nonetheless, the distinction into M^{iNOS} and $M^{Arginase}$ cell populations remains convincing as the macrophages switch occurred as the lesion evolved.

Population exchange versus single cell switch?

Several assumptions exist regarding the presence of differently polarized pro- and anti-inflammatory macrophages in the context of CNS inflammation. On the one hand, classical theories support the view of a sequential infiltration of polarized macrophages in the CNS (Auffray et al, 2009; Shechter et al, 2013) by means of sequential waves of different phagocyte populations over time. On the other hand, an alternative hypothesis proposes a phenotype adaptation on a single cell level. This potential switch would happen locally from a pro-inflammatory to an anti-inflammatory phenotype, according to the molecular cues present in the neighboring cell environment (Arnold et al, 2007; Liddiard & Taylor, 2015). To investigate these hypotheses, we performed a set of experiments. First, we tracked individual mononuclear phagocytes over time to follow their phenotypes using *in vivo* imaging. We found that a single cell could switch its polarization state over the entire course of the disease after the CNS entry. We noticed that at initial stage of the disease (i.e. weight loss) Arginase mRNA expression was already increased in pro-inflammatory macrophages compared to unpolarized cells, thus suggesting an immediate “shield” mechanism to counter attack the

ensuing inflammation. Moreover, fate-tracking experiment confirmed that a considerable proportion of macrophages undergoes a phenotypic switch. Also, we noticed that a substantial amount of Arginase^{+} macrophages never expressed iNOS and thus acquired the M^{Arginase} polarization *de novo*. All in all, these results suggest that both hypotheses were accurate, i.e. both an infiltration of differently polarized cells and a local phenotypic switch take place in the inflamed CNS correlating with the formation to the resolution of neuroinflammatory lesions.

Why is the study of the plasticity of mononuclear phagocytes relevant for MS?

Firstly, mononuclear phagocytes are the predominant cellular infiltrates in CNS demyelinating lesions, both in MS patients and in its animal model EAE (Mishra & Yong, 2016; Prinz & Priller, 2017). Due to complex integration of stimuli coming from their microenvironments, macrophages play a dual role in MS pathology by acquiring a pro- or an anti- inflammatory phenotype. Numerous studies have identified the association of deleterious pro-inflammatory macrophages with lesion formation in MS (Mikita et al, 2011; Lucchinetti et al, 2001). Moreover, high reactive species production (e.g. NO, peroxinitrite $ONOO^{-}$; Smith et al, 1999) and pro-inflammatory cytokines generation (e.g. TNFα and IFNγ) have been described in humans with the presence of iNOS and high amount of M1 markers - CD40, CD86, CD64 and CD32 – found in microglia in normal appearing white matter (NAWM) and in activated macrophages/microglia in active demyelinating MS lesions (Vogel et al, 2013; Lassmann, 2014). Infiltration of mononuclear phagocytes has been shown to be located near damaged axons and phagocytosed myelin (Trapp et al, 1998; Yamasaki et al, 2014; Romanelli et al, 2016). Among other relevant molecules, a tyrosine phosphatase protein, SHP-1, has been demonstrated to be involved in MS. SHP-1 is a negative regulator of pro-inflammatory cytokines signaling (i.e. through TLR activation) expressed mostly in

macrophages. SHP-1 deficiency found in MS patients had increased susceptibility to CNS demyelination, with a high expression of inflammatory markers (i.e. STAT1, STAT6, NFκB) (Christophi et al, 2009). Contrariwise, anti-inflammatory mononuclear phagocytes have been linked to tissue healing, lesion at remission stage and disease resolution (Miron et al, 2013). Assuming that regulatory mechanisms are conserved between MS and its animal model, targeting mononuclear phagocytes is of potential therapeutic interest. Our data suggests that mononuclear phagocytes entered in the CNS unpolarized and became pro-inflammatory after CNS entry. This initial polarization event needs to be prevented if we consider that this phenotype is linked to lesion initiation and tissue destruction. However, as we showed that lesion evolve over the entire course of the disease from a pro- to an anti-inflammatory phenotype, the timing of the prevention of M1 cells is critical as it may have different outcome at a later stage of the disease.

Immune cell interactions and microenvironments

Another potential topic of investigation remains the interaction of mononuclear phagocytes with other immune cells present in the CNS such as T cells or astrocytes. Recent studies have shown the crucial role of the meningeal compartment for the trafficking and lymphatic drainage of immune cells (i.e. T cells, Engelhardt et al., 2017) in particular during neuroinflammatory conditions (Bartholmäus et al, 2009; Schläger et al, 2016). The investigation of mononuclear phagocytes interaction with T cells in the different CNS microenvironments represents an intriguing area to examine, especially since different polarized macrophages express distinct type of T cell and cytokines sets (Biswas & Mantovani, 2010). M1 macrophages have been associated with Th1 cells while M2 macrophages have been linked to Th2 cells.

The interaction of T cells with mononuclear phagocytes in the meningeal compartment and the white matter will be further investigated, using multi-photon imaging in a shared project with Prof. Naoto Kawakami. Visualization of T cell activation will be achievable thanks to the genetically encoded fluorescence indicator (GECI) Twitch2b, a ratio-metric calcium sensor based on a Fluorescence resonance energy transfer (FRET) (Thestrup et al, 2014).

Targeting iron metabolism

Iron plays a crucial role in the metabolism at steady state, especially in the CNS. Iron is required in sufficient quantity for oxygen consumption, ATP production, oxidative metabolism and myelination (Connor et al, 1996; Ikeda & Long, 1990, Todorich et al 2009), and iron deficiency leads to permanent cognitive and motor damages. However, iron metabolism has to be tightly regulated as an iron accumulation could lead to free radicals production (i.e. NO^-) and oxidative injury. As stated previously, an aberrant accumulation of iron has been shown after spinal cord injury (Boven et al 2006, Kroner et al 2014; Liu et al 2006) and in neurodegenerative diseases such as Alzheimer's disease, Parkinson's and MS (Drayer et al, 1987; Olanow, 1993; Swaiman, 1991, Popescu et 2017). During lesion progression in MS, iron is released by oligodendrocytes resulting into accumulation of iron and its phagocytosis by macrophages and microglia at the lesion edges (Craelius et al, 1982, Lassmann 2014, Hametner et al, 2013). Thus, targeting iron metabolism molecules associated with macrophages could also be an appealing potential therapeutic target.

Therapeutic targets

The goal of our study was to shed light on the mechanisms and timing of macrophage polarization, in order to clarify macrophage-related aspects of MS treatment. Macrophages,

due to their potential dual role in MS, are certainly relevant and very attractive therapeutic targets. Understanding the trigger of the switch from a pro- to an anti-inflammatory macrophage would highlight a potential modulation of phagocyte phenotype leading to disease resolution.

Using genetically modified mice that lack important cytokines may be useful to understand potential candidates that may participate into macrophages switch (e.g. conditional knock-out of IL-4 and IL-13 cytokines, Voehringer et al 2009; Oeser et al, 2015). An interesting follow-up of our project could be the use of a conditional inactivation of IL-4 and IL-13 cytokines responsible for an anti-inflammatory macrophage polarization, during an EAE time course. Indeed, the timing of the inactivation of the anti-inflammatory macrophage population may have different outcome depending on the stage of the EAE lesion.

Another experimental approach in the search of novel therapeutic targets for MS would be a powerful technology recently implemented, the CRISPR-Cas9 method (Ran et al, 2013). CRISPR associated protein 9 nuclease (Cas9) from *Streptococcus pyogenes* is a relatively new technique in molecular biology created to manipulate functions of selected genes. This novel approach consists in targeting changes in the genome of living cells and enables genomic editing with a very high precision and efficiency at a relatively low cost. This technique can be used to speed up the selective inactivation of specific gene candidates necessary for the differentiation of macrophages into pro- or anti-inflammatory phenotypes (e.g. LPS, IFNγ, IL-4, IL-13, IL-10). Moreover, specific chemokine receptors reported fundamental for pro- or anti-inflammatory macrophage function could be as well targeted (i.e. CCR7 and CCR2, respectively). Preventing the influx of the pro- or anti- inflammatory macrophages population at different time points of the disease course could help us decipher the timing of the beneficial or detrimental impact of the distinct macrophages populations.

Other cytokines such as the pro-inflammatory immune mediator GM-CSF, involved in macrophages activation and in the pathogenicity of Th17 cells, could be as well targeted. Indeed, it has been shown that GM-CSF inhibition has beneficial effects in animal models of autoimmune disorders such as MS. GM-CSF knockout mice are resistant to EAE development (McQualter et al, 2001). Thus, many studies have focused on the development of molecular drugs targeting GM-CSF in order to ameliorate the disease course (Shiomi et al, 2016). T cell transfer experiments could be performed followed by the inactivating GM-CSF with the CRISPR-Cas9 method that would help decipher the timing of this cytokine action. Moreover, glucocorticoid hormones could be likewise targeted with a similar effect to Dexamethasone. This hormone has been associated with beneficial anti-inflammatory effects in cell culture. The action of Dexamethasone consists in decreasing in a dose-dependently manner the NO and iNOS production in murine macrophages formerly stimulated with LPS (Korhonen et al, 2002).

Thus, increasing our knowledge on the evolution of macrophage phenotype in neuroinflammatory lesions could help us better delineate potential therapeutic targets.

6. References

Adams AB, Williams MA, Jones TR, Shirasugi N, Durham MM, Kaech SM, Wherry EJ, Onami T, Lanier JG, Kokko KE, Pearson TC, Ahmed R, Larsen CP. Heterologous immunity provides a potent barrier to transplantation tolerance. *J Clin Invest.* 2003 Jun;111(12):1887-95.

Ahn M, Yang W, Kim H, Jin JK, Moon C, Shin T. Immunohistochemical study of arginase-1 in the spinal cords of Lewis rats with experimental autoimmune encephalomyelitis. *Brain Res.* 2012 May 9;1453:77-86.

Ajami B, Bennett JL, Krieger C, Tetzlaff W, Rossi FM. Local self-renewal can sustain CNS microglia maintenance and function throughout adult life. *Nat Neurosci.* 2007 Dec;10(12):1538-43.

Ajami B, Bennett JL, Krieger C, McNagny KM, Rossi FM. Infiltrating monocytes trigger EAE progression, but do not contribute to the resident microglia pool. *Nat Neurosci.* 2011 Jul 31;14(9):1142-9.

Amit I, Winter DR, Jung S. The role of the local environment and epigenetics in shaping macrophage identity and their effect on tissue homeostasis. *Nat Immunol.* 2016 Jan;17(1):18-25.

Arnold L, Henry A, Poron F, Baba-Amer Y, van Rooijen N, Plonquet A, Gherardi RK, Chazaud B. Inflammatory monocytes recruited after skeletal muscle injury switch into antiinflammatory macrophages to support myogenesis. *J Exp Med.* 2007 May 14;204(5):1057-69.

Auffray C, Fogg DK, Narni-Mancinelli E, Senechal B, Trouillet C, Saederup N, Leemput J, Bigot K, Campisi L, Abitbol M, Molina T, Charo I, Hume DA, Cumano A, Lauvau G, Geissmann F. CX3CR1+ CD115+ CD135+ common macrophage/DC precursors and the role of CX3CR1 in their response to inflammation. *J. Exp. Med.* 2009 Mar 16,206, 595–606.

Auffray C, Fogg D, Garfa M, Elain G, Join-Lambert O, Kayal S, Sarnacki S, Cumano A, Lauvau G, Geissmann F. Monitoring of blood vessels and tissues by a population of monocytes with patrolling behavior. *Science*. 2007 Aug 3;317(5838):666-70.

Auffray C, Sieweke MH, Geissmann F. Blood monocytes: development, heterogeneity, and relationship with dendritic cells. *Annu Rev Immunol.* 2009;27:669-92.

Bar-Or A, Pachner A, Menguy-Vacheron F, Kaplan J, Wiendl H. Teriflunomide and its mechanism of action in multiple sclerosis. *Drugs*. 2014; 74(6): 659–674

Bartholomäus I, Kawakami N, Odoardi F, Schläger C, Miljkovic D, Ellwart JW, Klinkert WE, Flügel-Koch C, Issekutz TB, Wekerle H, Flügel A. Effector T cell interactions with meningeal vascular structures in nascent autoimmune CNS lesions. *Nature*. 2009 Nov 5;462(7269):94-8

Bechade C, Colasse S, Diana MA, Rouault M, Bessis A. NOS2 expression is restricted to neurons in the healthy brain but is triggered in microglia upon inflammation. *Glia*. 2014 Jun;62(6):956-63.

Belge KU, Dayyani F, Horelt A, Siedlar M, Frankenberger M, Frankenberger B, Espevik T, Ziegler-Heitbrock L. The proinflammatory CD14+CD16+DR++ monocytes are a major source of TNF. *J. Immunol.* 2002, Apr 1, 168, 3536–3542.

Bishop D, Misgeld T, Kerschensteiner M. A reversible form of axon damage in experimental autoimmune encephalomyelitis and multiple sclerosis. *Nat Med.* 2011 Apr;17(4):495-9.

Biswas SK, Mantovani A. Macrophage plasticity and interaction with lymphocyte subsets: cancer as a paradigm. *Nat Immunol.* 2010 Oct;11(10):889-96.

Bitsch A, Schuchardt J, Bunkowski S, Kuhlmann T, Brück W. Acute axonal injury in multiple sclerosis. Correlation with demyelination and inflammation. *Brain*. 2000 Jun;123 (Pt 6):1174-83.

Bjartmar C, Wujek JR, Trapp BD. Axonal loss in the pathology of MS: consequences for understanding the progressive phase of the disease. *J Neurol Sci.* 2003 Feb 15;206(2):165-71.

Bogdan C. Nitric oxide synthase in innate and adaptive immunity: an update. *Trends Immunol.* 2015 Mar;36(3):161-78.

Boven, L.A., Van Meurs, M., Van Zwam, M., Wierenga-Wolf, A., Hintzen, R.Q., Boot, R.G., Aerts, J.M., Amor, S., Nieuwenhuis, E.E., and Laman, J.D. Myelin-laden macrophages are anti-inflammatory, consistent with foam cells in multiple sclerosis. 2006 *Brain* 129, 517–526.

Bronte V, Zanovello P. Regulation of immune responses by L-arginine metabolism. *Nat Rev Immunol.* 2005 Aug;5(8):641-54.

Brückener KE, el Bayâ A, Galla HJ, Schmidt MAJ. Permeabilization in a cerebral endothelial barrier model by pertussis toxin involves the PKC effector pathway and is abolished by elevated levels of cAMP. *Cell Sci.* 2003 May 1;116(Pt 9):1837-46.

Campbell GR, Kraytsberg Y, Krishnan KJ, Ohno N, Ziabreva I, Reeve A, Trapp BD, Newcombe J, Reynolds R, Lassmann H, Khrapko K, Turnbull DM, Mahad DJ. Clonally expanded mitochondrial DNA deletions within the choroid plexus in multiple sclerosis. *Acta Neuropathol.* 2012 Aug;124(2):209-20.

Campbell L, Saville CR, Murray PJ, Cruickshank SM, Hardman MJ. Local arginase 1 activity is required for cutaneous wound healing. *J Invest Dermatol*. 2013 Oct;133(10):2461-70.

Charo, I. F. & Ransohoff, R. M. The many roles of chemokines and chemokine receptors in inflammation. *N. Engl. J. Med.* 2006*,* Feb 9, 354, 610–621.

Christophi GP, Panos M, Hudson CA, Christophi RL, Gruber RC, Mersich AT, Blystone SD, Jubelt B, Massa PT. Macrophages of multiple sclerosis patients display deficient SHP-1 expression and enhanced inflammatory phenotype. *Lab Invest*. 2009 Jul;89(7):742-59.

Clausen BH, Lambertsen KL, Babcock AA, Holm TH, Dagnaes-Hansen F, Finsen B.J Interleukin-1beta and tumor necrosis factor-alpha are expressed by different subsets of microglia and macrophages after ischemic stroke in mice. *Neuroinflammation*. 2008 Oct 23;5:46.

Compston A, Coles A. Multiple sclerosis. *Lancet*. 2008 Oct 25;372(9648):1502-17.

Connor JR, Menzies SL. Relationship of iron to oligodendrocytes and myelination. *Glia*. 1996 Jun;17(2):83-93.

Corradin SB, Mauël J, Donini SD, Quattrocchi E, Ricciardi-Castagnoli P. Inducible nitric oxide synthase activity of cloned murine microglial cells. *Glia*. 1993 Mar;7(3):255-62.

Craelius, W., Migdal, M.W., Luessenhop, C.P., Sugar, A., and Mihalakis, I. Iron deposits surrounding multiple sclersosis plaques. *Arch. Pathol. Lab. Med.* 1982, 106:397.

Cumano, A. & Godin, I. Ontogeny of the hematopoietic system. *Annu. Rev. Immunol.* 2007, 25, 745–785.

Davies LC, Jenkins SJ, Allen JE, Taylor PR. Tissue-resident macrophages. *Nat Immunol.* 2013 Oct;14(10):986-95.

Dendrou CA, Fugger L, Friese MA. Immunopathology of multiple sclerosis. *Nat Rev Immunol.* 2015 Sep 15;15(9):545-58.

Dendrou CA, Plagnol V, Fung E, Yang JH, Downes K, Cooper JD, Nutland S, Coleman G, Himsworth M, Hardy M, Burren O, Healy B, Walker NM, Koch K, Ouwehand WH, Bradley JR, Wareham NJ, Todd JA, Wicker LS. Cell-specific protein phenotypes for the autoimmune locus IL2RA using a genotype-selectable human bioresource. *Nat Genet*. 2009 Sep;41(9):1011-5.

Dobin A, Davis CA, Schlesinger F, Drenkow J, Zaleski C, Jha S, Batut P, Chaisson M, Gingeras TR. STAR: ultrafast universal RNA-seq aligner. *Bioinformatics*. 2013 Jan 1;29(1):15-21.

Dranoff G. Cytokines in cancer pathogenesis and cancer therapy.*Nat Rev Cancer*. 2004 Jan;4(1):11-22.

Drayer, B., Burger, P., Hurwita, B., Dawson, D., and Cain, J. Reduced signal intensity on MR images of thalamus and putamen in multiple sclerosis: Increased iron content? *AJNR*. 1987. 8:413-419.

Edwards, J.P., Zhang, X., Frauwirth, K.A., and Mosser, D.M. Biochemical and functional characterization of three activated macrophage populations. 2006. *J Leukoc Biol* 80, 1298-1307.

Engelhardt B, Sorokin L. The blood-brain and the blood-cerebrospinal fluid barriers: function and dysfunction. *Semin Immunopathol.* 2009 Nov;31(4):497-511.

Engelhardt B, Vajkoczy P, Weller RO. The movers and shapers in immune privilege of the CNS. *Nat Immunol.* 2017 Feb;18(2):123-131.

Feger U, Luther C, Poeschel S, Melms A, Tolosa E, Wiendl H. Increased frequency of CD4+ CD25+ regulatory T cells in the cerebrospinal fluid but not in the blood of multiple sclerosis patients. *Clin Exp Immunol.* 2007 Mar;147(3):412-8.

Fletcher JM, Lalor SJ, Sweeney CM, Tubridy N, Mills KHG. T cells in multiple sclerosis and experimental autoimmune encephalomyelitis. *Clin Exp Immunol.* 2010 Oct; 162(1): 1–11.

Frischer JM, Bramow S, Dal-Bianco A, Lucchinetti CF, Rauschka H, Schmidbauer M, Laursen H, Sorensen PS, Lassmann H. The relation between inflammation and neurodegeneration in multiple sclerosis brains. *Brain*. 2009 May;132(Pt 5):1175-89.

Galboiz Y, Shapiro S, Lahat N, Miller A. Modulation of monocytes matrix metalloproteinase-2, MT1-MMP and TIMP-2 by interferon-gamma and -beta: implications to multiple sclerosis. *J Neuroimmunol.* 2002 Oct;131(1-2):191-200.

Galea I, Palin K, Newman TA, Van Rooijen N, Perry VH, Boche D. Mannose receptor expression specifically reveals perivascular macrophages in normal, injured, and diseased mouse brain. *Glia*. 2005 Feb;49(3):375-84.

Ginhoux F, Jung S. Monocytes and macrophages: developmental pathways and tissue homeostasis. *Nat Rev Immunol.* 2014 Jun;14(6):392-404.

Ginhoux F, Schultze JL, Murray PJ, Ochando J, Biswas SK. New insights into the multidimensional concept of macrophage ontogeny, activation and function. *Nat Immunol.* 2016 Jan;17(1):34-40.

Goldmann T, Wieghofer P, Jordão MJ, Prutek F, Hagemeyer N, Frenzel K, Amann L, Staszewski O, Kierdorf K, Krueger M, Locatelli G, Hochgerner H, Zeiser R, Epelman S, Geissmann F, Priller J, Rossi FM, Bechmann I, Kerschensteiner M, Linnarsson S, Jung S, Prinz M. Origin, fate and dynamics of macrophages at central nervous system interfaces. *Nat Immunol.* 2016 Jul;17(7):797-805.

Goverman J, Woods A, Larson L, Weiner LP, Hood L, Zaller DM. Transgenic mice that express a myelin basic protein-specific T cell receptor develop spontaneous autoimmunity. *Cell*. 1993 Feb 26;72(4):551-60.

Guglielmetti C, Le Blon D, Santermans E, Salas-Perdomo A, Daans J, De Vocht N, Shah D, Hoornaert C, Praet J, Peerlings J, Kara F, Bigot C, Mai Z, Goossens H, Hens N, Hendrix S, Verhoye M, Planas AM, Berneman Z, van der Linden A, Ponsaerts P. Interleukin-13 immune gene therapy prevents CNS inflammation and demyelination via alternative activation of microglia and macrophages. *Glia*. 2016 Dec;64(12):2181-2200.

Greter M, Merad M. Regulation of microglia development and homeostasis. *Glia*. 2013 Jan;61(1):121-7.

Gundra UM, Girgis NM, Gonzalez MA, San Tang M, Van Der Zande HJP, Lin JD, Ouimet M, Ma LJ, Poles J, Vozhilla N, Fisher EA, Moore KJ, Loke P. Vitamin A mediates conversion of monocyte-derived macrophages into tissue-resident macrophages during alternative activation. *Nat Immunol.* 2017 Jun;18(6):642-653.

Haider L, Fischer MT, Frischer JM, Bauer J, Höftberger R, Botond G, Esterbauer H,

Binder CJ, Witztum JL, Lassmann. Oxidative damage in multiple sclerosis lesions.H. *Brain*. 2011 Jul;134(Pt 7):1914-24.

Hametner S, Wimmer I, Haider L, Pfeifenbring S, Brück W, Lassmann H. Iron and neurodegeneration in the multiple sclerosis brain. *Ann Neurol.* 2013 Dec;74(6):848-61.

Hamilton JA, Achuthan A. 2013. Colony stimulating factors and myeloid cell biology in health and disease. *Trends Immunol*. 2013 Feb;34(2):81-9.

Hartmann FJ, Khademi M, Aram J, Ammann S, Kockum I, Constantinescu C, Gran B, Piehl F, Olsson T, Codarri L, Becher B. Multiple sclerosis-associated IL2RA polymorphism controls GM-CSF production in human TH cells. *Nat Commun.* 2014 Oct 3;5:5056.

Haure-Mirande JV, Audrain M, Fanutza T, Kim SH, Klein WL, Glabe C, Readhead B, Dudley JT, Blitzer RD, Wang M, Zhang B, Schadt EE, Gandy S, Ehrlich ME. Deficiency of TYROBP, an adapter protein for TREM2 and CR3 receptors, is neuroprotective in a mouse model of early Alzheimer's pathology. *Acta Neuropathol*. 2017 Jun 13.

Hauser SL, Oksenberg JR. The neurobiology of multiple sclerosis: genes, inflammation, and neurodegeneration. *Neuron*. 2006 Oct 5;52(1):61-76.

Hedström AK, Bäärnhielm M, Olsson T, Alfredsson L. Tobacco smoking, but not Swedish snuff use, increases the risk of multiple sclerosis. *Neurology*. 2009 Sep 1;73(9):696-701.

Helming L, Tomasello E, Kyriakides TR, Martinez FO, Takai T, Gordon S, Vivier E. Essential role of DAP12 signaling in macrophage programming into a fusion-competent state. *Sci Signal* 2008 Oct 28;1(43):ra11

Hemmer B, Archelos JJ, Hartung HP. New concepts in the immunopathogenesis of multiple sclerosis. *Nat Rev Neurosci.* 2002 Apr;3(4):291-301.

Huang SC, Everts B, Ivanova Y, O'Sullivan D, Nascimento M, Smith AM, Beatty W, Love-Gregory L, Lam WY, O'Neill CM, Yan C, Du H, Abumrad NA, Urban JF Jr,

Artyomov MN, Pearce EL, Pearce EJ. Cell-intrinsic lysosomal lipolysis is essential for alternative activation of macrophages. *Nat Immunol.* 2014 Sep;15(9):846-55.

Hussien Y, Sanna A, Söderström M, Link H, Huang YM. Multiple sclerosis: expression of CD1a and production of IL-12p70 and IFN-gamma by blood mononuclear cells in patients on combination therapy with IFN-beta and glatiramer acetate compared to monotherapy with IFN-beta. *Mult Scler.* 2004 Feb;10(1):16-25.

Iarlori C, Gambi D, Lugaresi A, Patruno A, Felaco M, Salvatore M, Speranza L, Reale M. Reduction of free radicals in multiple sclerosis: effect of glatiramer acetate (Copaxone). *Mult Scler.* 2008 Jul;14(6):739-48.

Ikeda Y, Long DM. The molecular basis of brain injury and brain edema: the role of oxygen free radicals. *Neurosurgery*. 1990 Jul;27(1):1-11.

Iqbal AJ, McNeill E, Kapellos TS, Regan-Komito D, Norman S, Burd S, Smart N, Machemer DE, Stylianou E, McShane H, Channon KM, Chawla A, Greaves DR. Human CD68 promoter GFP transgenic mice allow analysis of monocyte to macrophage differentiation *in vivo*. *Blood*. 2014 Oct 9;124(15):e33-44.

Jha AK, Huang SC, Sergushichev A, Lampropoulou V, Ivanova Y, Loginicheva E, Chmielewski K, Stewart KM, Ashall J, Everts B, Pearce EJ, Driggers EM, Artyomov MN. Network integration of parallel metabolic and transcriptional data reveals metabolic modules that regulate macrophage polarization. *Immunity*. 2015 Mar 17;42(3):419-30.

Jia T, Serbina NV, Brandl K, Zhong MX, Leiner IM, Charo IF, Pamer EG. Additive roles for MCP-1 and MCP-3 in CCR2-mediated recruitment of inflammatory monocytes during *Listeria monocytogenes* infection. *J Immunol.* 2008 May 15;180(10):6846-53.

Kerschensteiner M, Schwab ME, Lichtman JW, Misgeld T. *In vivo* imaging of axonal degeneration and regeneration in the injured spinal cord. *Nat Med.* 2005 May;11(5):572-7.

Kerschensteiner M, Reuter MS, Lichtman JW, Misgeld T. *Ex vivo* imaging of motor axon dynamics in murine triangularis sterni explants. *Nat Protoc.* 2008;3(10):1645-53.

Kigerl KA, Gensel JC, Ankeny DP, Alexander JK, Donnelly DJ, Popovich PG. Identification of two distinct macrophage subsets with divergent effects causing either neurotoxicity or regeneration in the injured mouse spinal cord. *J Neurosci.* 2009 Oct 28;29(43):13435-44.

Kim HJ, Ifergan I, Antel JP, Seguin R, Duddy M, Lapierre Y, Jalili F, Bar-Or A. Type 2 Monocyte and Microglia Differentiation Mediated by Glatiramer Acetate Therapy in Patients with Multiple Sclerosis. *J Immunol* June 1, 2004, 172 (11) 7144-7153

Kimura T, Nada S, Takegahara N, Okuno T, Nojima S, Kang S, Ito D, Morimoto K, Hosokawa T, Hayama Y, Mitsui Y, Sakurai N, Sarashina-Kida H, Nishide M, Maeda Y, Takamatsu H, Okuzaki D, Yamada M, Okada M, Kumanogoh A. Polarization of M2 macrophages requires Lamtor1 that integrates cytokine and amino-acid signals. *Nat Commun.* 2016 Oct 12;7:13130.

Kolodziejski PJ, Koo JS, Eissa NT. Regulation of inducible nitric oxide synthase by rapid cellular turnover and cotranslational down-regulation by dimerization inhibitors. *Proc Natl Acad Sci U S A.* 2004 Dec 28;101(52):18141-6.

Korhonen R, Lahti A, Hämäläinen M, Kankaanranta H, Moilanen E. Dexamethasone inhibits inducible nitric-oxide synthase expression and nitric oxide production by destabilizing mRNA in lipopolysaccharide-treated macrophages. *Mol Pharmacol.* 2002 Sep;62(3):698-704.

Kreider T, Anthony RM, Urban JFJr, Gause WC. Alternatively activated macrophages in helminth infections. 2007. *Curr. Opin. Immunol.* 19,448-453.

Kroner A, Greenhalgh AD, Zarruk JG, Passos Dos Santos R, Gaestel M, David S. TNF and increased intracellular iron alter macrophage polarization to a detrimental M1 phenotype in the injured spinal cord. *Neuron*. 2014 Sep 3;83(5):1098-116.

Kumaravelu P, Hook L, Morrison AM, Ure J, Zhao S, Zuyev S, Ansell J, Medvinsky A. Quantitative developmental anatomy of definitive haematopoietic stem cells/longterm repopulating units (HSC/RUs): role of the aorta–gonad–mesonephros (AGM) region and the yolk sac in colonisation of the mouse embryonic liver. *Development* 2002, Nov, 129, 4891–4899.

Kurihara, T., Warr, G., Loy, J. & Bravo, R. - Defects in macrophage recruitment and host defense in mice lacking the CCR2 chemokine receptor. *J. Exp. Med.* 186, 1757–1762 (1997).

Lang R, Patel D, Morris JJ, Rutschman RL, Murray PJ. Shaping gene expression in activated and resting primary macrophages by IL-10. *J Immunol.* 2002 Sep 1;169(5):2253-63.

Lassmann H. Mechanisms of white matter damage in multiple sclerosis. *Glia*. 2014 Nov;62(11):1816-30.

Lassmann H, Bradl M. Multiple sclerosis: experimental models and reality. *Acta Neuropathol.* 2017; 133(2): 223–244.

Lawrence T, Natoli G. Transcriptional regulation of macrophage polarization: enabling diversity with identity. *Nat Rev Immunol.* 2011 Oct 25;11(11):750-61.

Lavin Y, Mortha A, Rahman A, Merad M. Regulation of macrophage development and function in peripheral tissues. *Nat Rev Immunol.* 2015 Dec;15(12):731-44.

Leon B, Ardavin C. Monocyte migration to inflamed skin and lymph nodes is differentially controlled by L-selectin and PSGL-1. *Blood*. 2008; 111:3126–3130.

Liddiard K & Taylor PR. Understanding Local Macrophage Phenotypes In Disease: Shape-shifting macrophages. *Nat Medicine*. 2015. 21, 119–120.

Liu, Y., Hao, W., Letiembre, M., Walter, S., Kulanga, M., Neumann, H., and Fassbender, K. Suppression of microglial inflammatory activity by myelin phagocytosis: role of p47-PHOX-mediated generation of reactive oxy- gen species. 2006. *J. Neurosci.* 26, 12904–12913.

Liu, Z., Pelfrey, C. M., Cotleur, A., Lee, J. C. & Rudick, R. A. Immunomodulatory effects of interferon beta-1a in multiple sclerosis. *J. Neuroimmunol.* 2001,112, 153–162.

Locatelli G, Wörtge S, Buch T, Ingold B, Frommer F, Sobottka B, Krüger M, Karram K, Bühlmann C, Bechmann I, Heppner FL, Waisman A, Becher B. Primary oligodendrocyte death does not elicit anti-CNS immunity. *Nat Neurosci.* 2012 Feb 26;15(4):543-50.

Logroscino G, Marder K, Graziano J, Freyer G, Slavkovich V, LoIacono N, Cote L, Mayeux R. Altered systemic iron metabolism in Parkinson's disease. *Neurology*. 1997 Sep;49(3):714-7.

London A, Cohen M, Schwartz M. Microglia and monocyte-derived macrophages: functionally distinct populations that act in concert in CNS plasticity and repair. *Front Cell Neurosci.* 2013 Apr 8;7:34.

Lucas, M., Rodriguez MC, Gata JM, Zayas MD, Solano F, Izquierdo G. Regulation by interferon β-1a of reactive oxygen metabolites production by lymphocytes and monocytes and serum sulfhydryls in relapsing multiple sclerosis patients. *Neurochem. Int.* 2003, 42, 67–71.

Lucchinetti C, Bruck W, Noseworthy J. Multiple sclerosis: recent developments in neuropathology, pathogenesis, magnetic resonance imaging studies and treatment. *Curr opin Neurol.* 2001, 14: 259–269.

Lucchinetti, C. F., Brück, W., Rodriguez, M., & Lassmann, H. Distinct patterns of multiple sclerosis pathology indicates heterogeneity on pathogenesis. *Brain Pathology* 1996, 6(3), 259–274.

Mantovani A, Sica A, Sozzani S, Allavena P, Vecchi A, Locati M. The chemokine system in diverse forms of macrophage activation and polarization. *Trends Immunol. 2004* Dec;25(12):677-86.

Martinez F.O. and Gordon S. The M1 and M2 paradigm of macrophage activation: time for reassessment. *F1000Prime Rep.* 2014; 6:13.

McQualter JL, Darwiche R, Ewing C, Onuki M, Kay TW, Hamilton JA, Reid HH, Bernard CC. Granulocyte macrophage colony-stimulating factor: a new putative therapeutic target in multiple sclerosis. *J Exp Med.* 2001 Oct 1;194(7):873-82.

Medawar P.B. Immunity to homologous grafted skin. III. The fate of skin homografts transplanted to the brain, the subcutaneous tissue and to the anterior chamber of the eye. *Br J Exp Pathol;* 1948 Feb;29(1):58-69.

Menche J, Sharma A, Kitsak M, Ghiassian SD, Vidal M, Loscalzo J, Barabási AL. Uncovering disease-disease relationships through the incomplete interactome. *Science*. 2015 Feb 20; 347(6224):1257601.

Mikita J, Dubourdieu-Cassagno N, Deloire MS, Vekris A, Biran M, Raffard G, Brochet B, Canron MH, Franconi JM, Boiziau C, Petry KG. Altered M1/M2 activation patterns of monocytes in severe relapsing experimental rat model of multiple sclerosis. Amelioration of clinical status by M2 activated monocyte administration. *Mult Scler.* 2011 Jan;17(1):2-15.

Mills CD, Kincaid K, Alt JM, Heilman JH, Hill AM. M-1/M-2 Macrophages and the Th1/Th1 Paradigm. 2000 *J Immunol;* 164:6166-6173.

Miron VE, Boyd A, Zhao JW, Yuen TJ, Ruckh JM, Shadrach JL, van Wijngaarden P, Wagers AJ, Williams A, Franklin RJM, Ffrench-Constant C. M2 microglia and macrophages drive oligodendrocyte differentiation during CNS remyelination. *Nat Neurosci.* 2013 Sep;16(9):1211-1218.

Misgeld T, Kerschensteiner M. *In vivo* imaging of the diseased nervous system. *Nat Rev Neurosci.* 2006 Jun;7(6):449-63.

Misgeld T, Nikic I, Kerschensteiner M. *In vivo* imaging of single axons in the mouse spinal cord. *Nat Protoc.* 2007;2(2):263-8.

Mishra MK, Yong VW. Myeloid cells – targets of medication in multiple sclerosis. *Nat Neurology* 2016, 2016 Sep;12(9):539-51.

Mitrovic B, St Pierre BA, Mackenzie-Graham AJ, Merrill JE. The role of nitric oxide in glial pathology. *Ann N Y Acad Sci.* 1994 Nov 17;738:436-46.

Mosser DM, Edwards JP. Exploring the full spectrum of macrophage activation. *Nat Rev Immunol.* 2008 Dec;8(12):958-69.

Murray PJ. Macrophage polarization. *Annu Rev Physiol.* 2017 Feb 10;79:541-566.

Murray PJ, Allen JE, Biswas SK, Fisher EA, Gilroy DW, Goerdt S, Gordon S, Hamilton JA, Ivashkiv LB, Lawrence T, Locati M, Mantovani A, Martinez FO, Mege JL, Mosser DM, Natoli G, Saeij JP, Schultze JL, Shirey KA, Sica A, Suttles J, Udalova I, van Ginderachter JA, Vogel SN, Wynn TA. Macrophage activation and polarization: nomenclature and experimental guidelines. *Immunity*. 2014 Jul 17;41(1):14-20.

Murray PJ, Wynn TA. Protective and pathogenic functions of macrophage subsets. *Nat Rev Immunol.* 2011 Oct 14;11(11):723-37.

Nahrendorf M, Swirski FK. Abandoning M1/M2 for a Network Model of Macrophage Function. *Circ Res.* 2016 Jul 22;119(3):414-7.

Nave KA, Werner HB. Myelination of the nervous system: mechanisms and functions. *Annu Rev Cell Dev Biol.* 2014;30:503-33.

Nikić I, Merkler D, Sorbara C, Brinkoetter M, Kreutzfeldt M, Bareyre FM, Brück W, Bishop D, Misgeld T, Kerschensteiner M. A reversible form of axon damage in experimental autoimmune encephalomyelitis and multiple sclerosis. Nat Med. 2011 Apr;17(4):495-9.

Nerlov C, Graf T. PU.1 induces myeloid lineage commitment in multipotent hematopoietic progenitors. *Genes Dev.* 1998 Aug 1;12(15):2403-12.

Obermeier B, Lovato L, Mentele R, Brück W, Forne I, Imhof A, Lottspeich F, Turk KW, Willis SN, Wekerle H, Hohlfeld R, Hafler DA, O'Connor KC, Dornmair K. Related B cell clones that populate the CSF and CNS of patients with multiple sclerosis produce CSF immunoglobulin. *J Neuroimmunol.* 2011 Apr; 233(1-2): 245–248.

Oeser K, Schwartz C, Voehringer D. Conditional IL-4/IL-13-deficient mice reveal a critical role of innate immune cells for protective immunity against gastrointestinal

helminths. *Mucosal Immunol.* 2015 May;8(3):672-82.

Ogawa K, Funaba M, Chen Y, Tsujimoto M. Activin A functions as a Th2 cytokine in the promotion of the alternative activation of macrophages. *J Immunol.* 2006 Nov 15;177(10):6787-94.

Okuda Y, Sakoda S, Fujimura H, Yanagihara T. Aminoguanidine, a selective inhibitor of the inducible nitric oxide synthase, has different effects on experimental allergic encephalomyelitis in the induction and progression phase. *J Neuroimmunol*. 1998 Jan;81(1-2):201-10.

Olanow, C.W. A radical hypothesis for neurodegeneration. *TINS*, 1993, 16:439-444.

Olson MC, Scott EW, Hack AA, Su GH, Tenen DG, Singh H, Simon C. PU.1 is not essential for early myeloid gene expression but is required for terminal myeloid differentiation. *Immunity. 3,* 1995, 703-714.

Oshiro S, Morioka MS, Kikuchi M. Dysregulation of iron metabolism in Alzheimer's disease, Parkinson's disease, and amyotrophic lateral sclerosis. *Adv Pharmacol Sci.* 2011;2011:378278.

Pachner AR. Experimental models of multiple sclerosis. *Curr Opin Neurol.* 2011 Jun;24(3):291-9.

Pakpoor J, Pakpoor J, Disanto G, Giovannoni G, Ramagopalan SV. Cytomegalovirus and multiple sclerosis risk. *J Neurol.* 2013 Jun;260(6):1658-60. *J Neuroimmunol*. 2007 March ; 184(1-2): 37–44.

Perdiguero EG, Geissmann F. The development and maintenance of resident macrophages. *Nat Immunol.* 2016 Jan;17(1):2-8.

Peterson LK, Robert S and BS, Fujinami. Inflammation, Demyelination, Neurodegeneration and Neuroprotection in the Pathogenesis of Multiple Sclerosis. *J Neuroimmunol.* 2007 Mar; 184(1-2): 37–44.

Polfliet MM, van de Veerdonk F, Döpp EA, van Kesteren-Hendrikx EM, van Rooijen N, Dijkstra CD, van den Berg TK. The role of perivascular and meningeal macrophages in experimental allergic encephalomyelitis. *J Neuroimmunol*. 2002 Jan;122(1-2):1-8.

Popescu BF, Frischer JM, Webb SM, Tham M, Adiele RC, Robinson CA, Fitz-Gibbon PD, Weigand SD, Metz I, Nehzati S, George GN, Pickering IJ, Brück W, Hametner S, Lassmann H, Parisi JE, Yong G, Lucchinetti CF. Pathogenic implications of distinct patterns of iron and zinc in chronic MS lesions. *Acta Neuropathol.* 2017 Jul;134(1):45-64.

Prinz M and and Priller J. The role of peripheral immune cells in the CNS in steady state and disease. *Nat. Neurosci. Rev* 2017 Feb;20(2):136-144.

Pul R, Morbiducci F, Škuljec J, Skripuletz T, Singh V, Diederichs U, Garde N, Voss EV, Trebst C, Stangel M. Glatiramer Acetate Increases Phagocytic Activity of Human Monocytes *In Vitro* and in Multiple Sclerosis Patients. *PLoS One.* 2012; 7(12): e51867.

Rangachari M, Kuchroo VK. Using EAE to better understand principles of immune function and autoimmune pathology. *J Autoimmun.* 2013 Sep;45:31-9.

Raj T, Ryan KJ, Replogle JM, Chibnik LB, Rosenkrantz L, Tang A, Rothamel K, Stranger BE, Bennett DA, Evans DA, De Jager PL, Bradshaw EM. CD33: increased inclusion of exon 2 implicates the Ig V-set domain in Alzheimer's disease susceptibility. *Hum Mol Genet.* 2014 May 15;23(10):2729-36.

Ran FA, Hsu PD, Wright J, Agarwala V, Scott DA, Zhang F. Genome engineering using the CRISPR-Cas9 system. *Nat Protoc.* 2013 Nov;8(11):2281-2308.

Ransohoff RM. A polarizing question: do M1 and M2 microglia exist? *Nat Neurosci.* 2016 Jul 26;19(8):987-91.

Ransohoff RM. How neuroinflammation contributes to neurodegeneration. *Science*. 2016 Aug 19;353(6301):777-83.

Readhead C, Hood L. The dysmyelinating mouse mutations shiverer (shi) and myelin deficient (shimld). *Behav Genet.* 1990 Mar;20(2):213-34.

Reboldi A, Coisne C, Baumjohann D, Benvenuto F, Bottinelli D, Lira S, Uccelli A, Lanzavecchia A, Engelhardt B, Sallusto F. C-C chemokine receptor 6-regulated entry of TH-17 cells into the CNS through the choroid plexus is required for the initiation of EAE, *Nat Immunol.* 2009 May;10(5):514-23.

Reese TA, Liang HE, Tager AM, Luster AD, Van Rooijen N, Voehringer D, Locksley RM. Chitin induces accumulation in tissue of innate immune cells associated with allergy. *Nature.* 2007 May 3;447(7140):92-6.

Ritchie ME, Phipson B, Wu D, Hu Y, Law CW, Shi W, Smyth GK. limma powers differential expression analyses for RNA-sequencing and microarray studies. *Nucleic Acids Res.* 2015 Apr 20;43(7):e47.

Romanelli E, Merkler D, Mezydlo A, Weil MT, Weber MS, Nikić I, Potz S, Meinl E, Matznick FE, Kreutzfeldt M, Ghanem A, Conzelmann KK, Metz I, Brück W, Routh M, Simons M, Bishop D, Misgeld T, Kerschensteiner M. Myelinosome formation represents an early stage of oligodendrocyte damage in multiple sclerosis and its animal model. *Nat Commun.* 2016 Nov 16;7:13275.

Romanelli E, Sorbara CD, Nikić I, Dagkalis A, Misgeld T, Kerschensteiner M. *Nat. Protoc.* 8(3):481-90 (2013).

Ruddle NH, Bergman CM, McGrath KM, Lingenheld EG, Grunnet ML, Padula SJ, Clark RB. An antibody to lymphotoxin and tumor necrosis factor prevents transfer of experimental allergic encephalomyelitis. *J Exp Med.* 1990 Oct 1;172(4):1193-200.

Schläger C, Körner H, Krueger M, Vidoli S, Haberl M, Mielke D, Brylla E, Issekutz T, Cabañas C, Nelson PJ, Ziemssen T, Rohde V, Bechmann I, Lodygin D, Odoardi F, Flügel A. Effector T-cell trafficking between the leptomeninges and the cerebrospinal fluid. *Nature*. 2016 Feb 18;530(7590):349-53.

Schwartz M, Baruch K. The resolution of neuroinflammation in neurodegeneration: leukocyte recruitment via the choroid plexus. *EMBO J.* 2014 Jan 7;33(1):7-22.

Shechter R, London A, Schwartz M. Orchestrated leukocyte recruitment to immune-privileged sites: absolute barriers versus educational gates. *Nat Rev Immunol.* 2013 Mar;13(3):206-18.

Shechter R, Miller O, Yovel G, Rosenzweig N, London A, Ruckh J, Kim KW, Klein E, Kalchenko V, Bendel P, Lira SA, Jung S, Schwartz M. Recruitment of beneficial M2 macrophages to injured spinal cord is orchestrated by remote brain choroid plexus. *Immunity*. 2013 Mar 21;38(3):555-69.

Selmaj KW, Raine CS. Tumor necrosis factor mediates myelin and oligodendrocyte damage *in vitro*. *Ann Neurol.* 1988 Apr;23(4):339-46.

Selmaj K, Raine CS, Cross AH. Anti-tumor necrosis factor therapy abrogates autoimmune demyelination. *Ann Neurol.* 1991 Nov;30(5):694-700.

Shiomi A, Usui T and Mimori T. GM-CSF as a therapeutic target in autoimmune diseases. *Inflammation and Regeneration* 2016 36:8.

Sica A, Erreni M, Allavena P, Porta C. Macrophage polarization in pathology. *Cell Mol Life Sci.* 2015 Nov;72(21):4111-26.

Siffrin V, Radbruch H, Glumm R, Niesner R, Paterka M, Herz J, Leuenberger T, Lehmann SM, Luenstedt S, Rinnenthal JL, Laube G, Luche H, Lehnardt S, Fehling HJ, Griesbeck O, Zipp F. *In vivo* imaging of partially reversible th17 cell-induced neuronal dysfunction in the course of encephalomyelitis. *Immunity*. 2010 Sep 24;33(3):424-36.

Shi C & Pamer EG. Monocyte recruitment during infection and inflammation. *Nat Rev Immunol.* 2011 Oct 10;11(11):762-74.

Skripuletz T, Gudi V, Hackstette D, Stangel M. De- and remyelination in the CNS white and grey matter induced by cuprizone: the old, the new, and the unexpected. *Histol Histopathol.* 2011 Dec;26(12):1585-97.

Smith KJ, Kapoor R, Felts PA. Demyelination: the role of reactive oxygen and nitrogen species. *Brain Pathol.* 1999 Jan;9(1):69-92.

Spath S, Komuczki J, Hermann M, Pelczar P, Mair F, Schreiner B, Becher B. Dysregulation of the Cytokine GM-CSF Induces Spontaneous Phagocyte Invasion and Immunopathology in the Central Nervous System. *Immunity*. 2017 Feb 21;46(2):245-260.

Stein M, Keshav S, Harris N, Gordon S. Interleukin 4 potently enhances murine macrophage mannose receptor activity: a marker of alternative immunologic macrophage activation. *J Exp Med.* 1992 Jul 1;176(1):287-92.

Stromnes IM, Goverman JM. Active induction of experimental allergic encephalomyelitis. *Nat Protoc.* 2006;1(4):1810-9.

Stromnes IM, Goverman JM. Passive induction of experimental allergic encephalomyelitis. *Nat Protoc*. 2006;1(4):1952-60.

Swaiman, K.F. Hallervorden-Spatz syndrome and brain iron metabolism. *Arch. Neurol.,* 1991, 48:1285-1293.

Taylor PR, Martinez-Pomares L, Stacey M, Lin HH, Brown GD, Gordon S. Macrophage receptors and immune recognition. *Annu Rev Immunol.* 2005; 23:901–944.

Taşan M, Musso G, Hao T, Vidal M, MacRae CA, Roth FP. Selecting causal genes from genome-wide association studies via functionally coherent subnetworks. *Nat Methods*. 2015 Feb;12(2):154-9.

't Hart BA, Gran B, Weissert R. EAE: imperfect but useful models of multiple sclerosis. *Trends Mol Med.* 2011 Mar;17(3):119-25.

'tHart BA, Kap YS, Morandi E, Laman JD, Gran B. EBV Infection and Multiple Sclerosis: Lessons from a Marmoset Model. *Trends Mol Med*. 2016 Dec;22(12):1012-1024.

Thestrup T, Litzlbauer J, Bartholomäus I, Mues M, Russo L, Dana H, Kovalchuk Y, Liang Y, Kalamakis G, Laukat Y, Becker S, Witte G, Geiger A, Allen T, Rome LC, Chen TW, Kim DS, Garaschuk O, Griesinger C, Griesbeck O. Optimized ratiometric calcium sensors for functional *in vivo* imaging of neurons and T lymphocytes. *Nat Methods.* 2014

Feb;11(2):175-82.

Todorich B, Pasquini JM, Garcia CI, Paez PM, Connor JR. Oligodendrocytes and myelination: the role of iron. *Glia*. 2009 Apr 1;57(5):467-78.

Toft-Hansen, H., Nuttall, R.K., Edwards, D.R., and Owens, T. (2004). Key metalloproteinases are expressed by specific cell types in experimental autoimmune encephalomyelitis. *Journal of immunology* 173, 5209-5218.

Trapp BD, Peterson J, Ransohoff RM, Rudick R, Mörk S, Bö L. Axonal transection in the lesions of multiple sclerosis. *N Engl J Med.* 1998 Jan 29;338(5):278-85.

Vanheusden M, Stinissen P, 't Hart BA, Hellings N. Cytomegalovirus: a culprit or protector in multiple sclerosis? *Trends Mol Med*. 2015 Jan;21(1):16-23.

Vanheusden M, Broux B, Welten SP, Peeters LM, Panagioti E, Van Wijmeersch B, Somers V, Stinissen P, Arens R, Hellings N. Cytomegalovirus infection exacerbates autoimmune mediated neuroinflammation. *Sci Rep.* 2017 Apr 6;7(1):663.

Van Waesberghe JH, Kamphorst W, De Groot CJ, van Walderveen MA, Castelijns JA, Ravid R, Lycklama à Nijeholt GJ, van der Valk P, Polman CH, Thompson AJ, Barkhof F. Axonal loss in multiple sclerosis lesions: magnetic resonance imaging insights into substrates of disability. *Ann Neurol.* 1999 Nov;46(5):747-54.

Verreck FA, de Boer T, Langenberg DM, Hoeve MA, Kramer M, Vaisberg E, Kastelein R, Kolk A, de Waal-Malefyt R, Ottenhoff TH. Human IL-23-producing type 1 macrophages promote but IL-10-producing type 2 macrophages subvert immunity to (myco)bacteria. *Proc Natl Acad Sci U S A*. 2004 Mar 30;101(13):4560-5.

Voehringer D, Wu D, Liang HE, Locksley RM. Efficient generation of long-distance conditional alleles using recombineering and a dual selection strategy in replicate plates. *BMC Biotechnol.* 2009 Jul 28;9:69.

Vogel DY, Vereyken EJ, Glim JE, Heijnen PD, Moeton M, van der Valk P, Amor S, Teunissen CE, van Horssen J, Dijkstra CD. Macrophages in inflammatory multiple

sclerosis lesions have an intermediate activation status. *J Neuroinflammation*. 2013 Mar 4;10:35.

Vom Berg J, Prokop S, Miller KR, Obst J, Kälin RE, Lopategui-Cabezas I, Wegner A, Mair F, Schipke CG, Peters O, Winter Y, Becher B, Heppner FL. Inhibition of IL-12/IL-23 signaling reduces Alzheimer's disease-like pathology and cognitive decline. *Nat Med*. 2012 Dec;18(12):1812-9.

Weber MS, Prod'homme T, Youssef S, Dunn SE, Rundle CD, Lee L, Patarroyo JC, Stüve O, Sobel RA, Steinman L, Zamvil SS. Type II monocytes modulate T cell-mediated central nervous system autoimmune disease. *Nat Med.* 2007 Aug;13(8):935-43

Wilms H, Sievers J, Rickert U, Rostami-Yazdi M, Mrowietz U, Lucius R. Dimethylfumarate inhibits microglial and astrocytic inflammation by suppressing the synthesis of nitric oxide, IL-1β, TNF-α and IL-6 in an in-vitro model of brain inflammation. *J. Neuroinflamm.* 2010, 7, 30.

Yaghmoor F, Noorsaeed A, Alsaggaf S, Aljohani W, Scholtzova H, Boutajangout A, Wisniewski T. The Role of TREM2 in Alzheimer's Disease and Other Neurological Disorders. *J Alzheimers Dis Parkinsonism.* 2014 Nov;4(5).

Yamasaki R, Lu H, Butovsky O, Ohno N, Rietsch AM, Cialic R, Wu PM, Doykan CE, Lin J, Cotleur AC, Kidd G, Zorlu MM, Sun N, Hu W, Liu L, Lee JC, Taylor SE, Uehlein L, Dixon D, Gu J, Floruta CM, Zhu M, Charo IF, Weiner HL, Ransohoff RM. Differential roles of microglia and monocytes in the inflamed central nervous system. *J Exp Med.* 2014 Jul 28;211(8):1533-49.

Yang L, Tan D, Piao H. Myelin Basic Protein Citrullination in Multiple Sclerosis: A Potential Therapeutic Target for the Pathology. *Neurochem Res*. 2016 Aug;41(8):1845-56.

Yoshida H, Hayashi S, Kunisada T, Ogawa M, Nishikawa S, Okamura H, Sudo T, Shultz LD, Nishikawa S. The murine mutation osteopetrosis is in the coding region of the macrophage colony stimulating factor gene. *Nature*. 1990; 345:442–444.

Ziemssen T, Schrempf W. Glatiramer acetate: mechanisms of action in multiple sclerosis. *Int Rev Neurobiol.* 2007;79:537-70.

7. List of abbreviations

aCSF, artificial cerebrospinal fluid

APC, antigen presenting cell

BBB, blood brain barrier

CCR, CC-chemokine receptor

CCL, CC-chemokine ligand

CD, cluster of differentiation

CIS, clinically isolated syndromes

CFA, complete freunds adjuvant

CNS, central nervous system

Cas9, CRISPR associated protein 9 nuclease

CSF, cerebrospinal fluid

CSF1R, macrophage colony stimulating factor 1 receptor

CX_3CL1, CX_3- C chemokine ligand

CX_3CR1, CX_3C-chemokine receptor 1

DAMPS, damage-associated molecular patterns

EAE, experimental autoimmune encephalomyelitis

EBV, Epstein-Barr virus

FAD, focal axonal degeneration

FDA, food and drug administration

FRET, fluorescence resonance energy transfer

FTD, frontotemporal dementia

GECI, genetically encoded fluorescence indicator

GFAP, glial fibrillary acidic protein

GFP, green fluorescent protein

GM-CSF, granulocyte macrophage colony stimulating factor

HLA, human leukocyte antigen

HSCs, hematopoietic stem cells

IFN, interferons

IgG, immunoglobulin

IL, interleukin

IL-1R, interleukin 1 receptor

iNOS, inducible Nitric Oxide Synthase

i.p. intraperitoneally

LFA1, lymphocyte function associated antigen 1

LPS, lipopolysaccharides

Ly6c, lymphocyte antigen 6 complex

MAC1, macrophage receptor 1

M-CSF, macrophage colony stimulating factor

MHC, major histocompatibility complex

MBP, myelin basic protein

MOG, myelin oligodendrocyte glycoprotein

MS, multiple sclerosis

NAWM, normal appearing white matter

NK, natural Killer

NFkB, nuclear factor κ B

NO, nitric Oxide

PAMPS, pathogen-associated molecular patterns

PECAM1, platelet endothelial cell adhesion molecule

PFA, paraformaldehyde

PLP, proteolipid protein

PNS, peripheral nervous system

PRMS, progressive-Relapsing MS

PSGL1, P-selectin glycoprotein, ligand 1

ROS, reactive oxygen species

RNS, reactive nitrogen species

S1P-R, sphingosine-1-phosphate receptors

SPMS, secondary-Progressive MS

TCR, T cell receptor

TGFβ, transforming growth factor β

Th1, T helper 1

Th2, T helper 2

TLRs, toll like receptors

TNF, tumor necrosis factor

TNFR1, tumor necrosis factor receptor 1

TREM2, triggering receptor expressed on myeloid cells

TYROBP, tyrosine kinase binding protein

VLA4, very late antigen 4

YFP, yellow gluorescent protein

8. Acknowledgements

To start, I would like to truly thank my supervisor Prof. Dr. Martin Kerschensteiner for giving me the chance to work in his lab and learn outstanding techniques on a very interesting project. I would like to particularly thank him for his guidance, help and valuable advices during my entire PhD. His genuine passion for science pushed me forward to become a better scientist.

I would like to profoundly thank Dr. Giuseppe Locatelli (Beppe), who I shared all projects with. I want to thank him especially for being a wonderful mentor, scientist and friend, all along my PhD and for the time spent to teach me *in vivo* imaging and flow cytometry. He always cheered me up even in sad moments.

I am also very grateful to the members of my committee meeting: Prof. Dr. Thomas Misgeld, Prof. Dr. Thomas Korn and Prof. Naoto Kawakami, who gave me very nice suggestions and feedbacks to help us for futures directions of our project.

Thanks to the coordinators of the Medical Life Science and Technology Program for the chance of being part of such a remarkable international program.

I was lucky enough to work with terrific former and current lab mates and also friends that made my PhD memorable with especially Mehrnoosh, Laura, Carmen, Alex, Peter, Cath, Naomi, Beppe and Daniel.

I am very thankful to have wonderful friends that I could always count on even though we are spread across different countries, especially Adeline, Alba, Mathilde, Tharshana, Thomas, Antoine, Maud, Elise, Matthieu, Raph, Guillaume, Romain, Max, Elena, Aurelien and Deniz.

Last but not least, I want to thank my amazing family for supporting me and giving me faith and love at any moment: my mother, my father, my brother Damien and Weiyue. I want to thank the one who at the same time makes my heart beat and who is my best friend, Daniel. One thing that is absolutely sure is that I would have never made it until here without him. We have been through a lot together and I love you.

9. Publication

- Locatelli G*, **Theodorou D***, Jordao MJC, Staszewski O, Dagkalis A, Bessis A, Prinz M, Kerschensteiner M. Mononuclear phagocytes locally specify and adapt their phenotype in the inflamed central nervous system. ***Submitted in Nature Neuroscience.***

***first co-author**